Nonequilibrium dynamical mean field theory

Philipp Werner

University of Fribourg

Jouvence, May 2024

Motivation

Ultrafast pump-probe spectroscopy

- Time resolution: ~10 fs ⟶ measures excitation and relaxation processes on the intrinsic timescale of the electrons

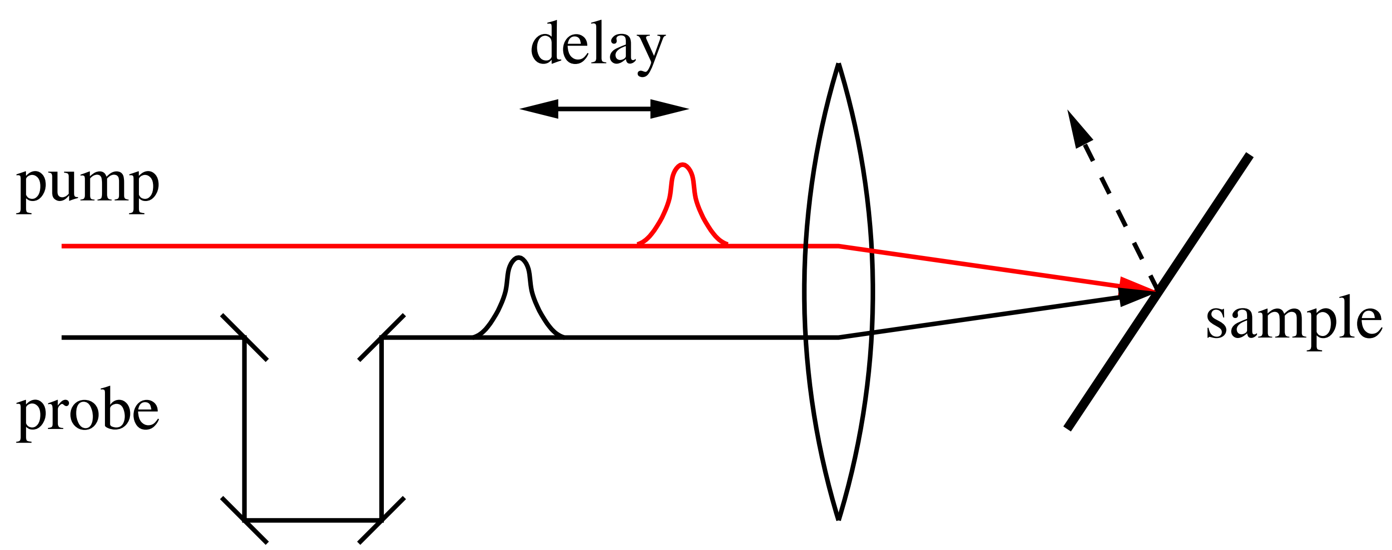

- Pump pulse drives system out of equilibrium
- Time evolution measured by subsequent probe pulses

- Possibility to "disentangle" competing effects on the time-axis

Motivation

"Tuning" of material properties by external driving

- Ultra-fast insulator-metal transition ("photo-doping")

Iwai et al. (2003)

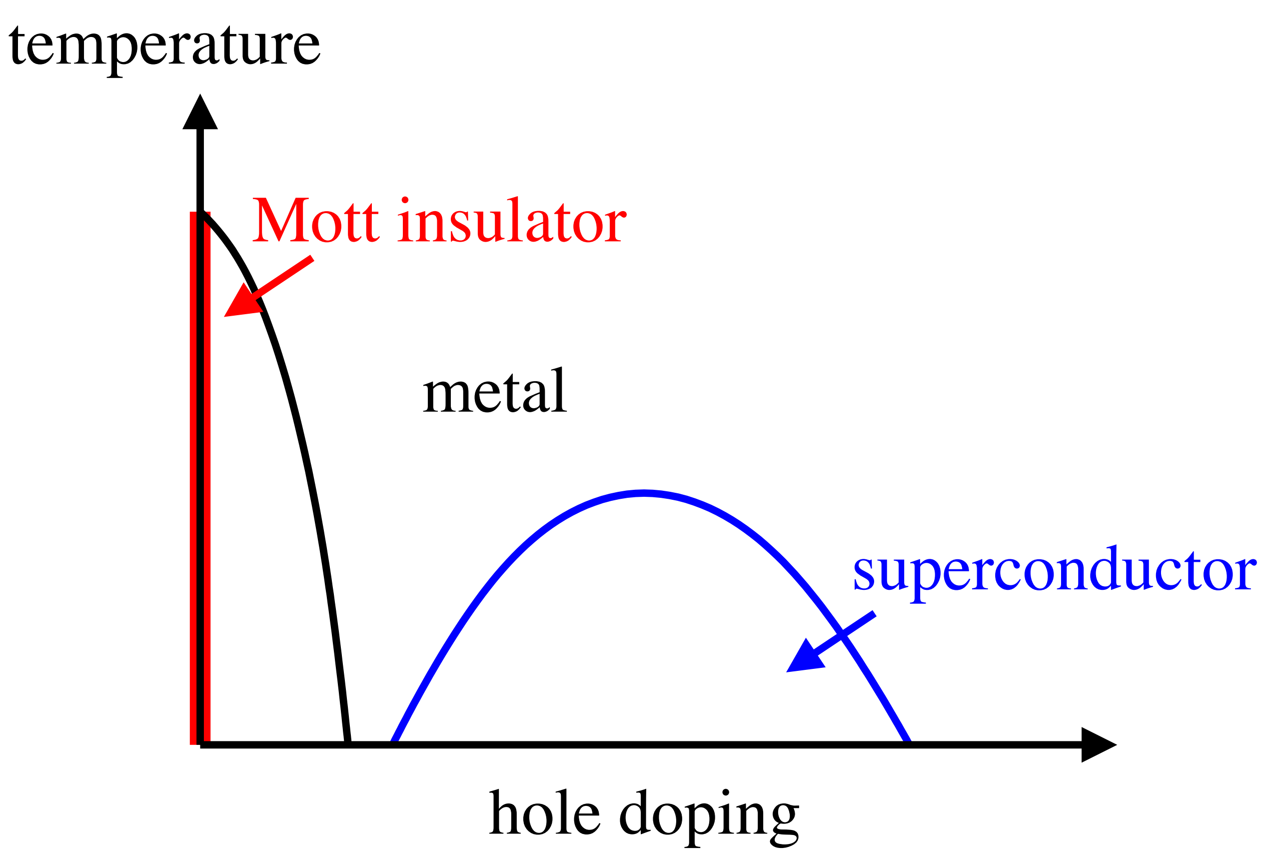

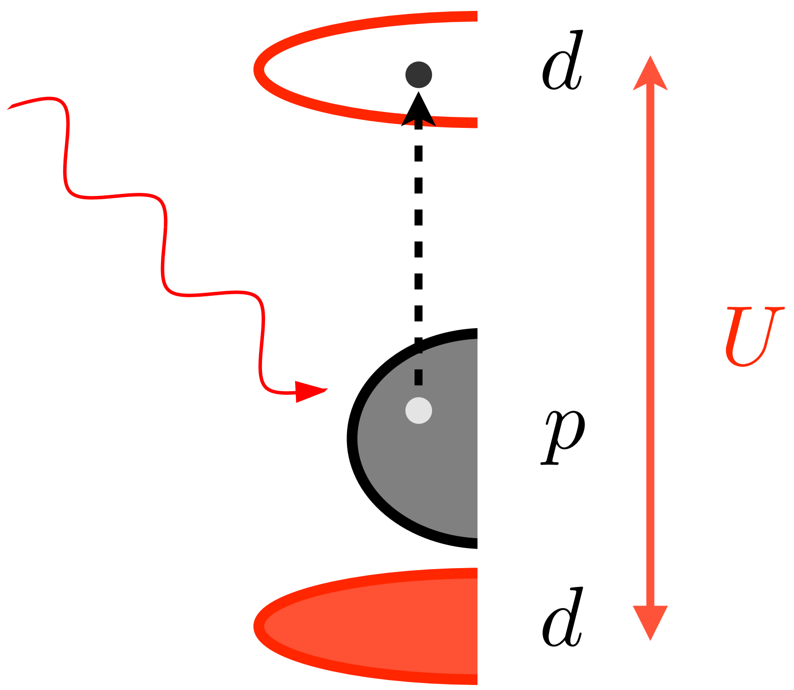

Motivation

“Tuning” of material properties by external driving

- Create long-lived transient states with novel properties

  e. g. *light-induced high-temperature superconductivity*

  Fausti et al. (2010), Kaiser et al. (2013)

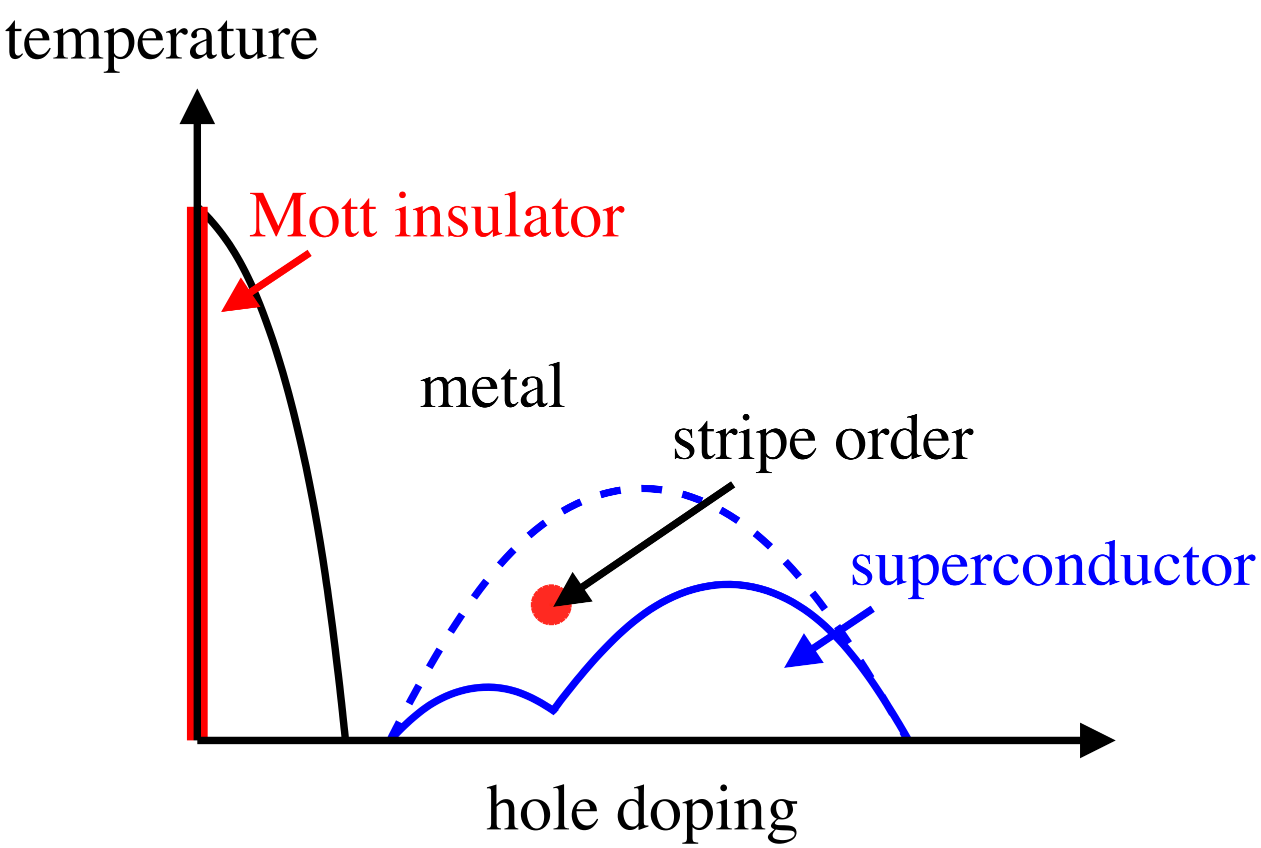

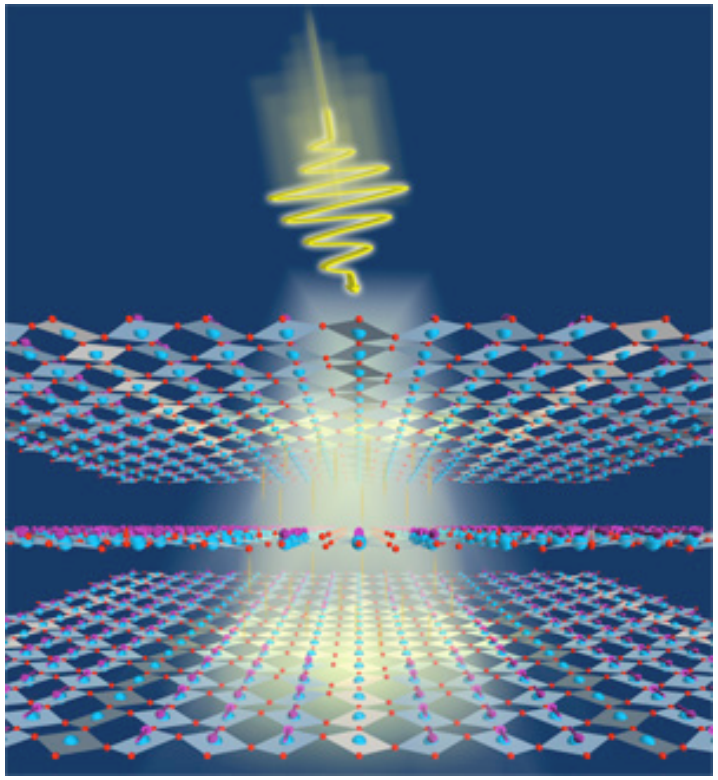

THz pulse couples to phonons

Motivation

“Tuning” of material properties by external driving

- Create long-lived transient states with novel properties

  e. g. *light-induced high-temperature superconductivity*

Mitrano et al. (2015)

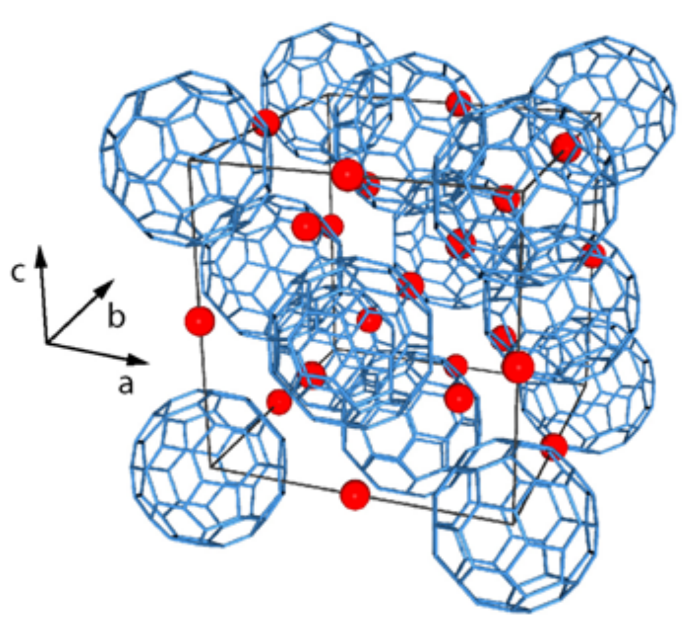

K_3C_{60}

equilibrium

driven state

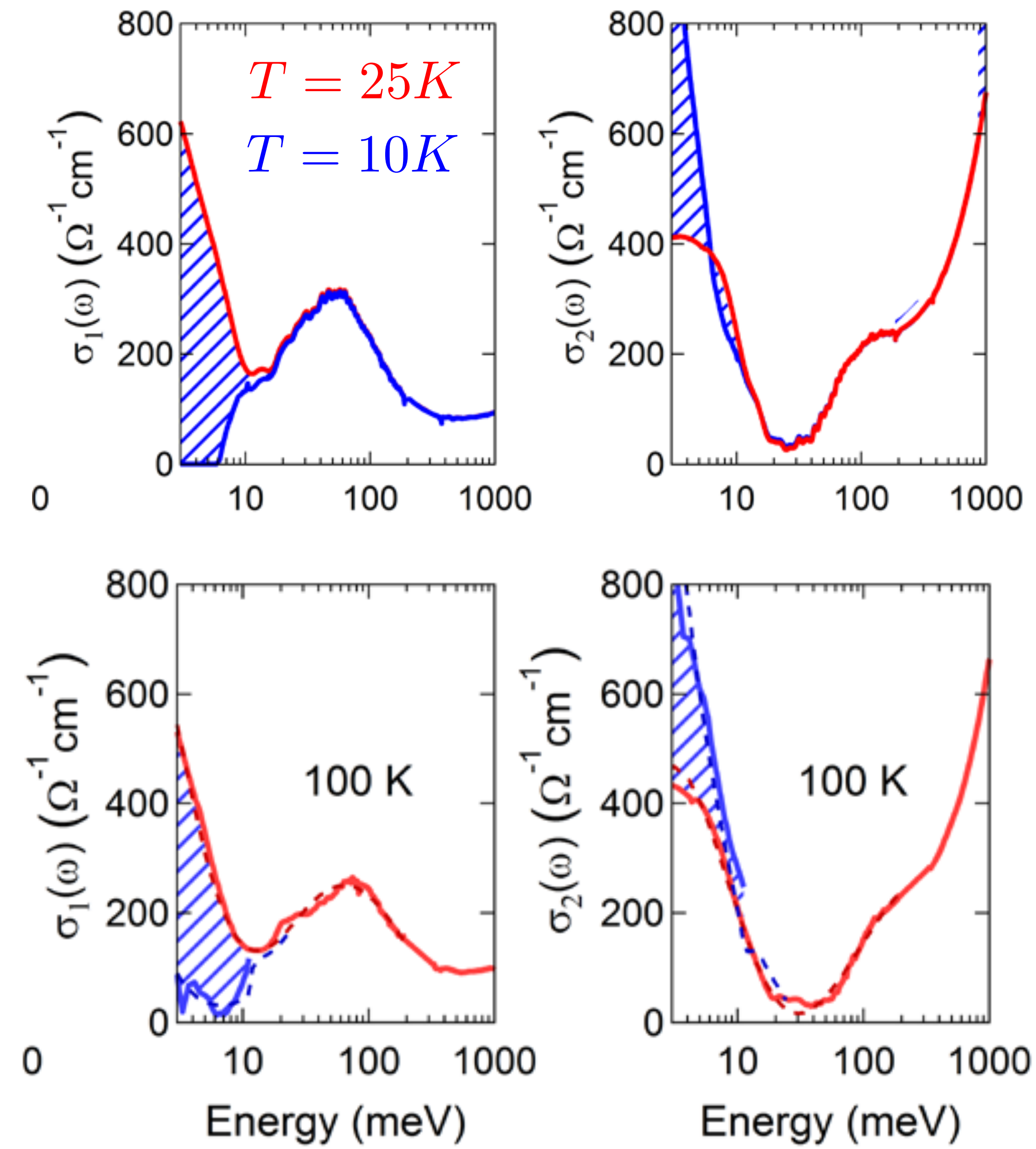

Motivation

"Tuning" of material properties by external driving

- Switching into metastable, but long-lived "hidden states"

  e. g. *Reversible switching of TaS_2 into / out of a metallic hidden state*

  Stojchevska et al. (2014)

equilibrium state (insulating)

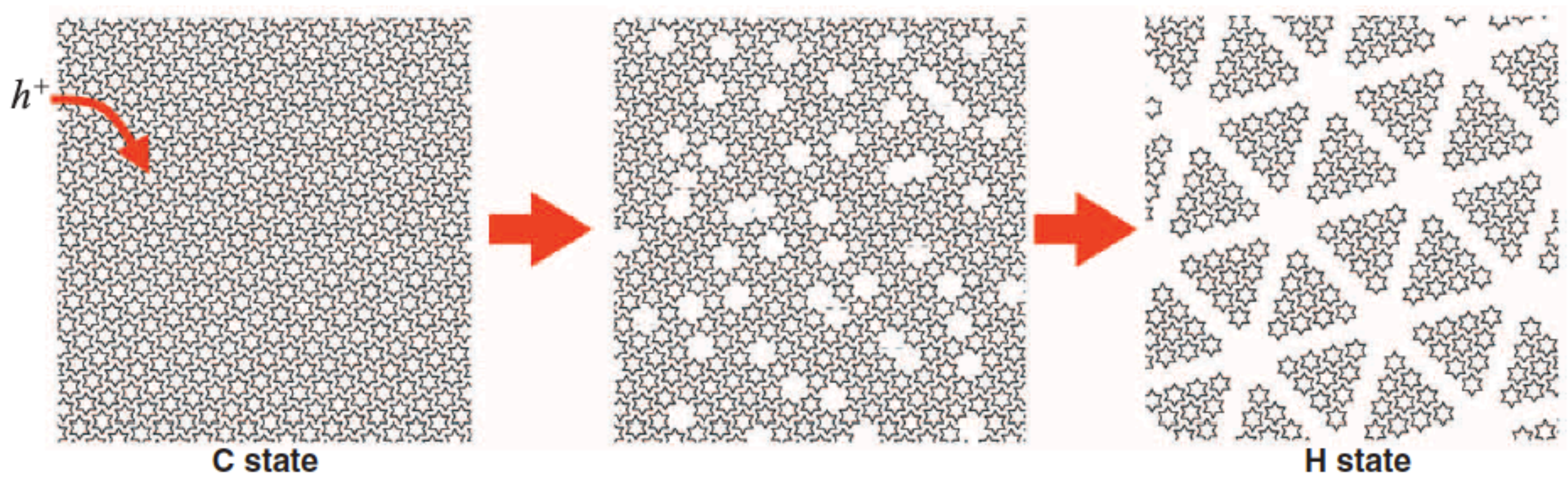

hidden state (conducting)

Motivation

"Tuning" of material properties by external driving

- Switching into metastable, but long-lived "hidden states"

  e. g. *Reversible switching of TaS_2 into / out of a metallic hidden state*

  Stojchevska et al. (2014)

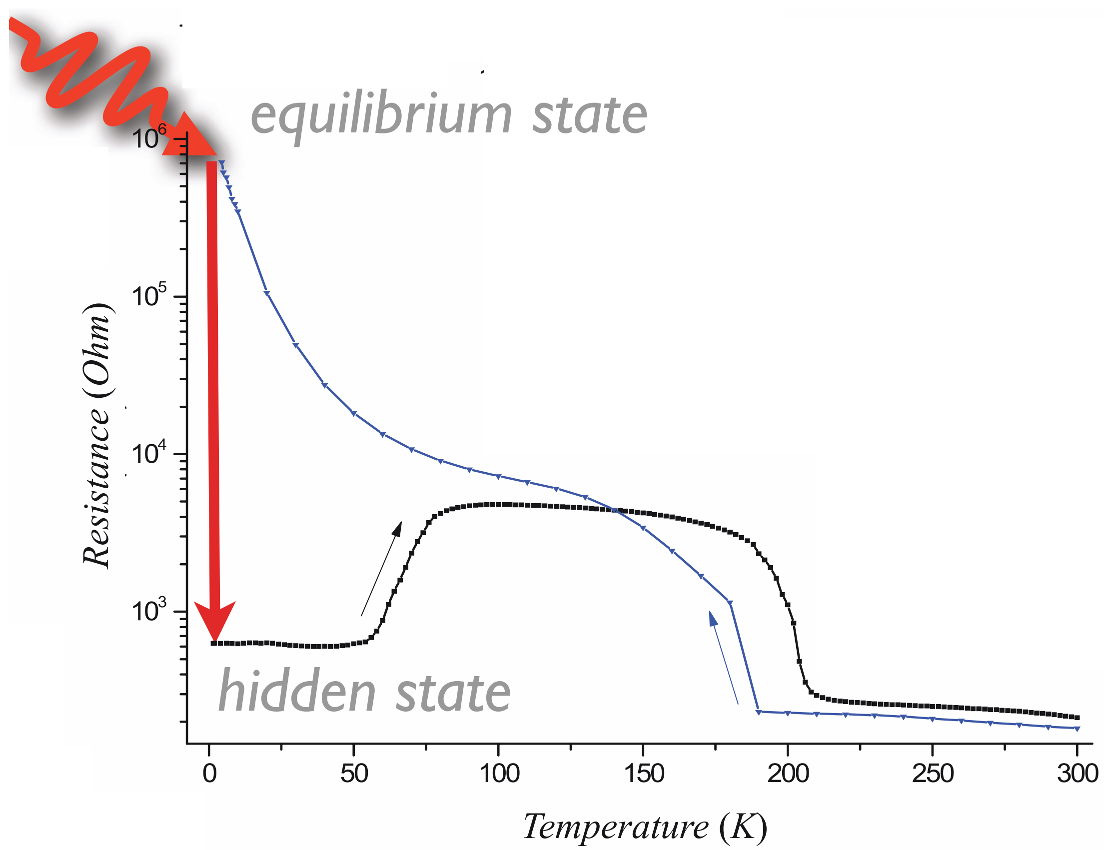

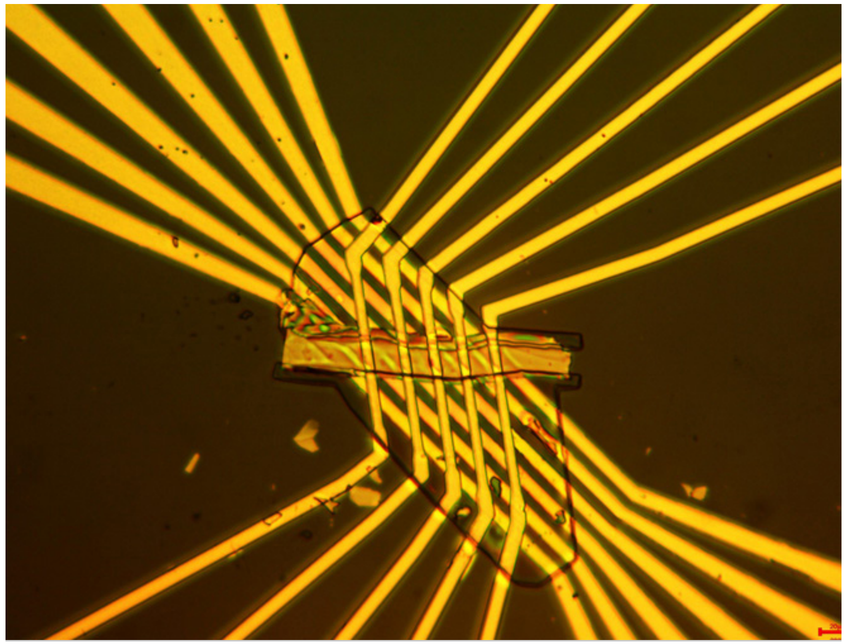

memory device with unprecedented speed and very low power consumption

Motivation

- Challenge for theory/numerics *Aoki et al. (2014)*

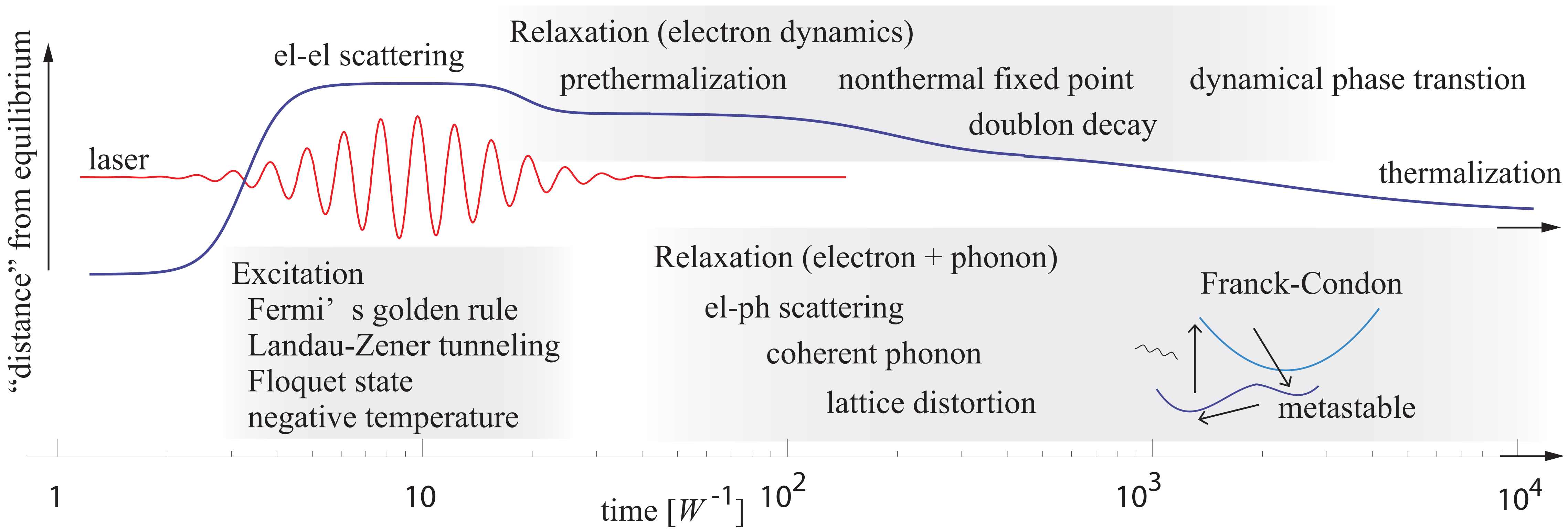

- Strongly interacting many-particle systems
- Strong perturbations
- Different relevant time scales

Overview

- *Dynamical mean field theory*
- *Cluster extension*
- *Nonequilibrium extension*
- *Nonequilibrium solvers and benchmarks*
- *Illustrations:*
  - *AC field quench - tuning of the interaction strength by external driving*
  - *Nonequilibrium phase transition - nonthermal fixed points*
  - *Cooling by photo-doping*

Model and method

- Static mean field theory: mapping to a single-site problem

  Weiss (1903)

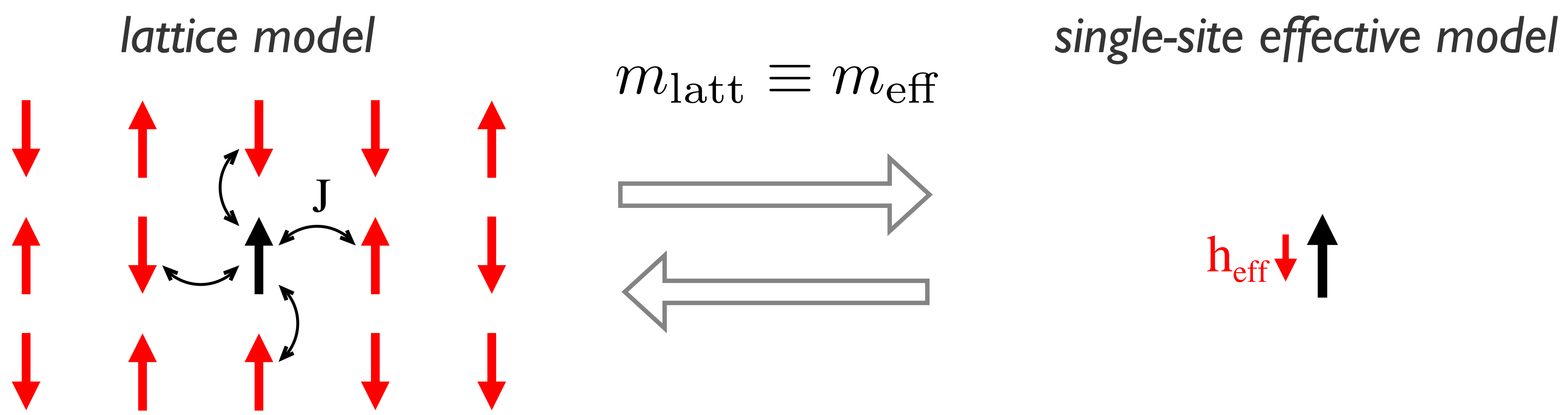

- Effective model: yields local observables (magnetization)

- Parameter of the effective model ("mean field"): optimized by requesting consistency between the lattice and single-site model

Model and method

- Dynamical mean field theory DMFT: mapping to an impurity problem

  Georges & Kotliar (1992)

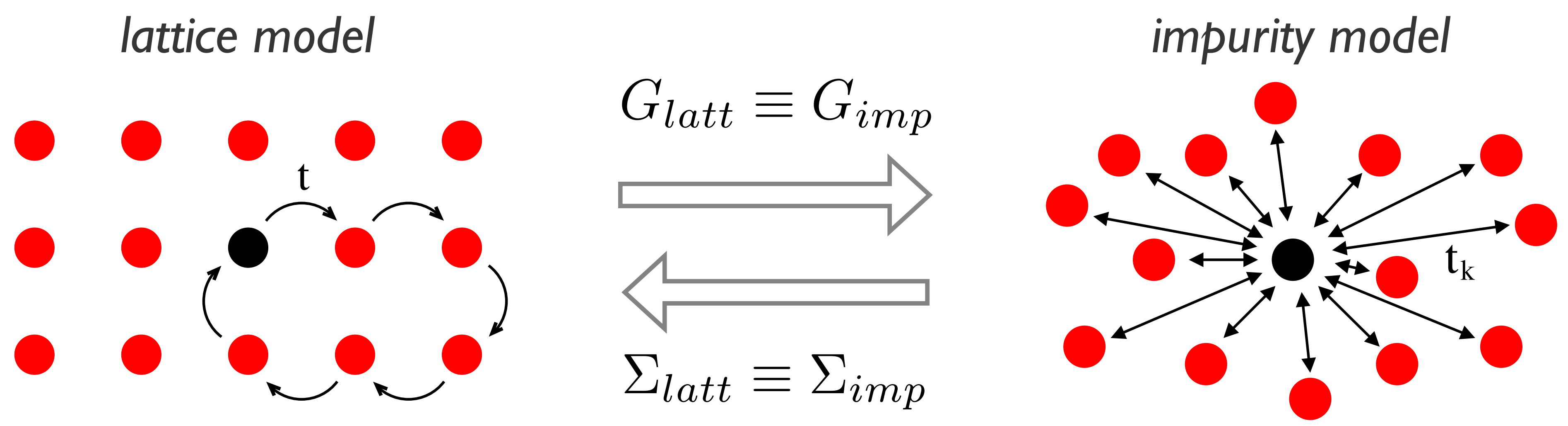

- Impurity solver: computes the Green's function of the correlated site

- Bath parameters = "mean field": optimized in such a way that the bath mimics the lattice environment

Model and method

- Dynamical mean field theory DMFT: mapping to an impurity problem

  Georges & Kotliar (1992)

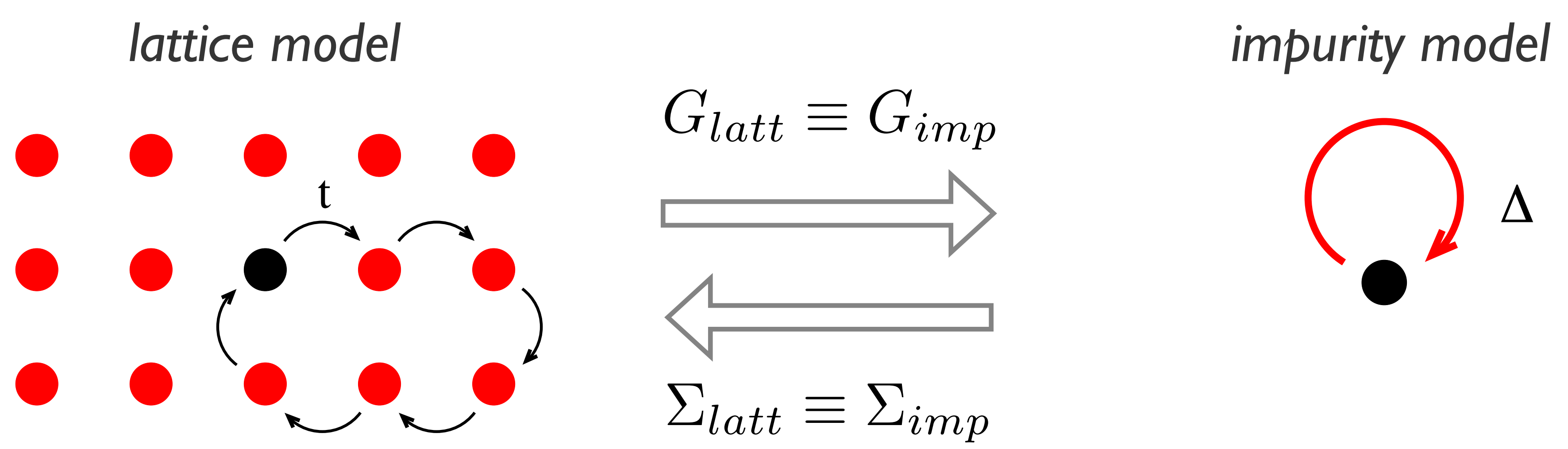

- Impurity solver: computes the Green's function of the correlated site

- Bath parameters = "mean field": optimized in such a way that the bath mimics the lattice environment

Model and method

- Dynamical mean field theory DMFT: mapping to an impurity problem

  Georges & Kotliar (1992)

lattice model *impurity model*

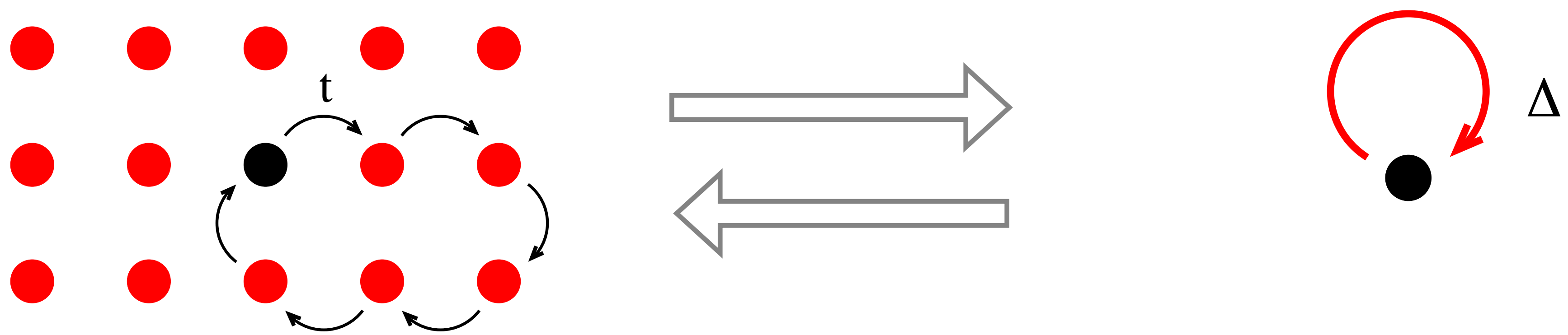

DMFT self-consistency

$$G^{\text{latt}}_{\text{loc}}(i\omega_n) \Rightarrow S_{\text{imp}}[\Delta(i\omega_n)]$$

$$G^{\text{latt}}_{\text{loc}} \equiv G_{\text{imp}}$$

momentum average ⇑ ⇓ *impurity solver*

$$\Sigma^{\text{latt}}_k \equiv \Sigma_{\text{imp}}$$

$$G^{\text{latt}}_k = \frac{1}{i\omega_n + \mu - \epsilon_k - \Sigma^{\text{latt}}_k} \Leftarrow G_{\text{imp}}(i\omega_n), \Sigma_{\text{imp}}(i\omega_n)$$

DMFT approximation

Model and method

- Dynamical mean field theory DMFT: mapping to an impurity problem
  Georges & Kotliar (1992)

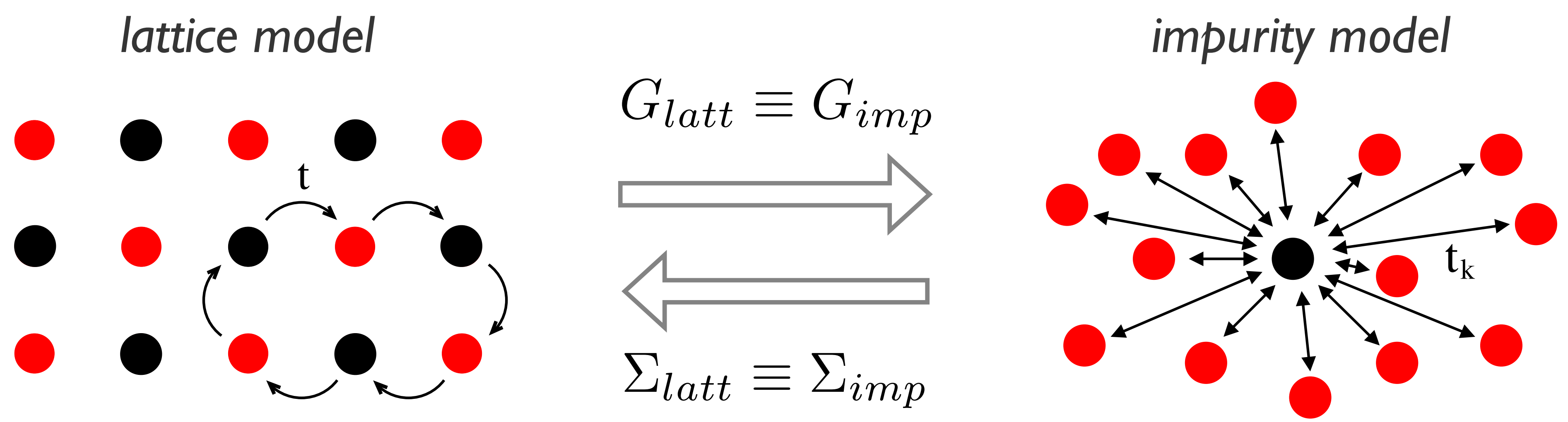

- Single-site DMFT can treat two-sublattice order (e. g. AFM)

$$\mathrm{Bath}_{B,\sigma}[G_{A,\sigma}], \quad \mathrm{Bath}_{A,\sigma}[G_{B,\sigma}]$$

- Pure Neel order: $\mathrm{Bath}_{B,\sigma} = \mathrm{Bath}_{A,\bar{\sigma}} \longrightarrow \mathrm{Bath}_{A,\bar{\sigma}}[G_{A,\sigma}]$

Model and method

- Equilibrium DMFT phase diagram (half-filling)
- Paramagnetic calculation: Metal - Mott insulator transition at low *T*
- Smooth crossover at high *T*

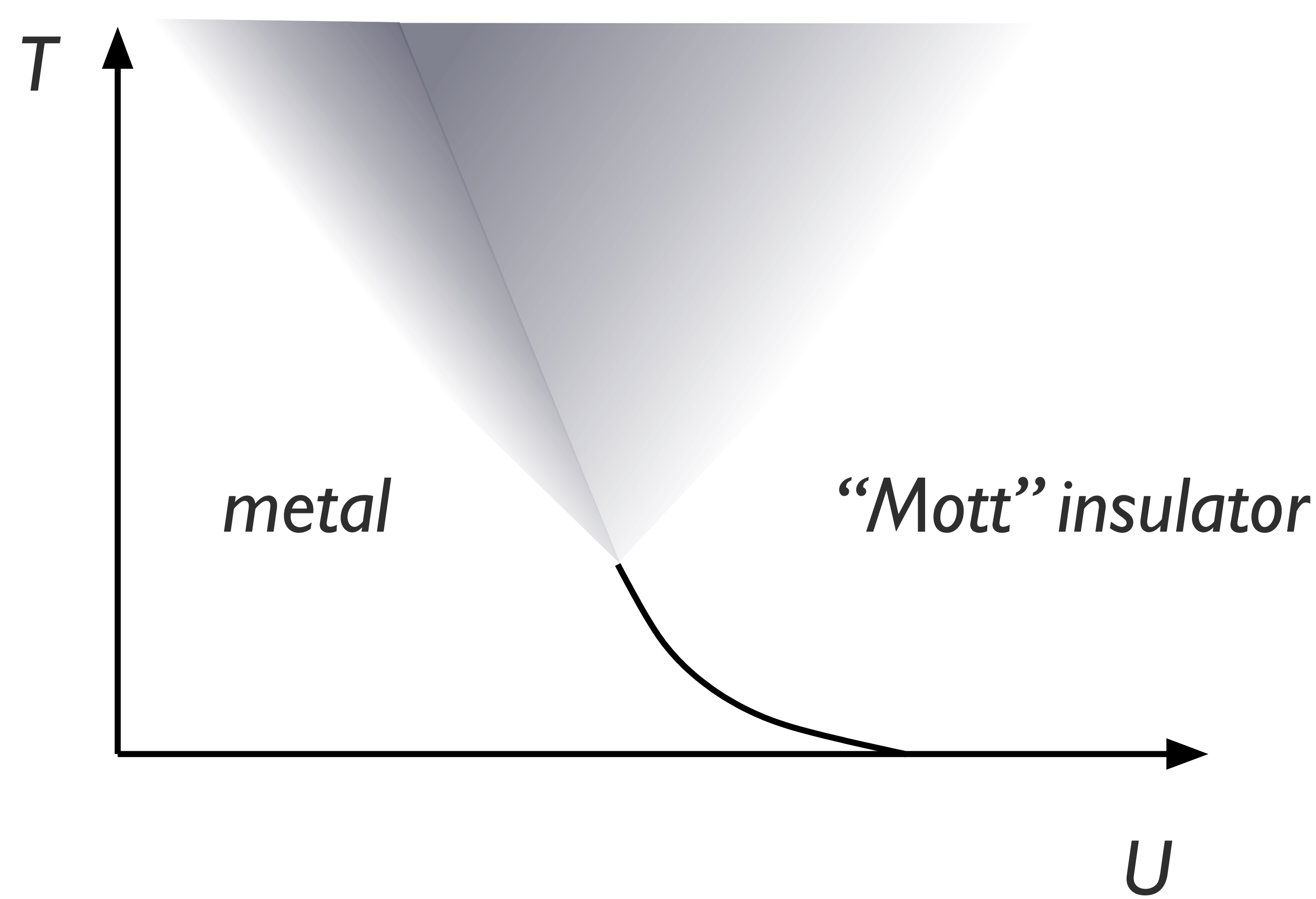

Model and method

- Equilibrium DMFT phase diagram (half-filling)
- With 2-sublattice order: Antiferromagnetic insulator at low *T*
- Smooth crossover at high *T*

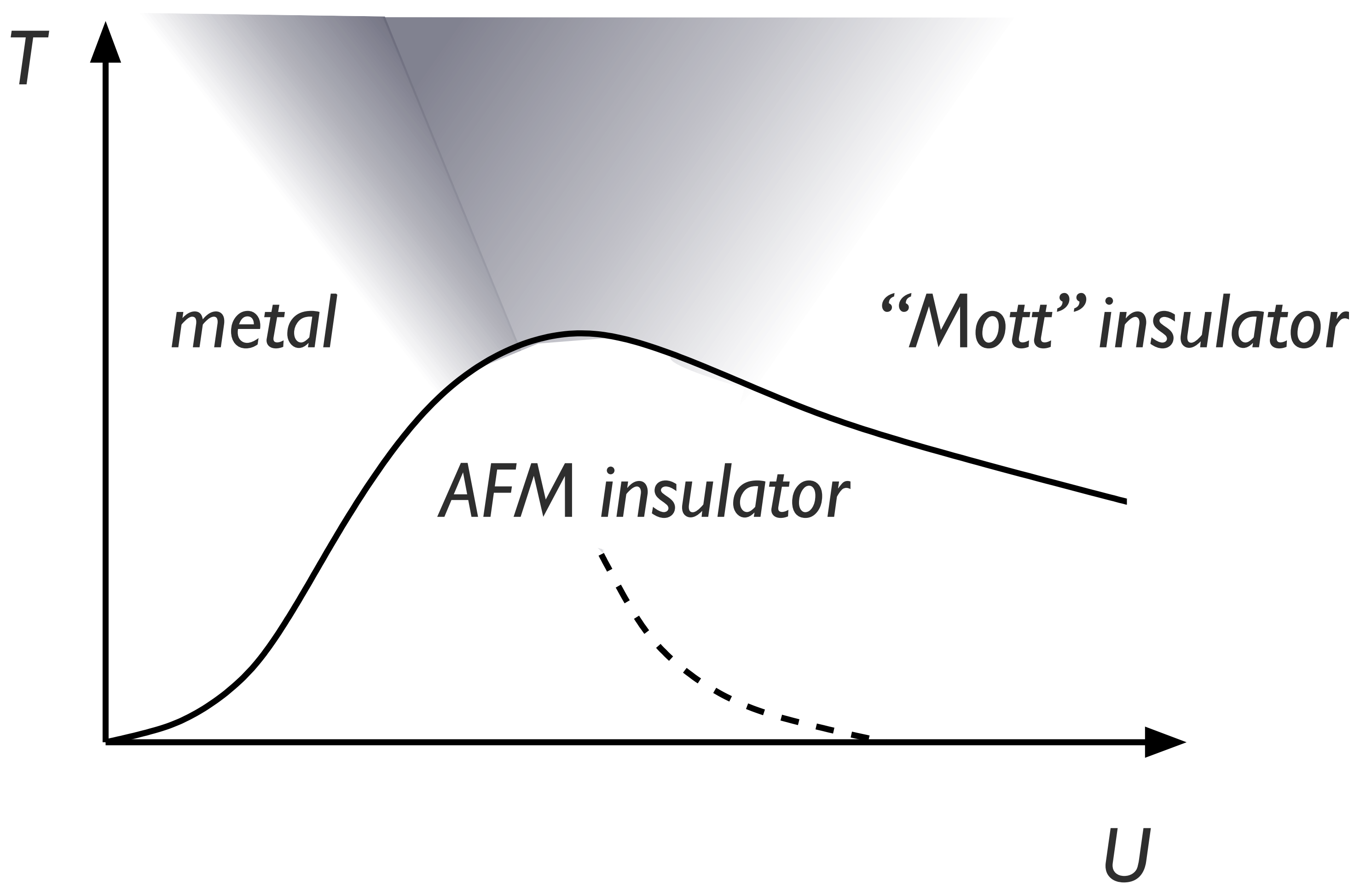

Model and method

- Equilibrium DMFT phase diagram (half-filling)
- Transformation $c_{i\uparrow} \to c_{i\uparrow}^\dagger \quad (i \in A), \quad c_{i\uparrow} \to -c_{i\uparrow}^\dagger \quad (i \in B)$

  maps repulsive model onto attractive model

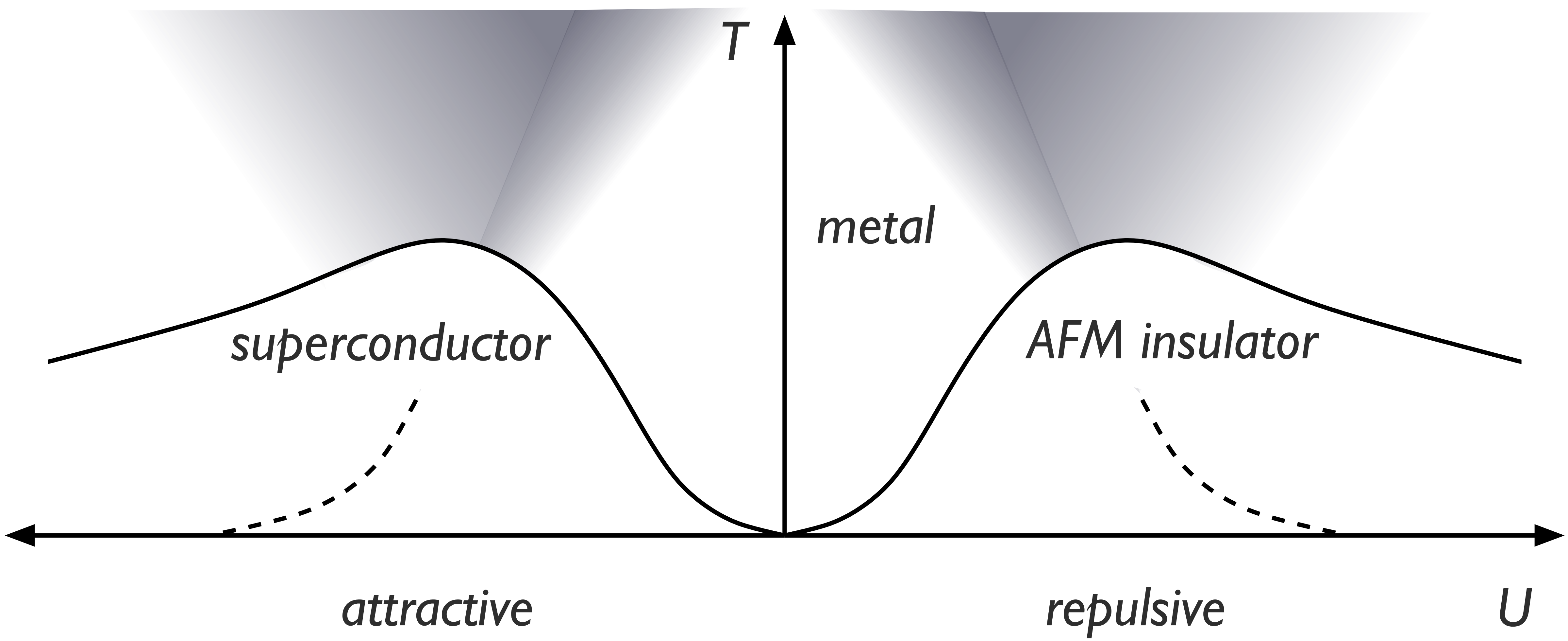

Model and method

- Equilibrium DMFT phase diagram
- Half-filling: transformation $c_{i\uparrow} \to c_{i\uparrow}^{\dagger} \quad (i \in A), \quad c_{i\uparrow} \to -c_{i\uparrow}^{\dagger} \quad (i \in B)$

  maps repulsive model onto attractive model

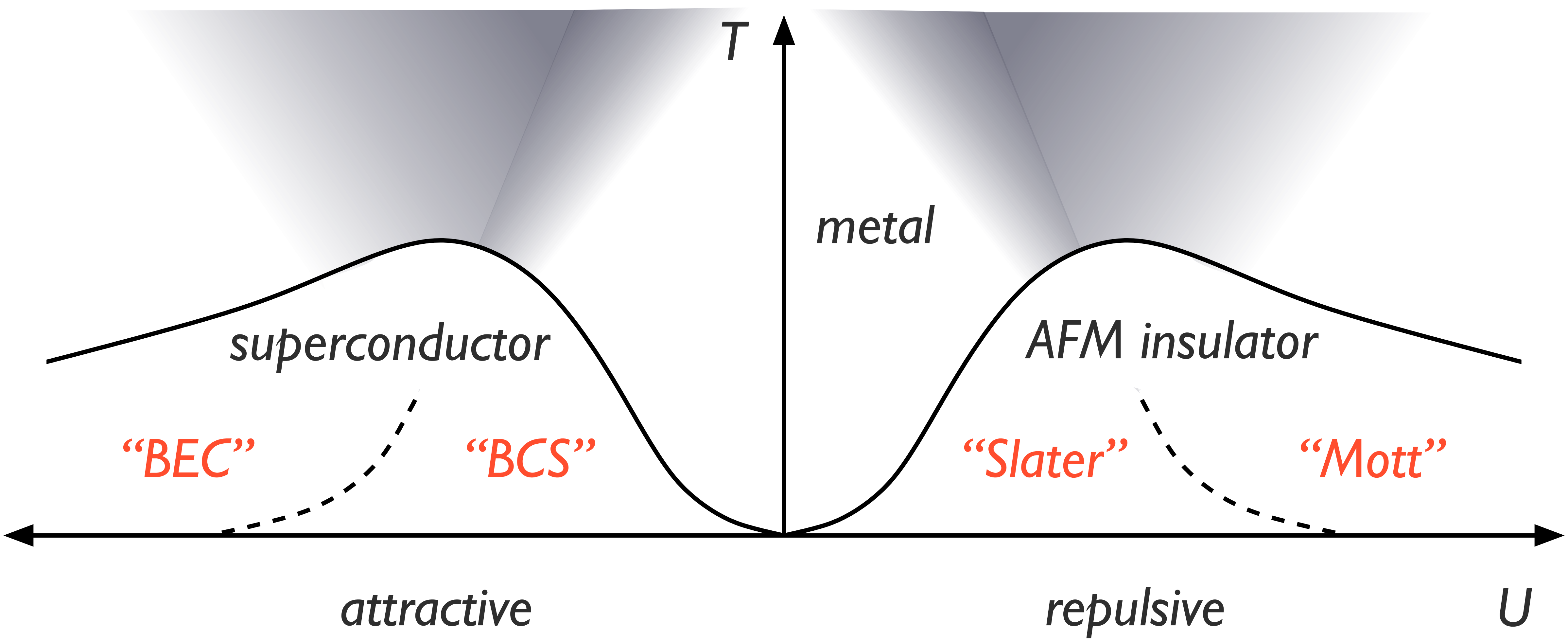

Cluster extension

- Low-dimensional systems
- DMFT is exact in $d = \infty$ *Metzner & Vollhardt (1989)*
- Neglect of spatial fluctuations problematic in $d < 3$
- $d = 2$ Hubbard model is believed to describe the physics of high-*Tc* (cuprate) superconductors

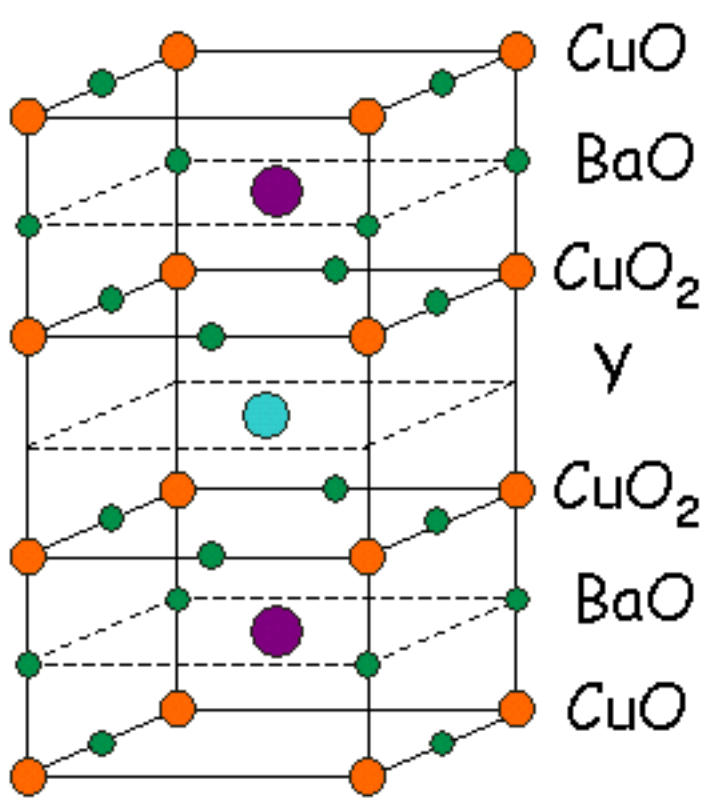

to describe the physics of the cuprates, we need a cluster extension of DMFT, with at least 4 sites

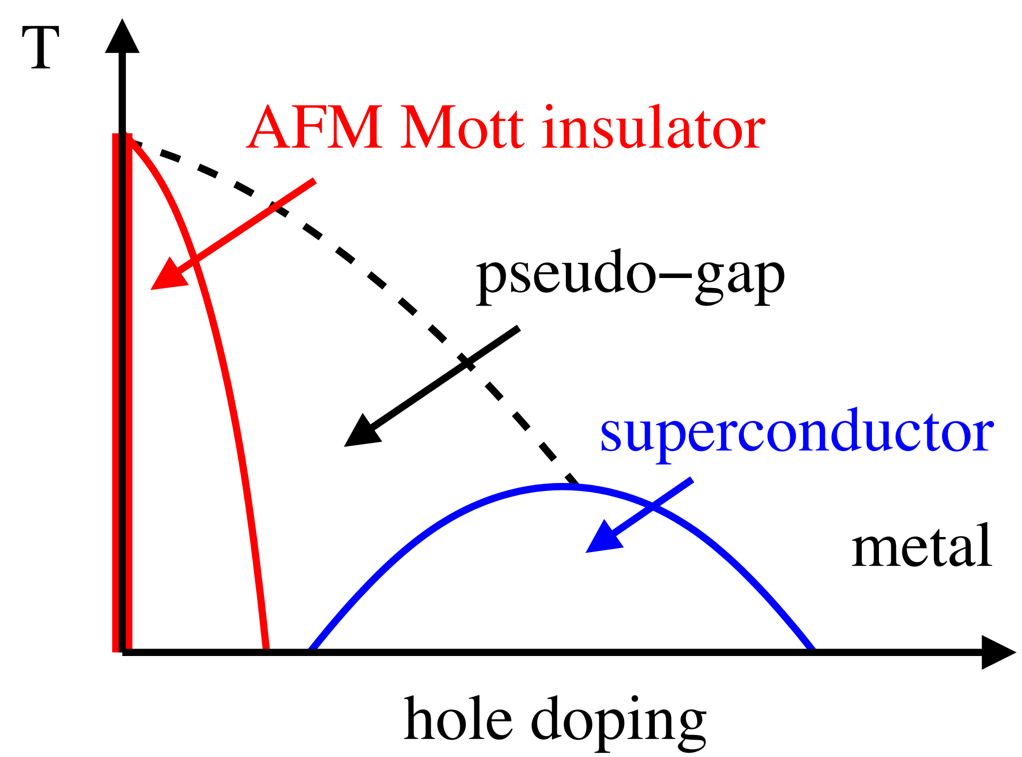

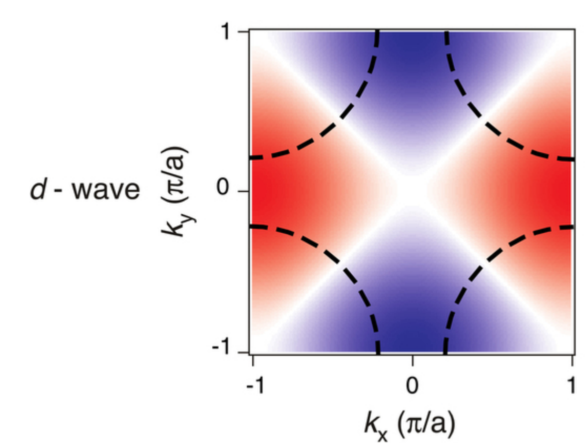

Cluster extension

- Low-dimensional systems
- Cluster DMFT self-consistently embeds a cluster of N_c sites into a fermionic bath *Hettler, Prushke, Krishnamurthy & Jarrell (1998)*
- If cluster is periodized: coarse-graining of the momentum-dependence

$$\Sigma(k,\omega) = \sum_a \phi_a(k)\Sigma_a(\omega)$$

- "Tiling" of the Brillouin zone

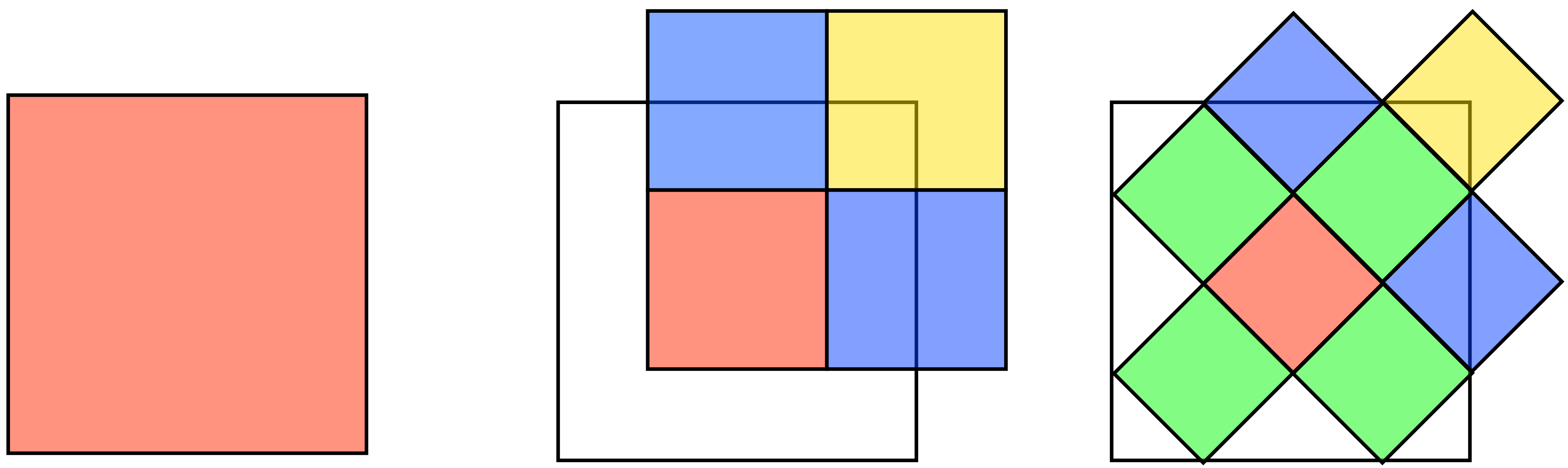

Cluster extension

- Dynamical cluster approach: mapping to an impurity cluster

  Hettler et al. (1998)

lattice model

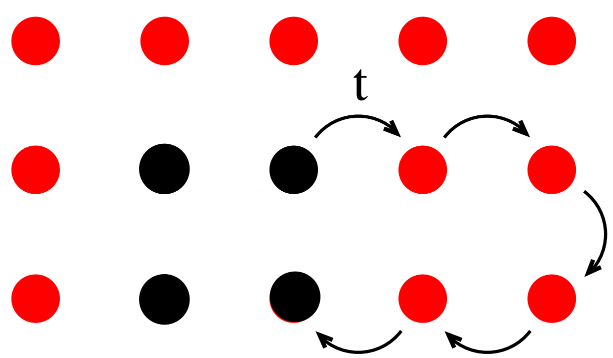

cluster impurity model

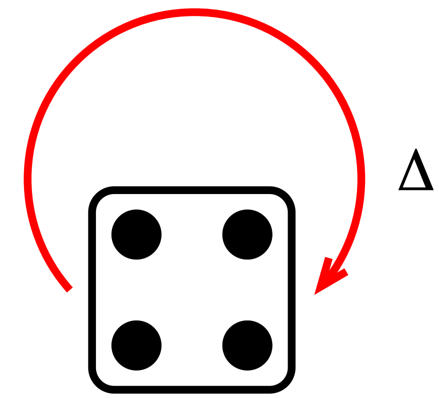

DMFT self-consistency

$$G_K^{\tilde{k}-\mathrm{av}}(i\omega_n) \Rightarrow S_{\mathrm{imp}}[\Delta_K(i\omega_n)]$$

$$G_K^{\tilde{k}\text{-av}} \equiv G_K^{\mathrm{imp}}$$

K-patch average

cluster solver

$$\Sigma_{K+\tilde{k}}^{\mathrm{latt}} \equiv \Sigma_K^{\mathrm{imp}}$$

$$G_k^{\mathrm{latt}} = \frac{1}{i\partial_t + \mu - \epsilon_k - \Sigma_k^{\mathrm{latt}}} \Leftarrow G_K^{\mathrm{imp}}(i\omega_n), \Sigma_K^{\mathrm{imp}}(i\omega_n)$$

DMFT approximation

Cluster extension

- Equilibrium DMFT phase diagram (half-filling)
- Paramagnetic calculation: Metal - Mott insulator transition at low *T*
- Smooth crossover at high *T*

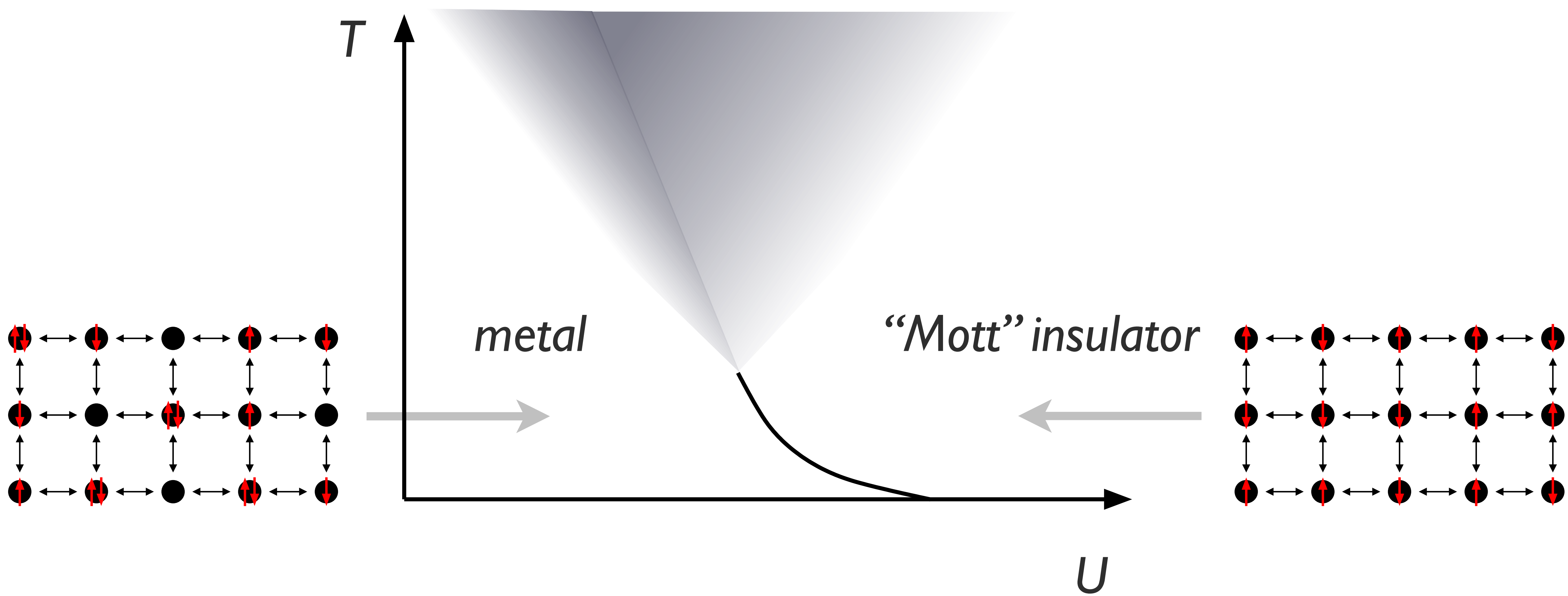

Cluster extension

- Equilibrium DMFT phase diagram (half-filling)
- Paramagnetic calculation: Metal - Mott insulator transition at low *T*
- Smooth crossover at high *T*

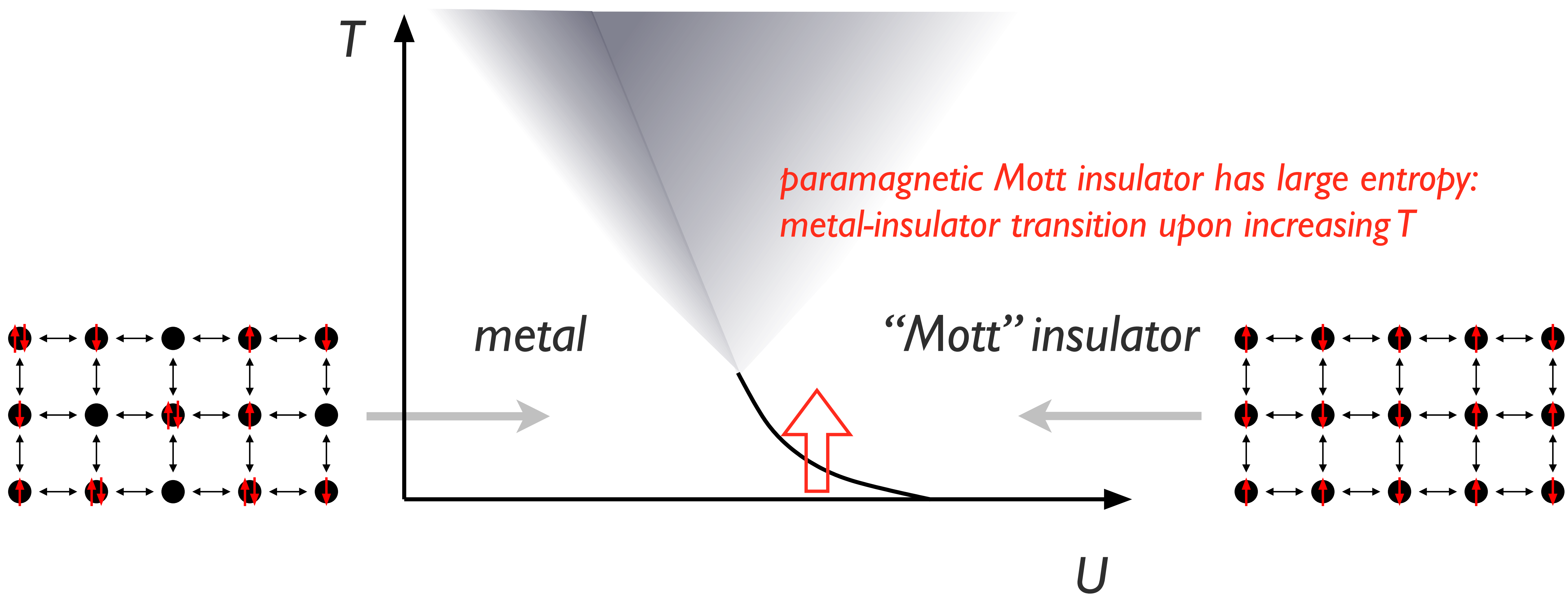

Cluster extension

- Equilibrium cluster DMFT phase diagram (half-filling)
- Paramagnetic calculation: Metal - Mott insulator transition at low *T*
- Smooth crossover at high *T*

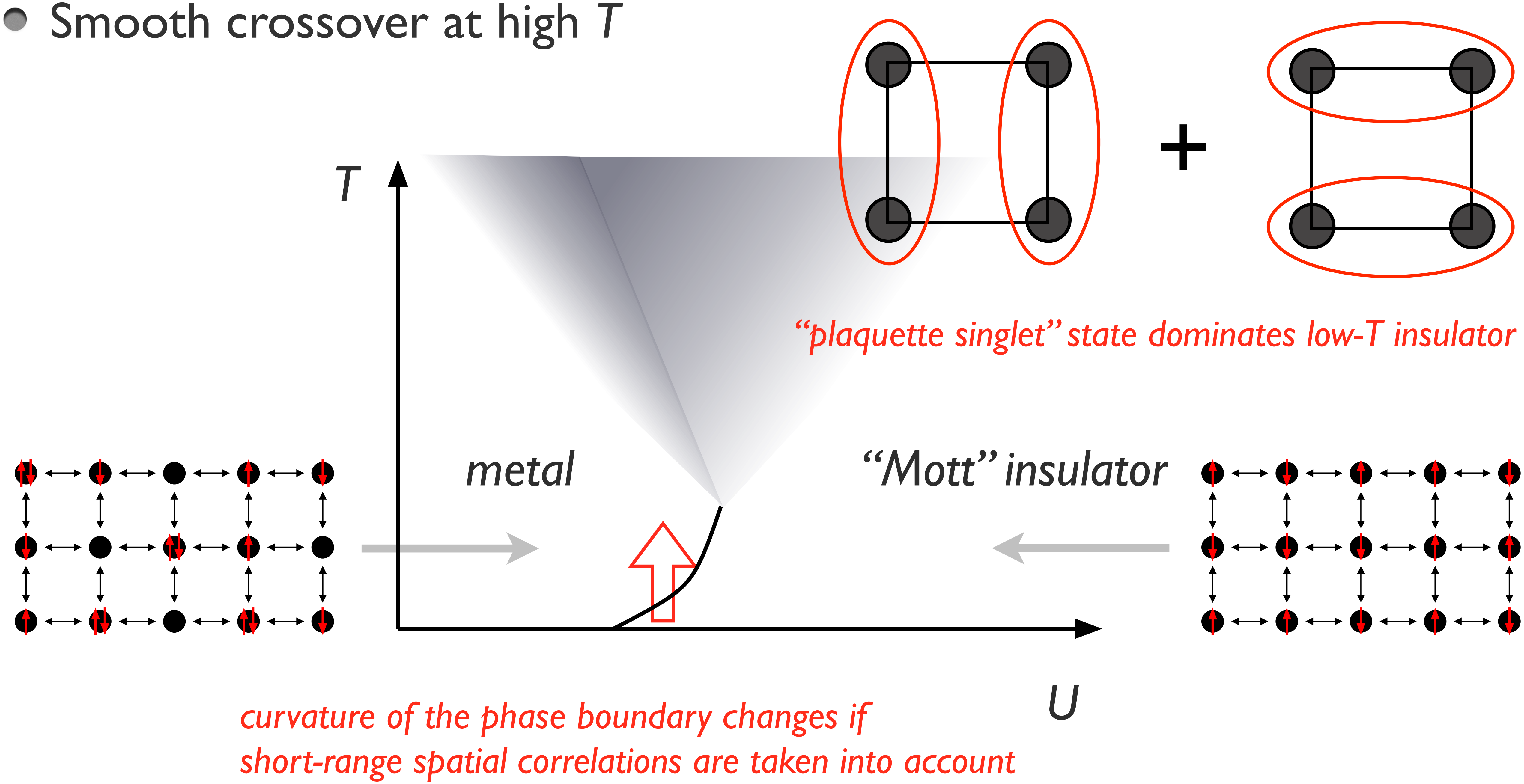

Nonequilibrium extension

- Kadanoff-Baym contour
- Initial state described by the density matrix $\rho(0) = \frac{1}{Z} e^{-\beta H(0)}$
- State at time *t* described by $\rho(t) = U(t,0)\,\rho(0)\,U(0,t)$

$$U(t,t') = \begin{cases} \mathcal{T} \exp\left(-i \int_{t'}^{t} d\bar{t}\, H(\bar{t})\right) & t > t' \\ \tilde{\mathcal{T}} \exp\left(-i \int_{t'}^{t} d\bar{t}\, H(\bar{t})\right) & t < t' \end{cases}$$

- Time dependent expectation value of observable $\mathcal{O}$

$$\langle \mathcal{O}(t) \rangle = \mathrm{Tr}\left[\rho(t)\mathcal{O}\right] = \mathrm{Tr}\left[U(t,0)\rho(0)U(0,t)\mathcal{O}\right]$$

Nonequilibrium extension

- Kadanoff-Baym contour
- Express $\rho(0)$ as time-propagation along an imaginary time branch

$$\langle\mathcal{O}\rangle(t) = \mathrm{Tr}\left[\frac{1}{Z}e^{-\beta H(0)}U(0,t)\mathcal{O}U(t,0)\right]$$

$$= \mathrm{Tr}\left[\frac{1}{Z}\left(\mathcal{T}_\tau e^{-\int_0^\beta d\tau H(\tau)}\right)\left(\tilde{\mathcal{T}} e^{i\int_0^t ds H(s)}\right)\mathcal{O}\left(\mathcal{T} e^{-i\int_0^t ds H(s)}\right)\right]$$

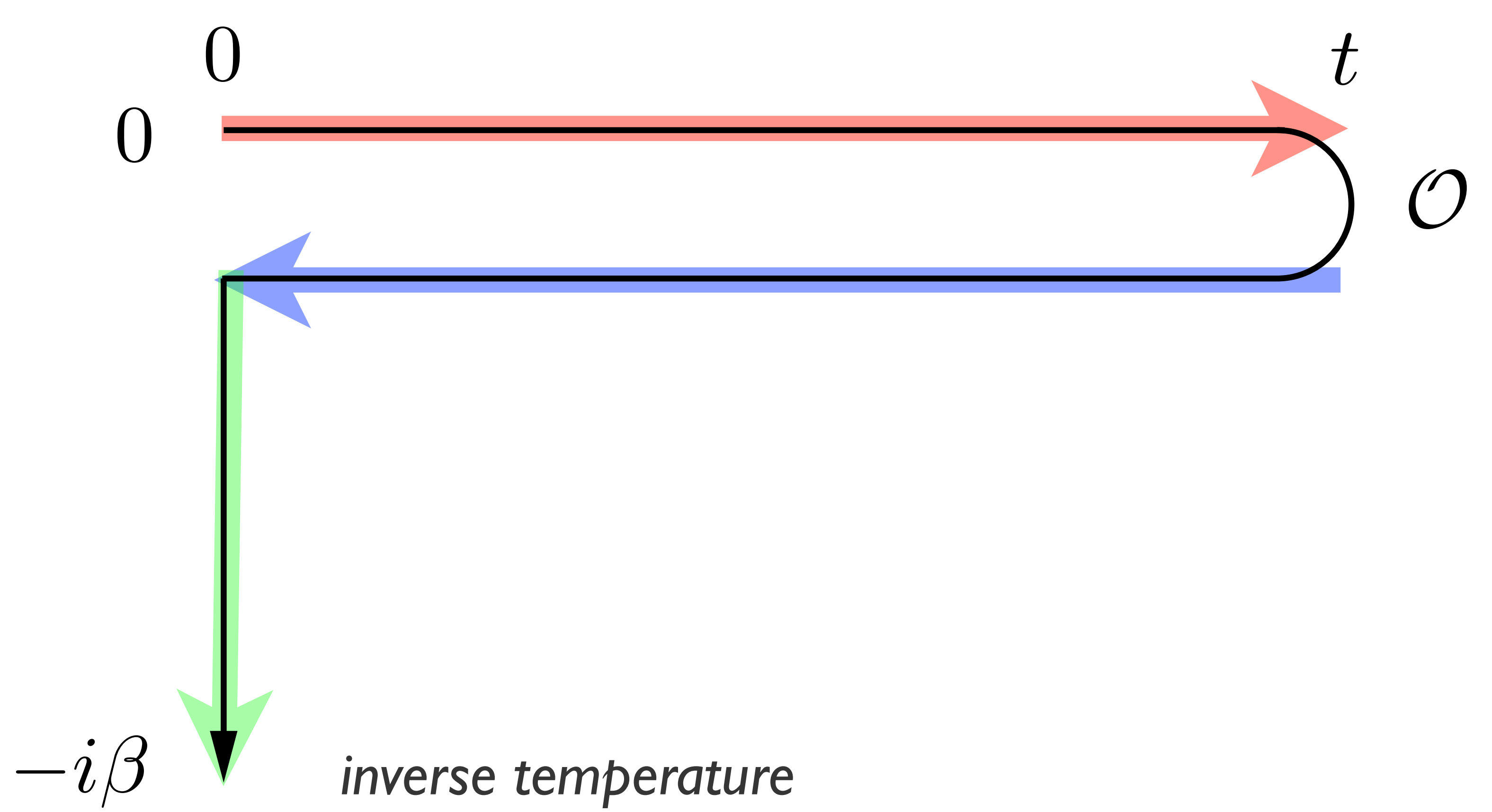

Nonequilibrium extension

- Kadanoff-Baym contour
- Define contour ordering $\mathcal{T}_\mathcal{C}$ on the contour $\mathcal{C} : 0 \to t \to 0 \to -i\beta$

$$\langle \mathcal{O}(t) \rangle = \frac{1}{Z} \mathrm{Tr}\Big[\mathcal{T}_\mathcal{C} \, e^{-i \int_\mathcal{C} ds \, H(s)} \mathcal{O}(t) \Big]$$

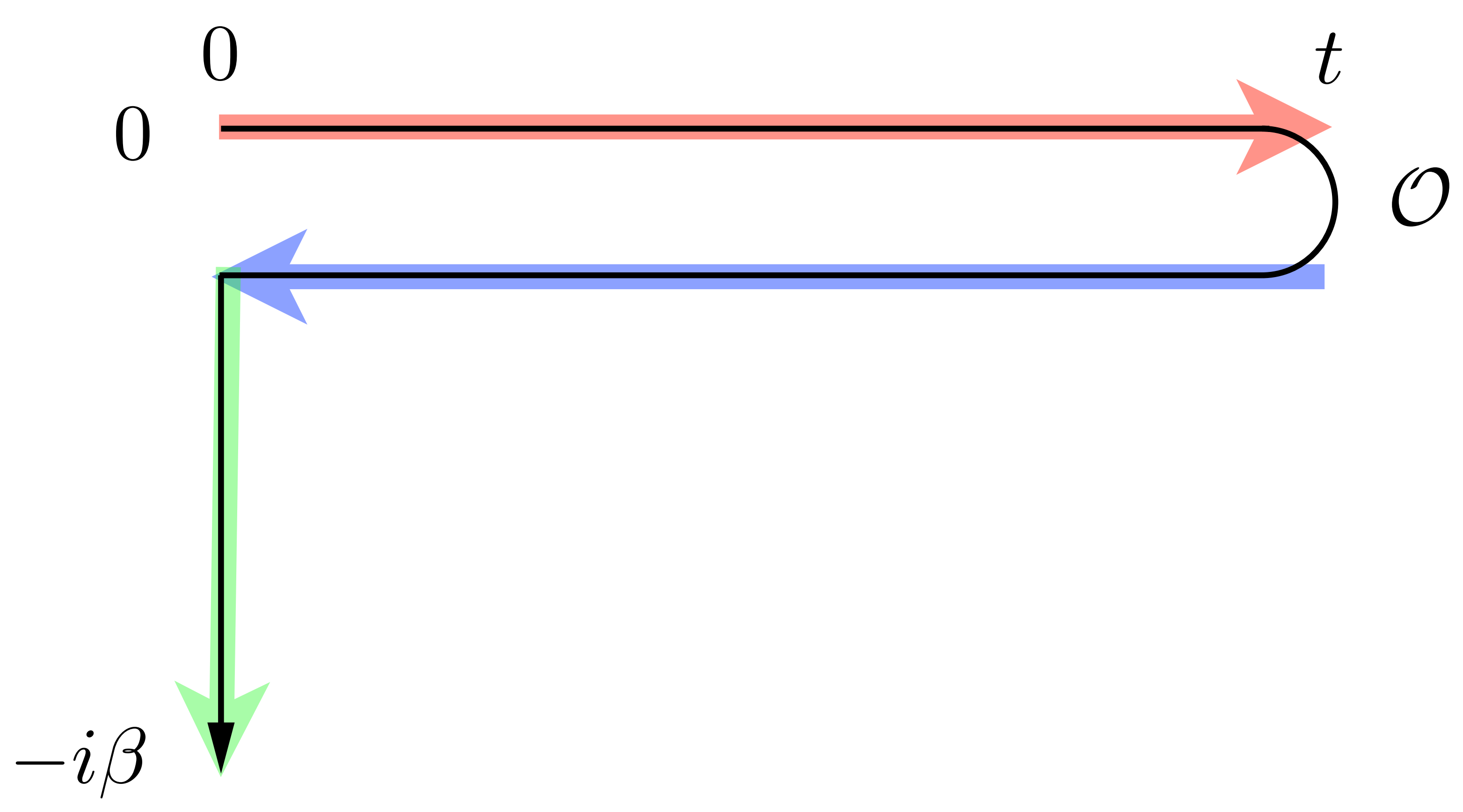

Nonequilibrium extension

- Kadanoff-Baym contour
- Define contour ordering $\mathcal{T}_{\mathcal{C}}$ on the contour $\mathcal{C} : 0 \to t \to 0 \to -i\beta$

$$\langle \mathcal{O}(t) \rangle = \frac{1}{Z} \mathrm{Tr} \left[\mathcal{T}_{\mathcal{C}}\, e^{-i \int_{\mathcal{C}} ds\, H(s)} \mathcal{O}(t) \right]$$

- Contour-ordered formalism can also be applied to 2-point functions

$$\langle \mathcal{T}_{\mathcal{C}}\, \mathcal{A}(t) \mathcal{B}(t') \rangle \equiv \frac{1}{Z} \mathrm{Tr} \left[\mathcal{T}_{\mathcal{C}}\, e^{-i \int_{\mathcal{C}} ds\, H(s)} \mathcal{A}(t) \mathcal{B}(t') \right]$$

- Particularly relevant: Green's function

$$G(t, t') \quad \equiv -i \langle \mathcal{T}_{\mathcal{C}}\, d(t)\, d^\dagger(t') \rangle$$

Nonequilibrium extension

- Kadanoff-Baym contour
- Due to the 3 branches, the Green's function has 9 components

$$G(t,t') \equiv G_{ij}(t,t'), \quad t \in \mathcal{C}_i, t' \in \mathcal{C}_j, \quad i,j = 1,2,3$$

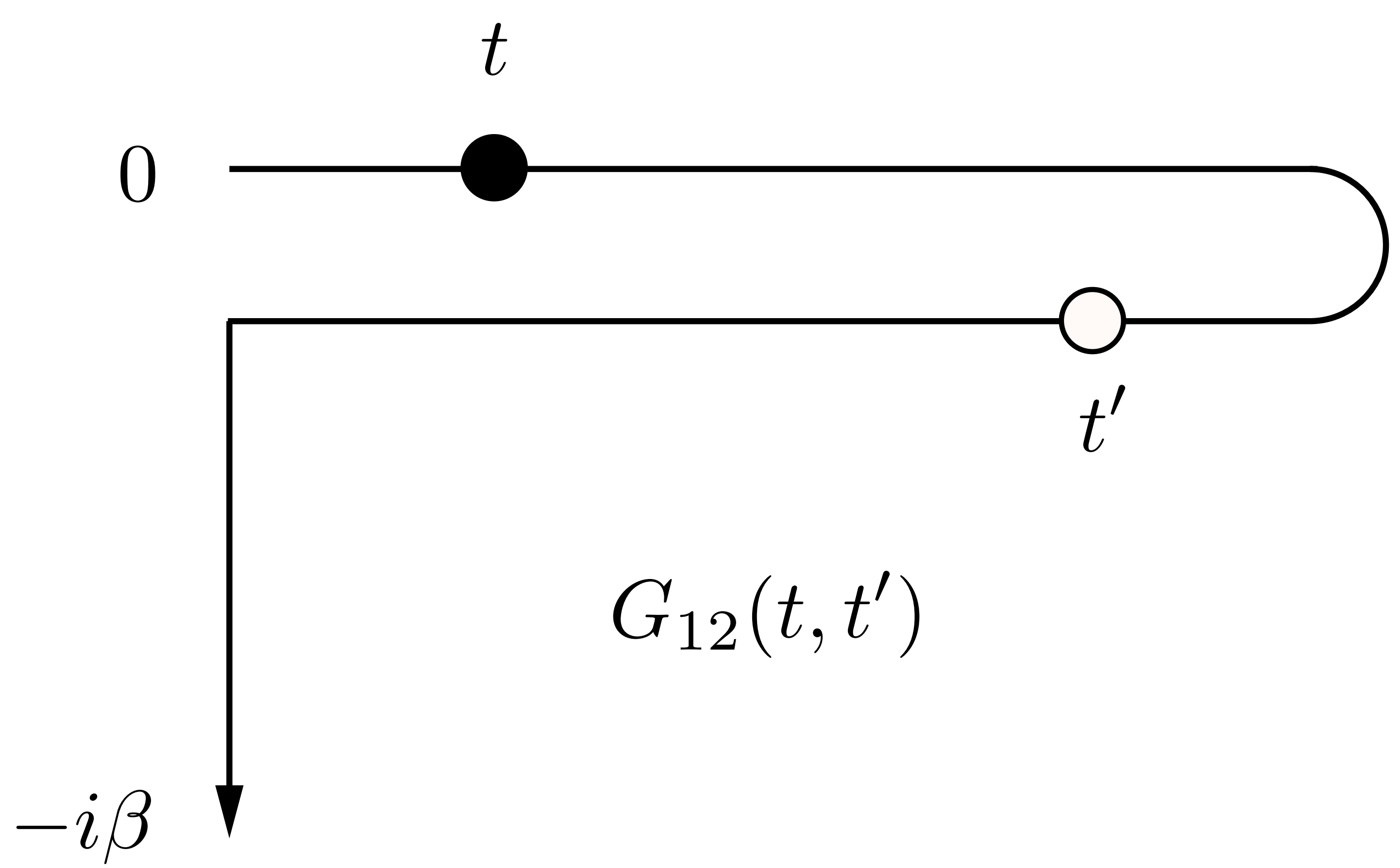

Nonequilibrium extension

- Kadanoff-Baym contour
- Due to the 3 branches, the Green's function has 9 components

$$G(t,t') \equiv G_{ij}(t,t'), \quad t \in \mathcal{C}_i, t' \in \mathcal{C}_j, \quad i,j = 1,2,3$$

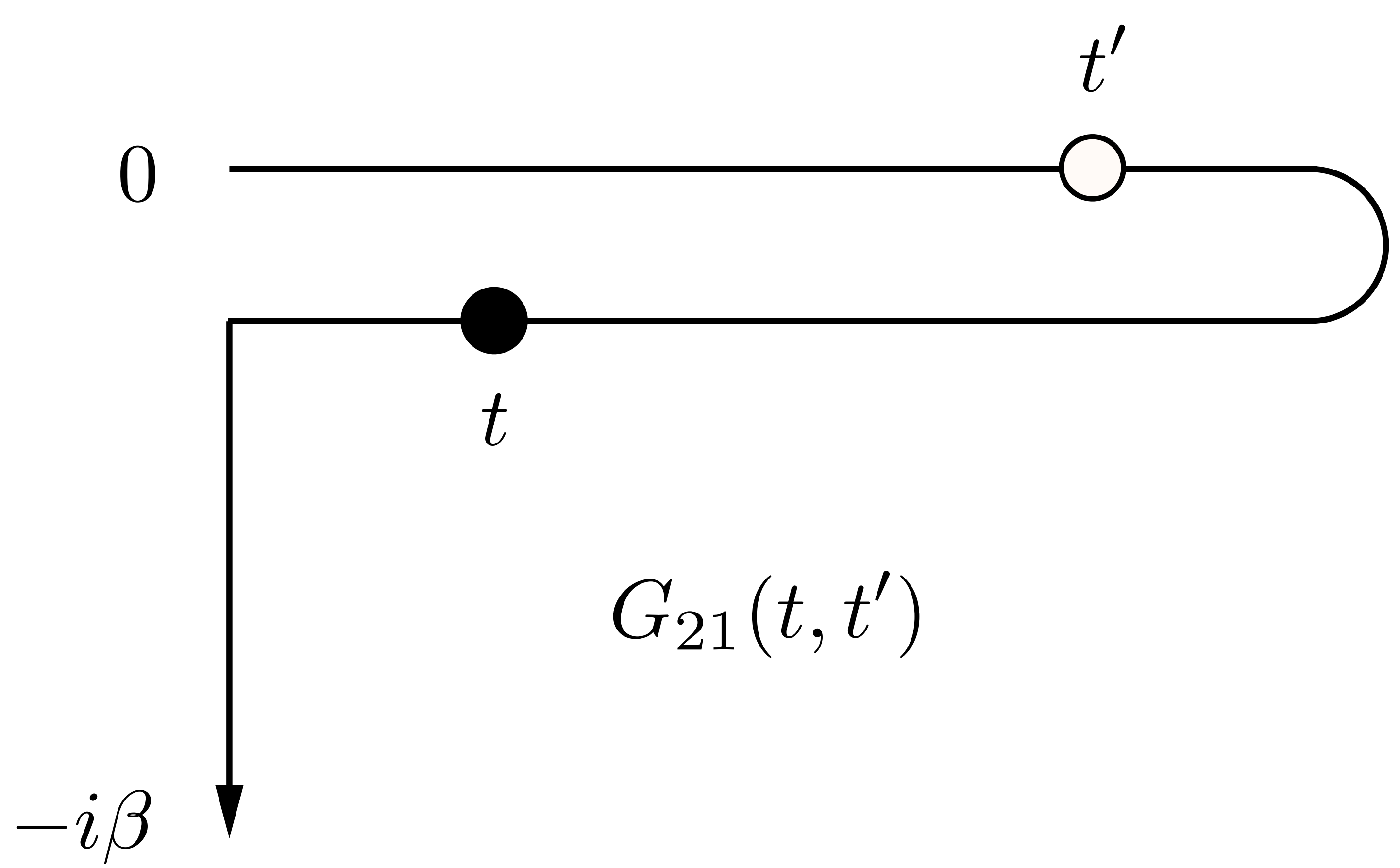

Nonequilibrium extension

- Nonequilibrium DMFT: Solve DMFT equations on the Kadanoff-Baym contour $\mathcal{C}$ *Freericks et al. (2006)*

lattice model *impurity model*

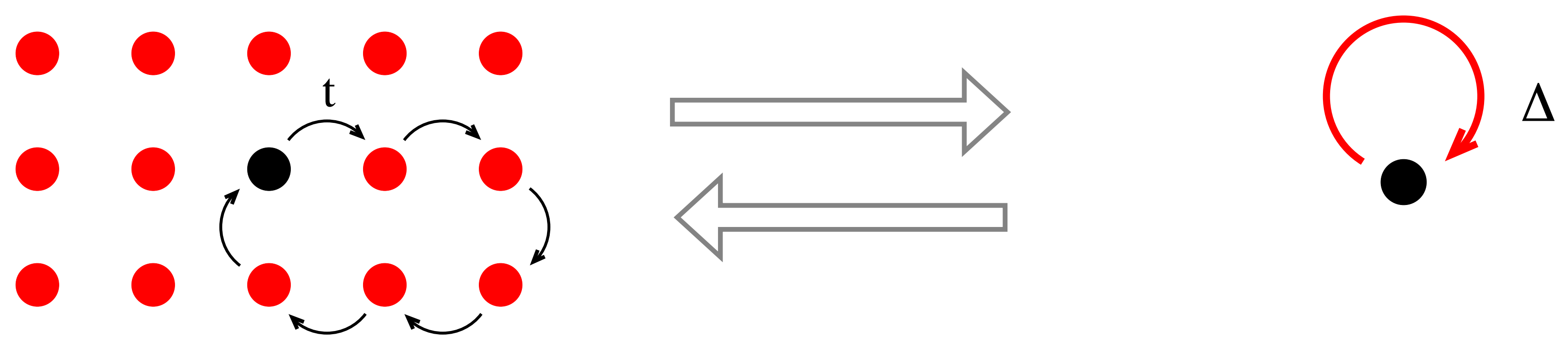

DMFT self-consistency

$$G_{\text{loc}}^{\text{latt}}(t,t') \Longrightarrow S_{\text{imp}}[\Delta(t,t')]$$

$$G_{\text{loc}}^{\text{latt}} \equiv G_{\text{imp}}$$

momentum average (↑) *impurity solver* (↓)

$$\Sigma_k^{\text{latt}} \equiv \Sigma_{\text{imp}}$$

$$G_k^{\text{latt}} = \frac{1}{i\partial_t + \mu - \epsilon_k - \Sigma_k^{\text{latt}}} \Longleftarrow G_{\text{imp}}(t,t'), \Sigma_{\text{imp}}(t,t')$$

DMFT approximation

Nonequilibrium extension

- Nonequilibrium DMFT: Solve DMFT equations on the Kadanoff-Baym contour $\mathcal{C}$ *Tsuji et al. (2014)*

lattice model *cluster impurity model*

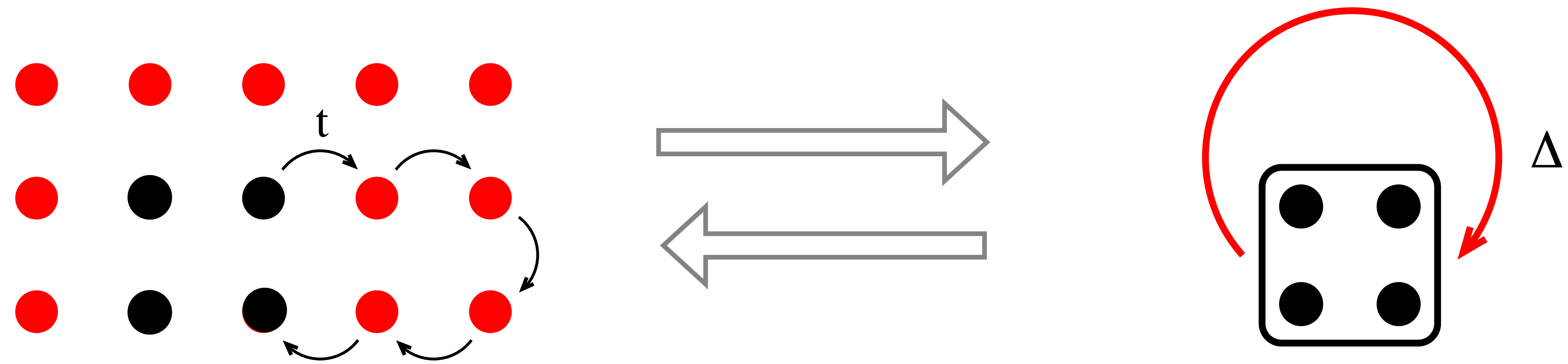

DMFT self-consistency

$$G_K^{\tilde{k}\text{-av}}(t,t') \Longrightarrow S_{\text{imp}}[\Delta_K(t,t')]$$

$$G_K^{\tilde{k}\text{-av}} \equiv G_K^{\text{imp}}$$

K-patch average *cluster solver*

$$\Sigma_{K+\tilde{k}}^{\text{latt}} \equiv \Sigma_K^{\text{imp}}$$

$$G_k^{\text{latt}} = \frac{1}{i\partial_t + \mu - \epsilon_k - \Sigma_k^{\text{latt}}} \Longleftarrow G_K^{\text{imp}}(t,t'), \Sigma_K^{\text{imp}}(t,t')$$

DMFT approximation

Nonequilibrium extension

- Nonequilibrium DMFT: Solve DMFT equations on the Kadanoff-Baym contour $\mathcal{C}$
- Nonequilibrium Anderson impurity model

$$S_{\mathrm{imp}} = -i \int_{\mathcal{C}} dt\, H_{\mathrm{loc}}(t) - i \sum_{\sigma} \int_{\mathcal{C}} dt\, dt'\, d_{\sigma}^{\dagger}(t) \Delta(t,t') d_{\sigma}(t')$$

⇧ *interaction and chemical potential terms* ⇧ *contour hybridization function*

- Hybridization function is equivalent to "Weiss" Green's function

$$\mathcal{G}_0(t,t') = (i\partial_t + \mu(t))\delta_{\mathcal{C}}(t,t') - \Delta(t,t')$$

Nonequilibrium extension

- Nonequilibrium DMFT: Solve DMFT equations on the Kadanoff-Baym contour $\mathcal{C}$

- Nonequilibrium Anderson impurity model

$$S_{\rm imp} = -i \int_{\mathcal{C}} dt\, H_{\rm loc}(t) - i \sum_\sigma \int_{\mathcal{C}} dt\, dt'\, d^\dagger_\sigma(t) \Delta(t,t') d_\sigma(t')$$

⇧ *interaction and chemical potential terms* ⇧ *contour hybridization function*

- Impurity Green's function

$$G_{\rm imp}(t,t') = -i \langle \mathcal{T}_{\mathcal{C}}\, d(t) d^\dagger(t') \rangle_{S_{\rm imp}}$$

$$\langle \cdots \rangle_{S_{\rm imp}} = \frac{\mathrm{Tr}[\mathcal{T}_{\mathcal{C}}\, \exp(S_{\rm imp}) \cdots]}{\mathrm{Tr}[\mathcal{T}_{\mathcal{C}}\, \exp(S_{\rm imp})]}$$

Nonequilibrium extension

- Impurity solver: weak-coupling continuous-time QMC *Werner et al. (2009)*

$$\langle\mathcal{O}\rangle(t) = Tr\left[\frac{1}{Z}e^{-\beta H}U(0,t)\mathcal{O}U(t,0)\right]$$

$$= Tr\left[\frac{1}{Z}e^{-\beta H_0}\left(T_\tau e^{-\int_0^\beta d\tau H_I(\tau)}\right)\left(\tilde{T}e^{i\int_0^t dsH_I(s)}\right)\mathcal{O}(t)\left(Te^{-i\int_0^t dsH_I(s)}\right)\right]$$

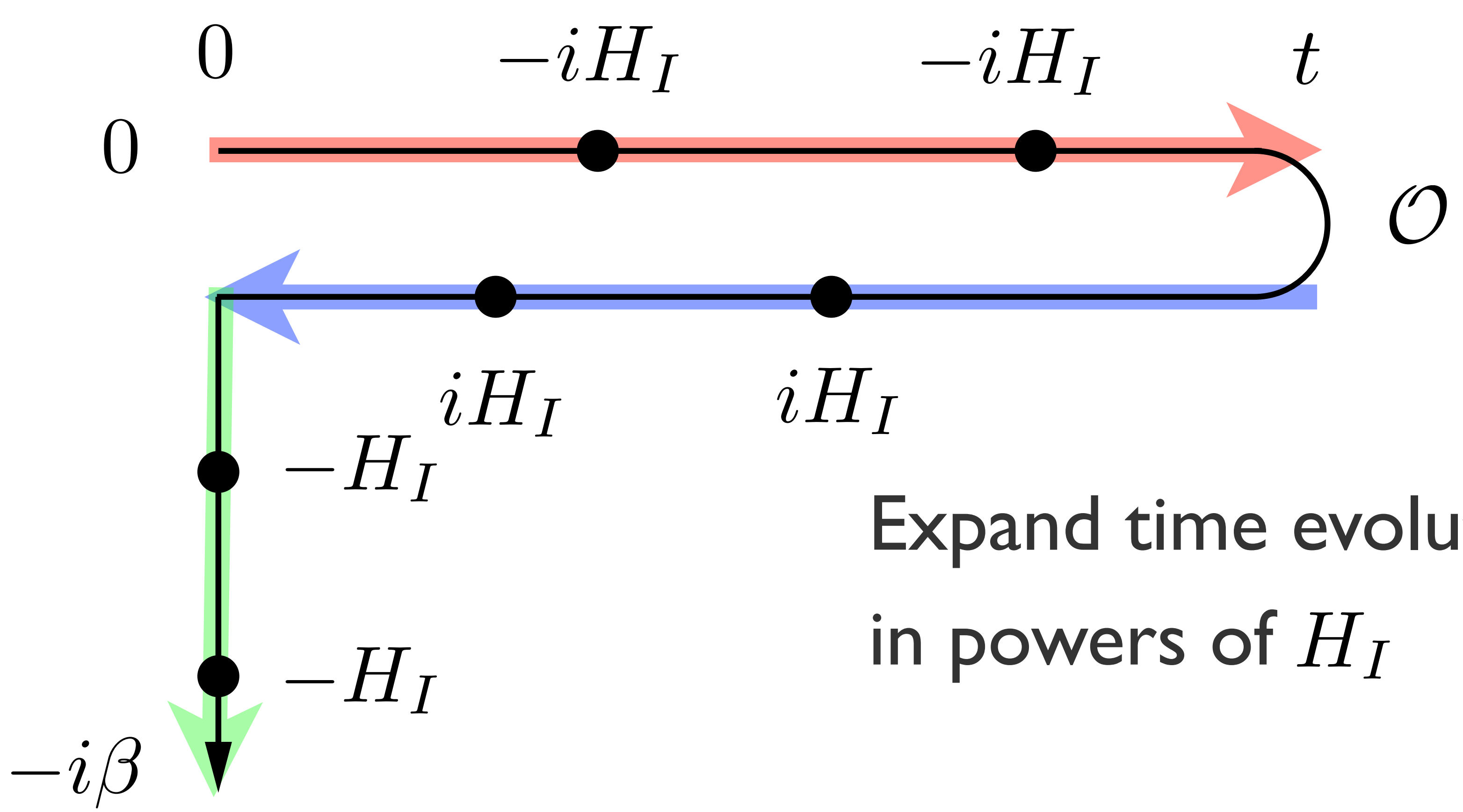

Expand time evolution operators in powers of H_I

Nonequilibrium extension

- Impurity solver: weak-coupling continuous-time QMC *Werner et al. (2009)*

$$\langle\mathcal{O}\rangle(t) = Tr\Big[\frac{1}{Z}e^{-\beta H}U(0,t)\mathcal{O}U(t,0)\Big]$$

$$= Tr\Big[\frac{1}{Z}e^{-\beta H_0}\Big(T_\tau e^{-\int_0^\beta d\tau H_I(\tau)}\Big)\Big(\tilde{T}e^{i\int_0^t dsH_I(s)}\Big)\mathcal{O}(t)\Big(Te^{-i\int_0^t dsH_I(s)}\Big)\Big]$$

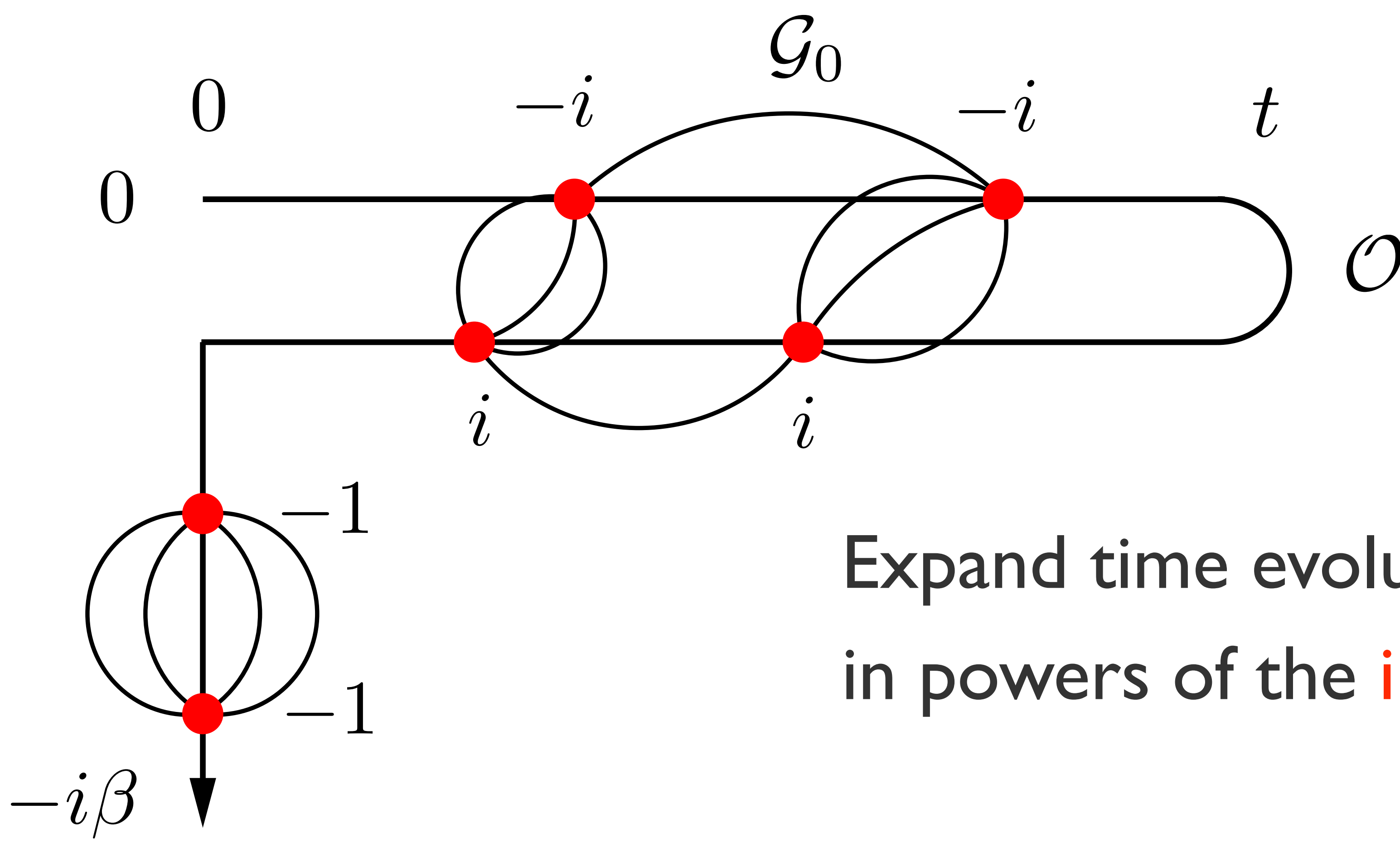

Expand time evolution operators in powers of the interaction term

Nonequilibrium extension

- Impurity solver: weak-coupling continuous-time QMC *Werner et al. (2009)*

$$\langle \mathcal{O} \rangle(t) = Tr\Big[\frac{1}{Z}e^{-\beta H} U(0,t)\mathcal{O}U(t,0)\Big]$$

$$= Tr\Big[\frac{1}{Z}e^{-\beta H_0}\Big(T_\tau e^{-\int_0^\beta d\tau H_I(\tau)}\Big)\Big(\tilde{T}e^{i\int_0^t ds H_I(s)}\Big)\mathcal{O}(t)\Big(Te^{-i\int_0^t ds H_I(s)}\Big)\Big]$$

- Time evolution of double occupation after a quench from *U*=0

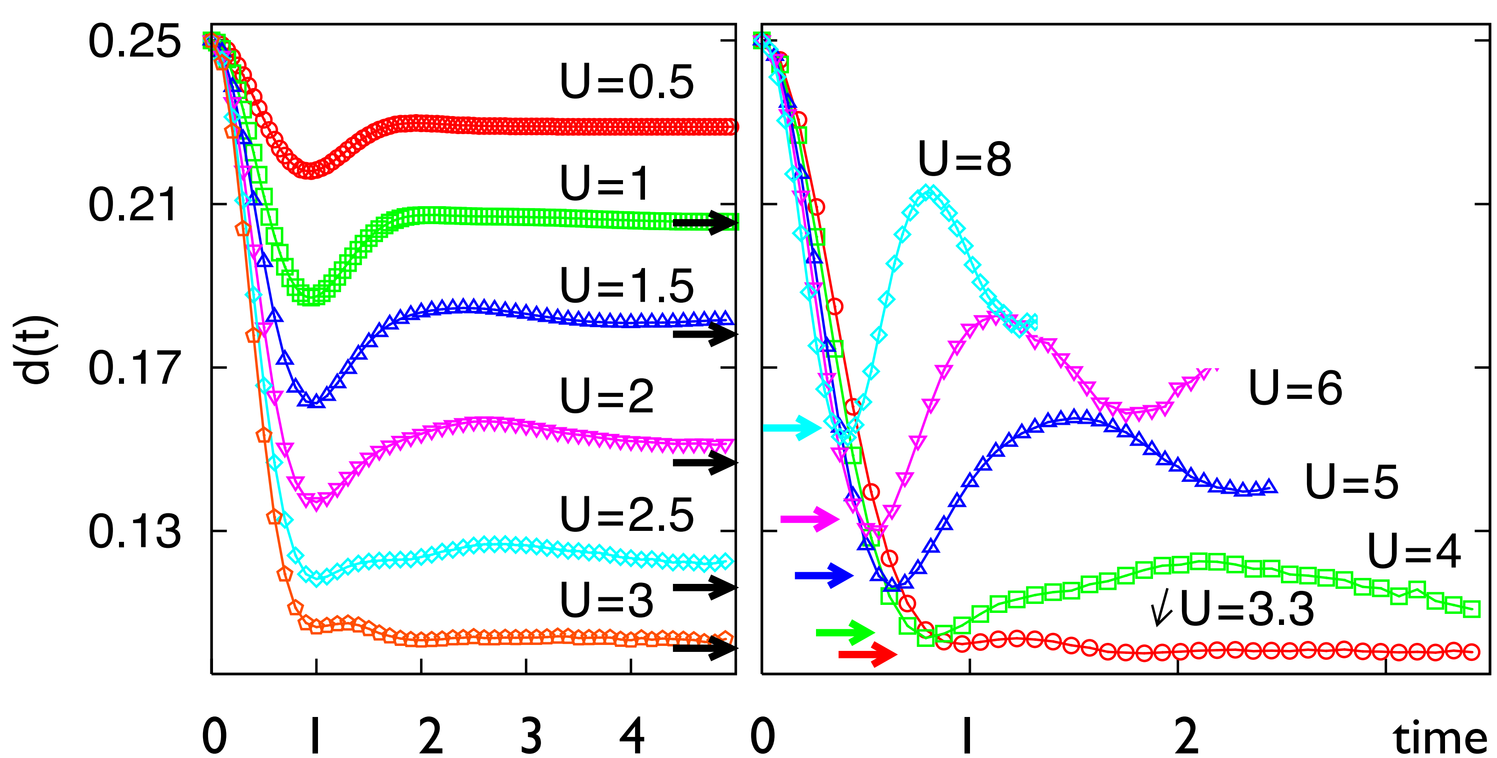

intermediate/strong correlation regime:

can reach a few inverse hopping times

Eckstein et al. (2009)

Nonequilibrium extension

- Impurity solver: weak-coupling perturbation theory
- Generate a subset of all weak-coupling diagrams by approximating the self-energy
- Truncation at second order: *Iterated Perturbation Theory (IPT)*

$\Sigma_{\mathrm{imp}} =$

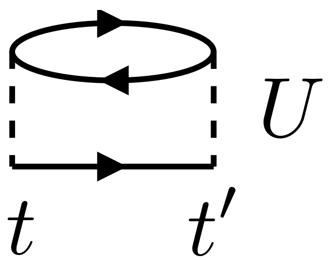

$$G_{\mathrm{imp}} = \mathcal{G}_0 + \mathcal{G}_0 \star \Sigma_{\mathrm{imp}} \star G_{\mathrm{imp}}$$

$G_{\mathrm{imp}} =$

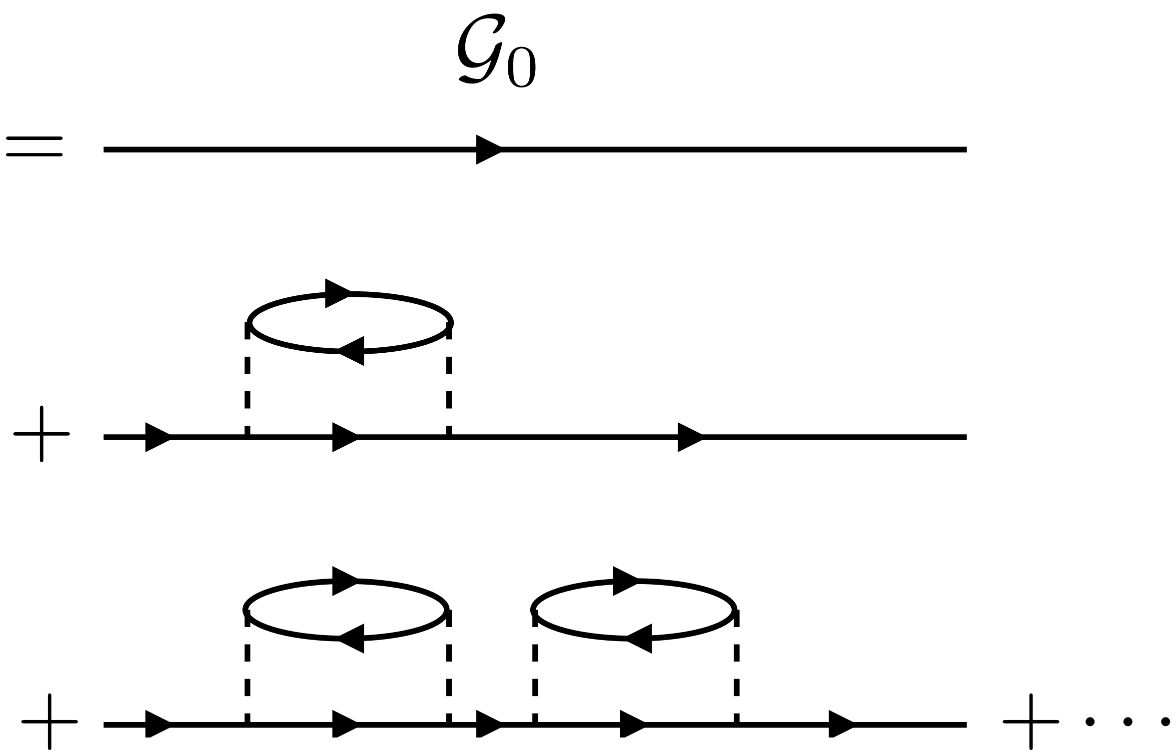

Nonequilibrium extension

- Impurity solver: weak-coupling perturbation theory
- Generate a subset of all weak-coupling diagrams by approximating the self-energy
- Boldified expansion: conserving, but not accurate

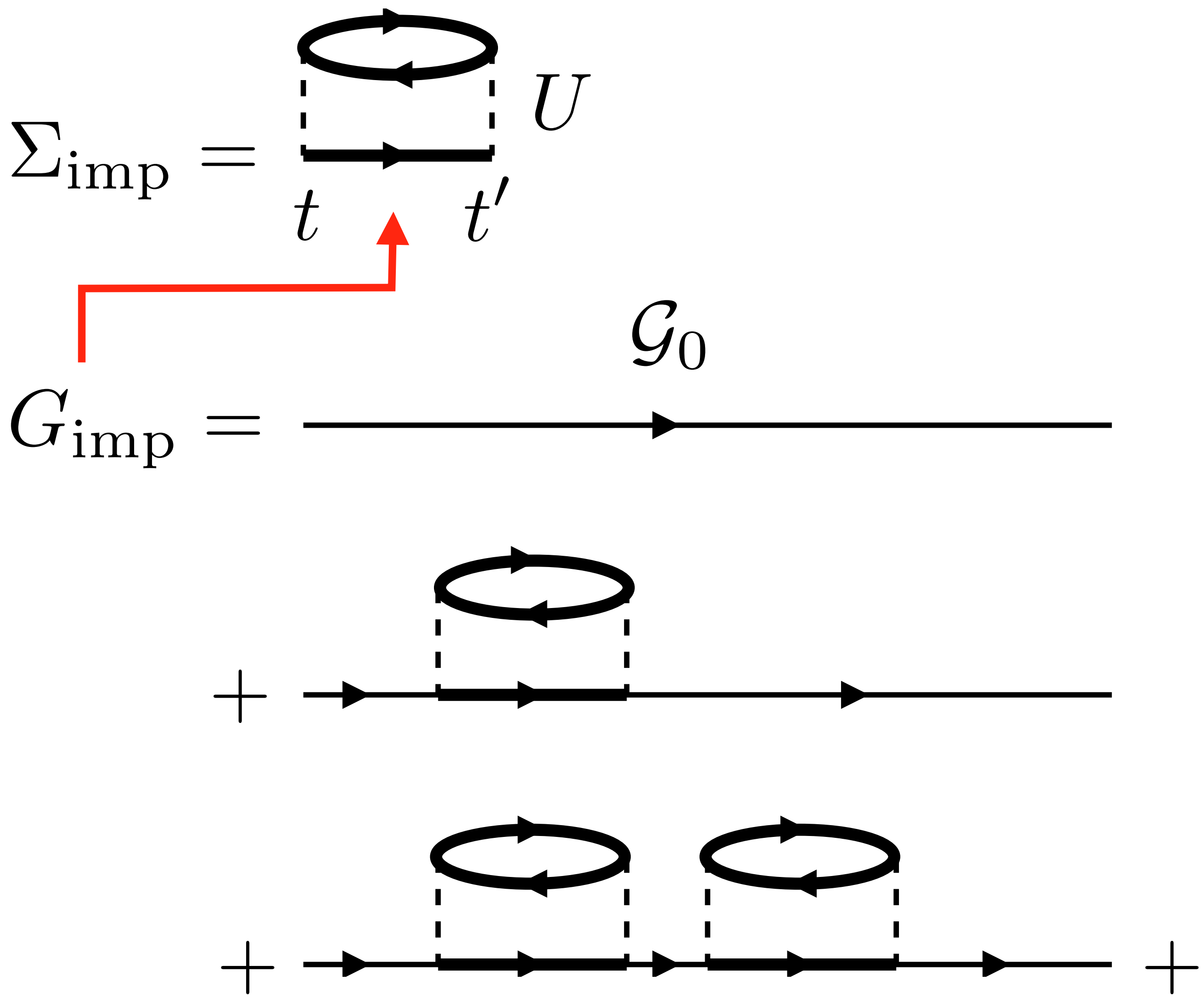

$$G_{\mathrm{imp}} = \mathcal{G}_0 + \mathcal{G}_0 \star \Sigma_{\mathrm{imp}} \star G_{\mathrm{imp}}$$

Nonequilibrium extension

- Impurity solver: weak-coupling perturbation theory
- Generate a subset of all weak-coupling diagrams by approximating the self-energy
- Boldified expansion: conserving, but not accurate *Eckstein et al. (2009)*

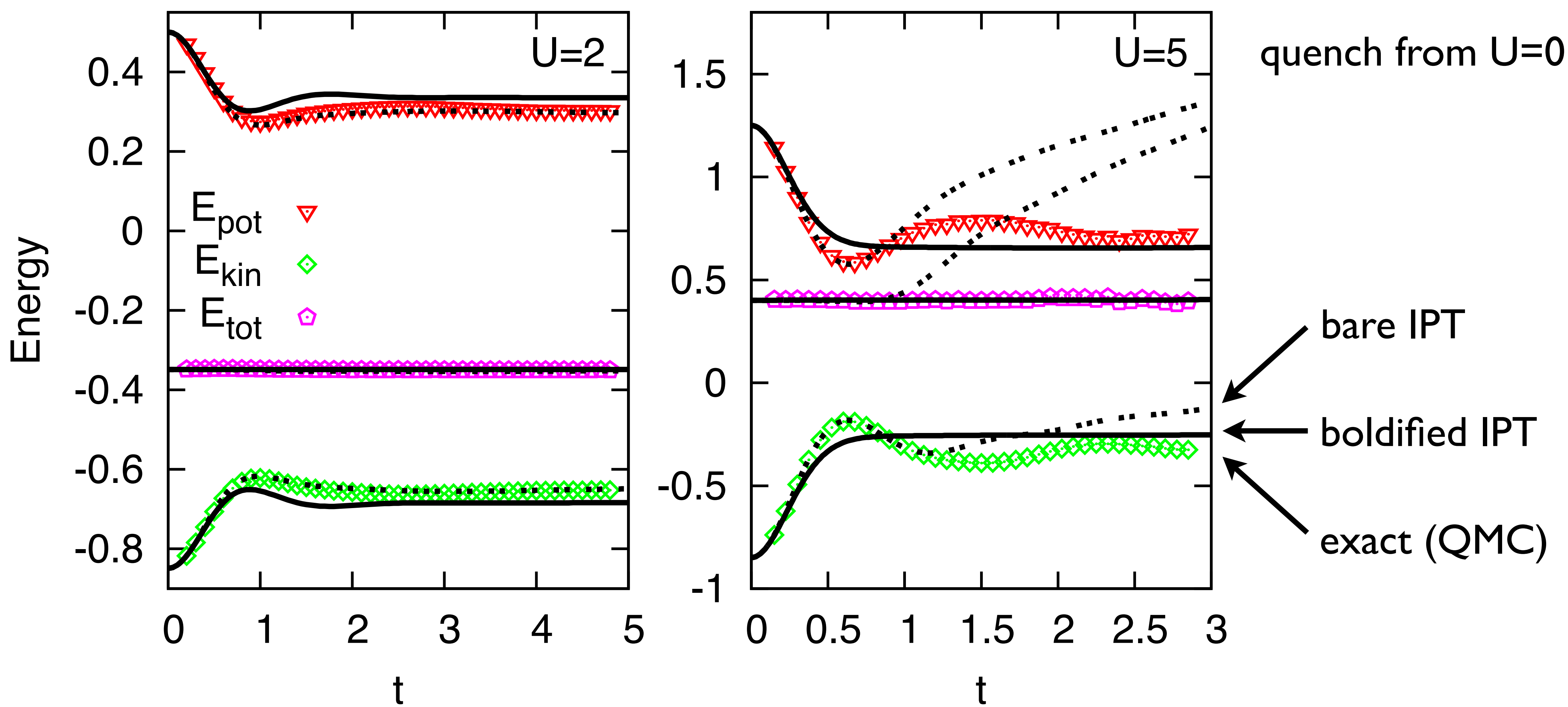

Nonequilibrium extension

- Impurity solver: Strong-coupling perturbation theory
- Introduce pseudo-particle propagators G_α for local states $\{0, \uparrow, \downarrow, \uparrow\downarrow\}$
- Approximate pseudo-particle self-energy

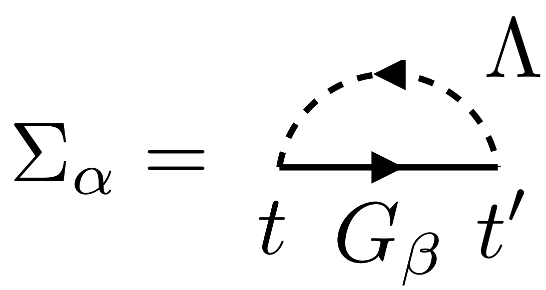

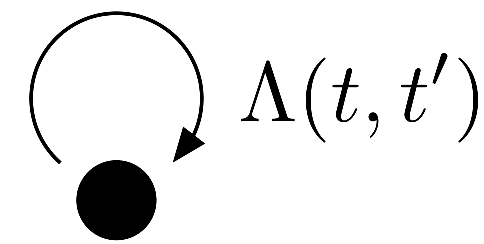

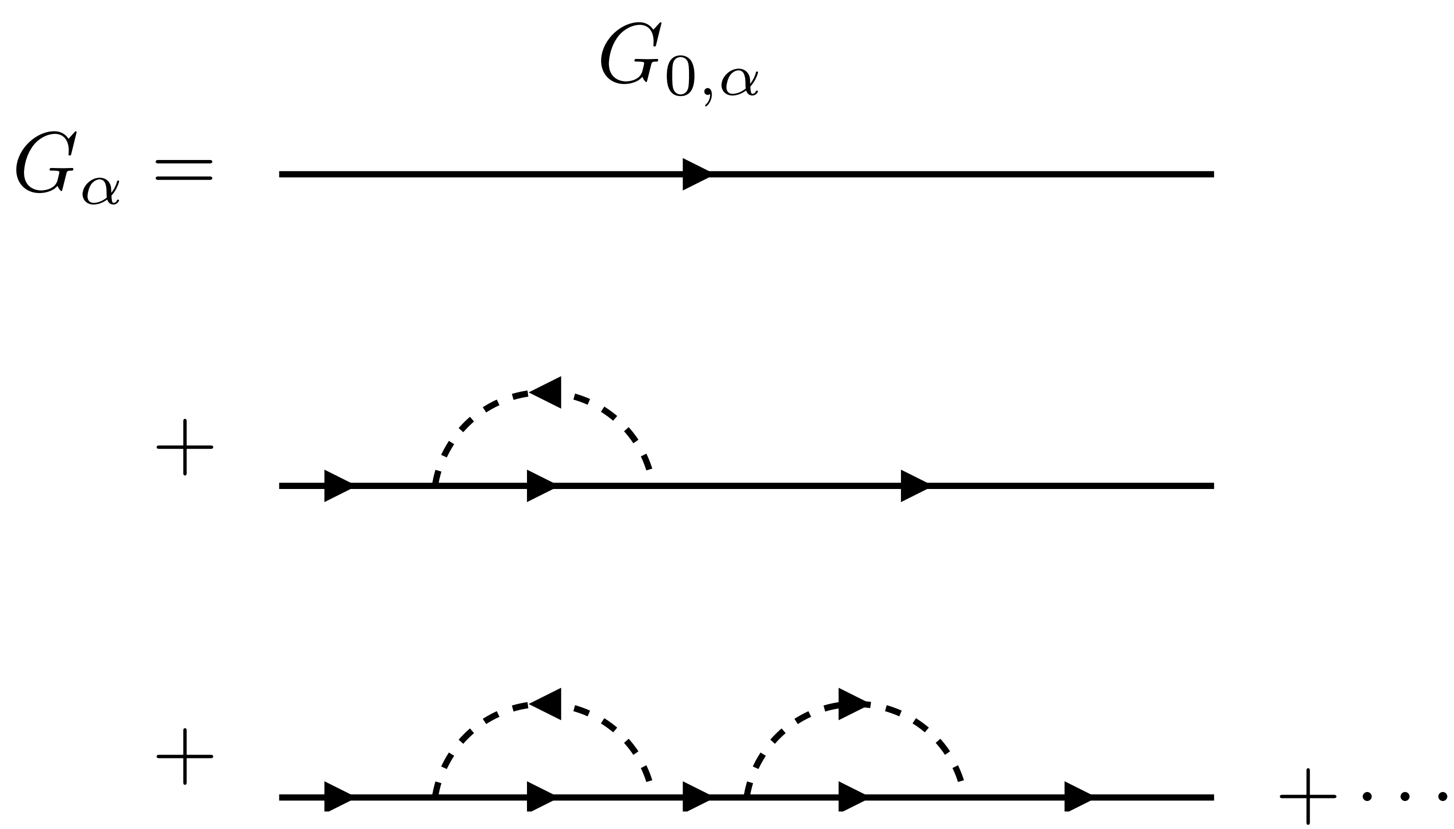

Non-crossing approximation (NCA)

Keiter & Kimball (2009)

Nonequilibrium extension

- Impurity solver: Strong-coupling perturbation theory
- Introduce pseudo-particle propagators G_α for local states $\{0, \uparrow, \downarrow, \uparrow\downarrow\}$
- Approximate pseudo-particle self-energy

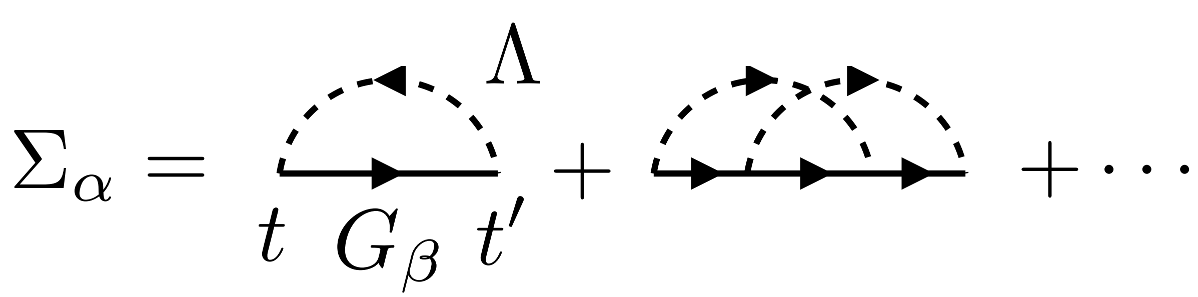

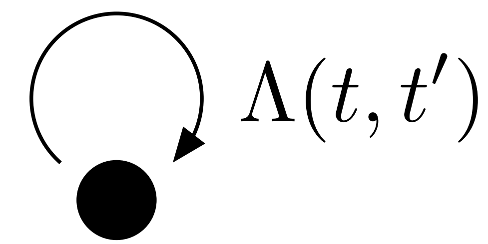

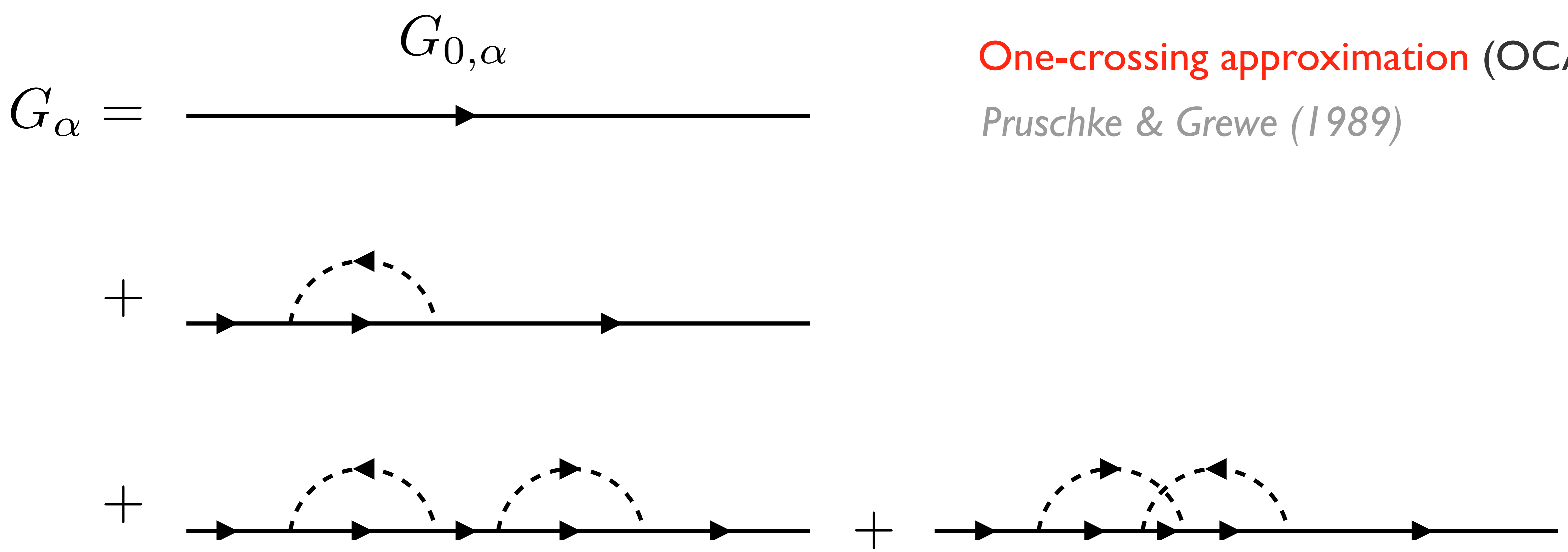

One-crossing approximation (OCA)

Pruschke & Grewe (1989)

Nonequilibrium extension

- Impurity solver: Strong-coupling perturbation theory
- Introduce pseudo-particle propagators G_α for local states $\{0, \uparrow, \downarrow, \uparrow\downarrow\}$
- Approximate pseudo-particle self-energy

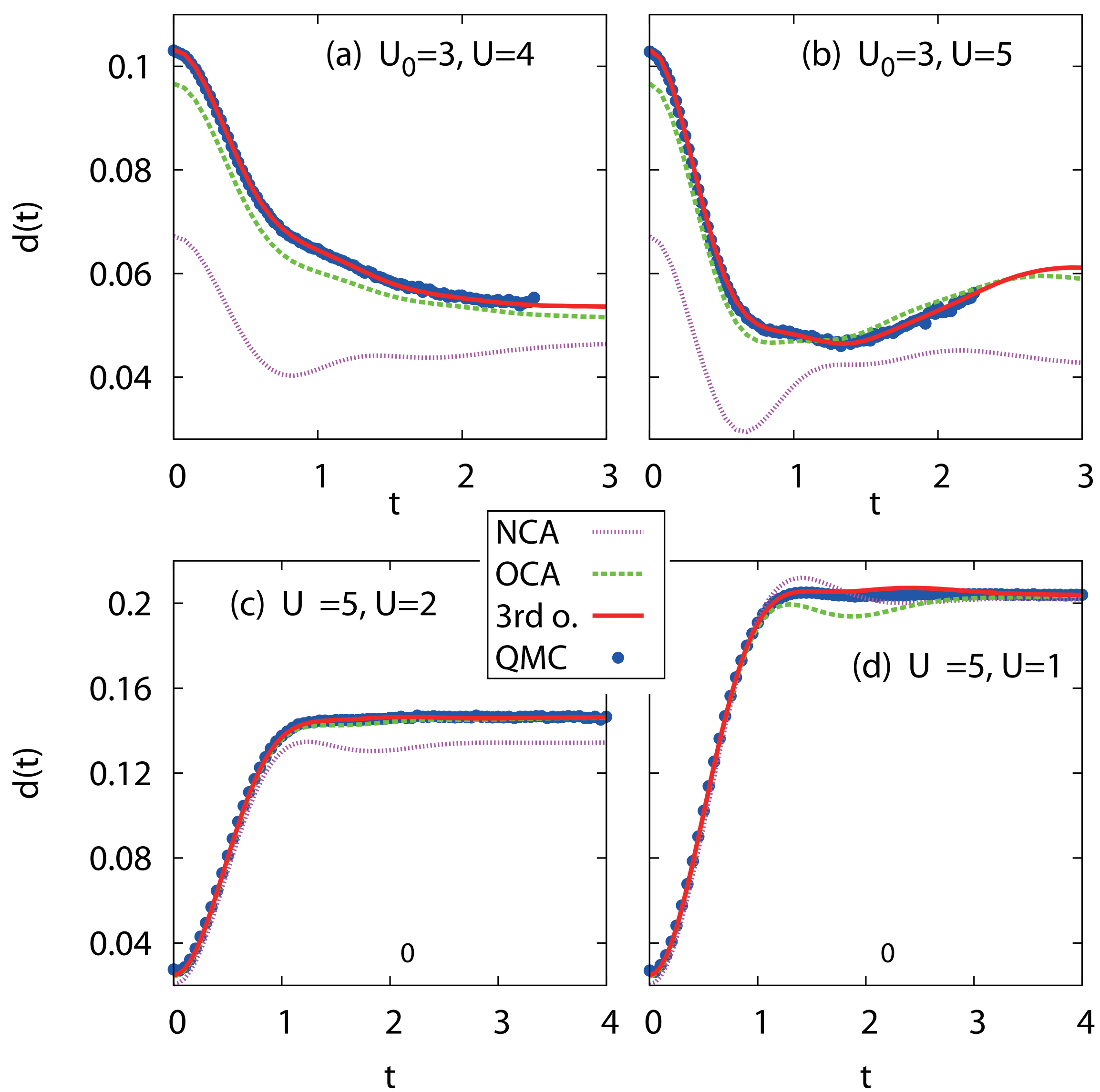

conserving approximation

systematically converging to the exact result

accurate in the strong-coupling regime

Eckstein & Werner (2010)

Nonequilibrium extension

- Calculation of the lattice Green's function
- Noninteracting lattice:

$$H_0(t) = \sum_k [\epsilon_k(t) - \mu(t)] d_k^\dagger d_k$$

$$G_{0,k}(t,t') = -i\langle \mathcal{T}_\mathcal{C} d_k(t) d_k^\dagger(t')\rangle_0$$

- Green's function satisfies:

$$[i\partial_t + \mu(t) - \epsilon_k(t)] G_{0,k}(t,t') = \delta_\mathcal{C}(t,t')$$

$$\Downarrow$$

Inverse lattice Green's function:

$$G_{0,k}^{-1}(t,t') = \delta_\mathcal{C}(t,t')[i\partial_t + \mu(t) - \epsilon_k(t)]$$

Nonequilibrium extension

- Calculation of the lattice Green's function
- Noninteracting lattice:

$$H_0(t) = \sum_k [\epsilon_k(t) - \mu(t)] d_k^\dagger d_k$$

$$G_{0,k}(t,t') = -i\langle \mathcal{T}_\mathcal{C} d_k(t) d_k^\dagger(t')\rangle_0$$

- Green's function satisfies:

$$[i\partial_t + \mu(t) - \epsilon_k(t)] G_{0,k}(t,t') = \delta_\mathcal{C}(t,t')$$

$$\Downarrow$$

Inverse lattice Green's function:

$$G_{0,k}^{-1}(t,t') = \delta_\mathcal{C}(t,t')[i\partial_t + \mu(t) - \epsilon_k(t)]$$

Nonequilibrium extension

- Calculation of the lattice Green's function
- Interacting lattice: Green's function satisfies Dyson equation

$$G_k = G_{0,k} + G_{0,k} \star \Sigma \star G_k$$ *integral form*

⇧ *impurity self-energy (DMFT)*

$$[G_{0,k}^{-1} - \Sigma] \star G_k = \delta_{\mathcal{C}}$$ *differential form*

- Imaginary-time branch: boundary-value problem ⟶ solve by FT

$$G_k(i\omega_n) = \frac{1}{G_{0,k}^{-1}(i\omega_n) - \Sigma(i\omega_n)} = \frac{1}{i\omega_n + \mu(0) - \epsilon_k(0) - \Sigma(i\omega_n)}$$

Usual equilibrium DMFT calculation for the initial equilibrium state

Nonequilibrium extension

- Calculation of the lattice Green's function
- Interacting lattice: Green's function satisfies Dyson equation

$$G_k = G_{0,k} + G_{0,k} \star \Sigma \star G_k$$ *integral form*

$$\Uparrow$$

impurity self-energy (DMFT)

$$[G_{0,k}^{-1} - \Sigma] \star G_k = \delta_{\mathcal{C}}$$ *differential form*

- Real-time branches: initial-value problem

$$[i\partial_t + \mu(t) - \epsilon_k(t)]G_k(t,t') - \int_{\mathcal{C}} d\bar{t}\, \Sigma(t,\bar{t}) G_k(\bar{t},t') = \delta_{\mathcal{C}}(t,t')$$

Defines time-propagation scheme for *G* in which the self-energy plays the role of a memory-kernel

Nonequilibrium extension

- Calculation of the lattice Green's function

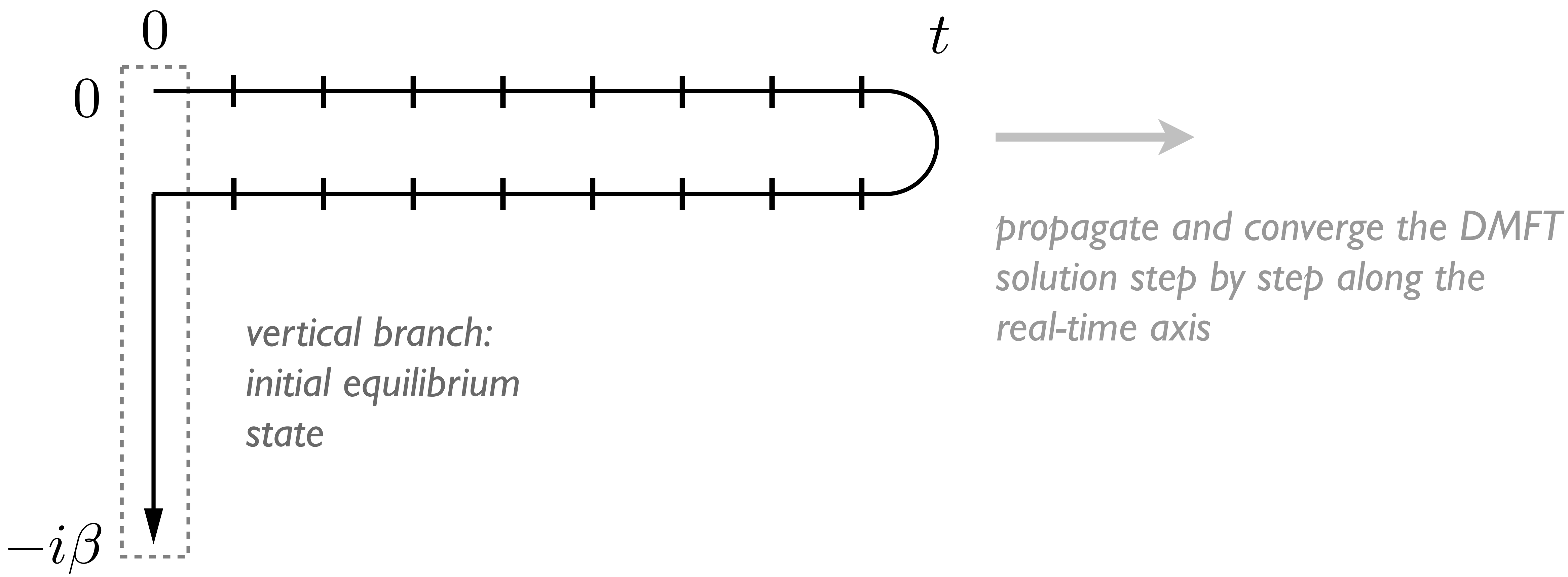

- Real-time branches: initial-value problem

$$[i\partial_t + \mu(t) - \epsilon_k(t)]G_k(t,t') - \int_{\mathcal{C}} d\bar{t}\, \Sigma(t,\bar{t})G_k(\bar{t},t') = \delta_{\mathcal{C}}(t,t')$$

Defines time-propagation scheme for G in which the self-energy plays the role of a memory-kernel

Nonequilibrium extension

- Calculation of the lattice Green's function

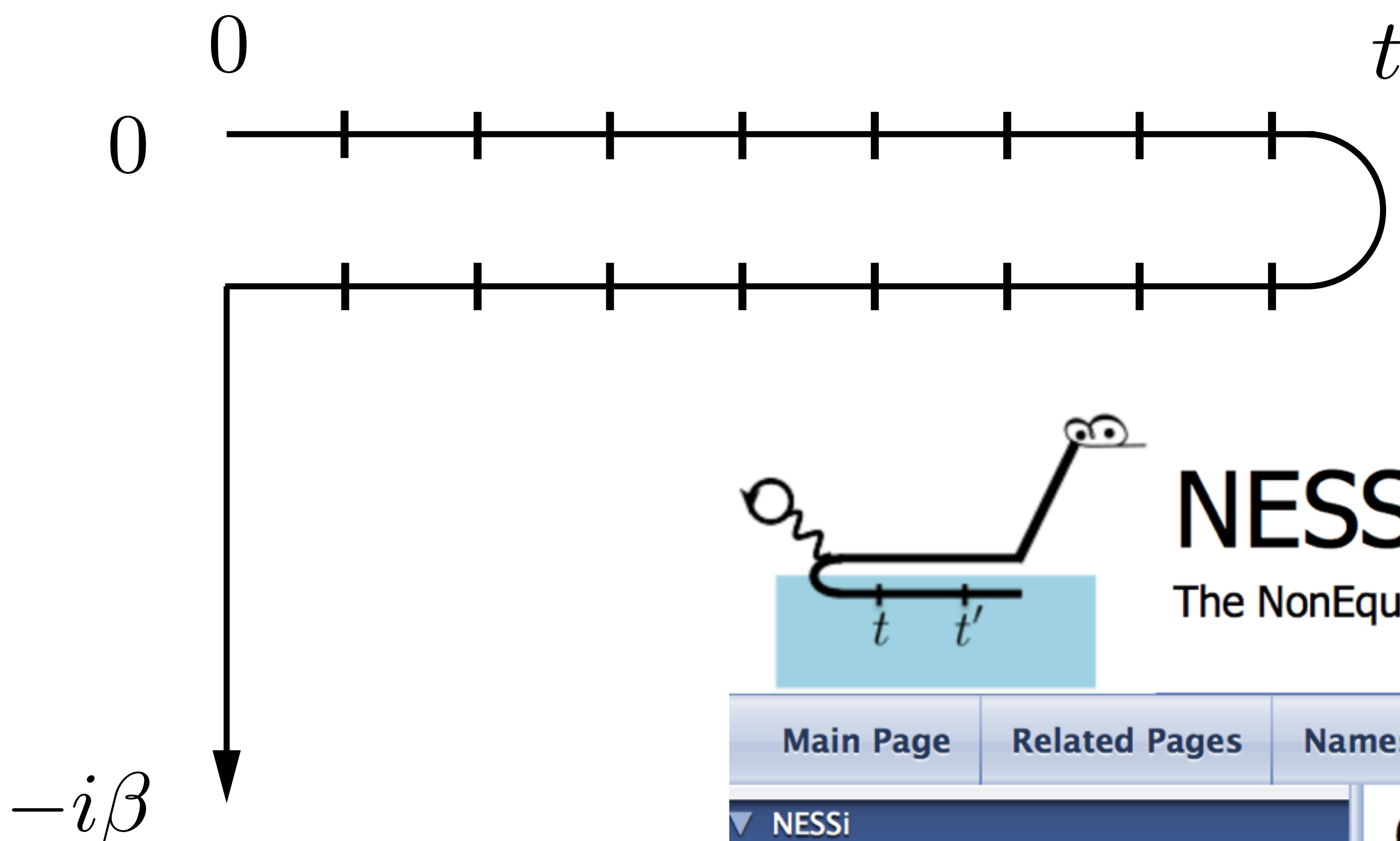

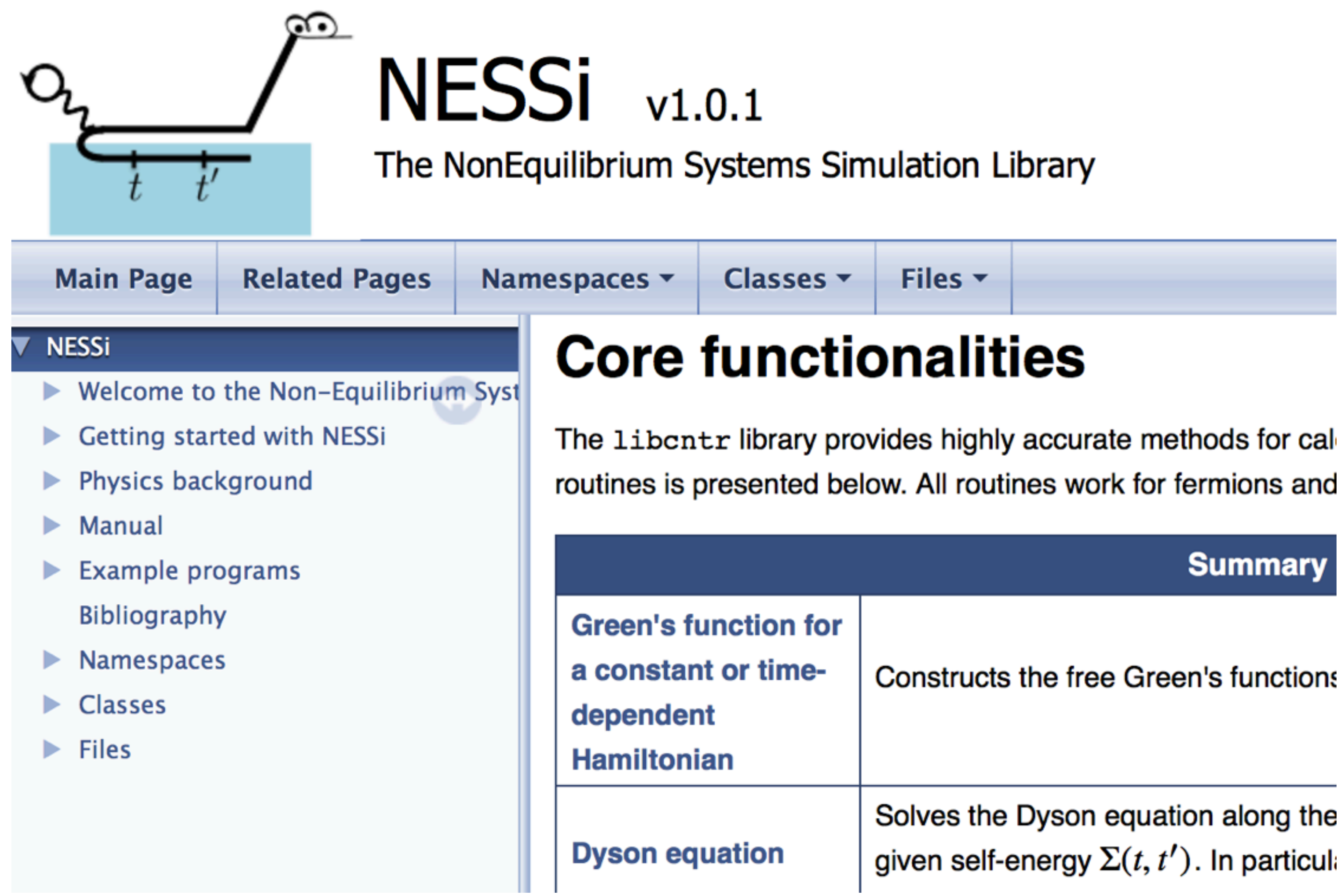

- Open source library:
  nessi.tuxfamily.org

Nonequilibrium extension

- Electric fields
- Vector potential $A(r,t)$, scalar potential $\Phi(r,t)$: $E = -\nabla\Phi - \partial_t A$

$$v_{ij}(t) = v_{ij} \exp\left(-ie \int_{R_i}^{R_j} dr\, A(r,t)\right)$$

$$\Downarrow$$

$$\begin{aligned} H(t) &= -\sum_{\langle ij\rangle\sigma} v_{ij}(t)(d_{i\sigma}^\dagger d_{j\sigma} + d_{j\sigma}^\dagger d_{i\sigma}) \\ &\quad + U(t)\sum_i n_{i\uparrow}n_{i\downarrow} - \sum_{i\sigma} \mu(t) n_{i\sigma} \end{aligned}$$

$$\Uparrow$$

$$\mu(t) = \mu + e\Phi(R_i,t)$$

- Convenient choice: gauge with pure vector potential:

$\Phi \equiv 0, E = -\partial_t A$

Nonequilibrium extension

- Electric fields
- Neglecting the *r*-dependence of *A* (assumption: field varies slowly on the atomic scale):

$$v_{ij}(t) = v_{ij} \exp\left(-ie \int_{R_i}^{R_j} dr\, A(t) \right) \qquad A(t) = -\int_0^t ds E(s)$$

⇓ *Fourier transformation*

$$\epsilon_k(t) = \epsilon_{k-eA(t)}$$

- Electric field enters in the lattice Dyson equation in the form of a time-dependent dispersion:

$$[i\partial_t + \mu(t) - \epsilon_k(t)]G_k(t,t') - \int_{\mathcal{C}} d\bar{t}\, \Sigma(t,\bar{t})G_k(\bar{t},t') = \delta_{\mathcal{C}}(t,t')$$

Spectroscopy

- "Physical" Green's functions
- The 9 elements of the 3x3 Green's function matrix

$$\hat{G} = \begin{pmatrix} G_{11} & G_{12} & G_{13} \\ G_{21} & G_{22} & G_{23} \\ G_{31} & G_{32} & G_{33} \end{pmatrix}$$

are not independent:

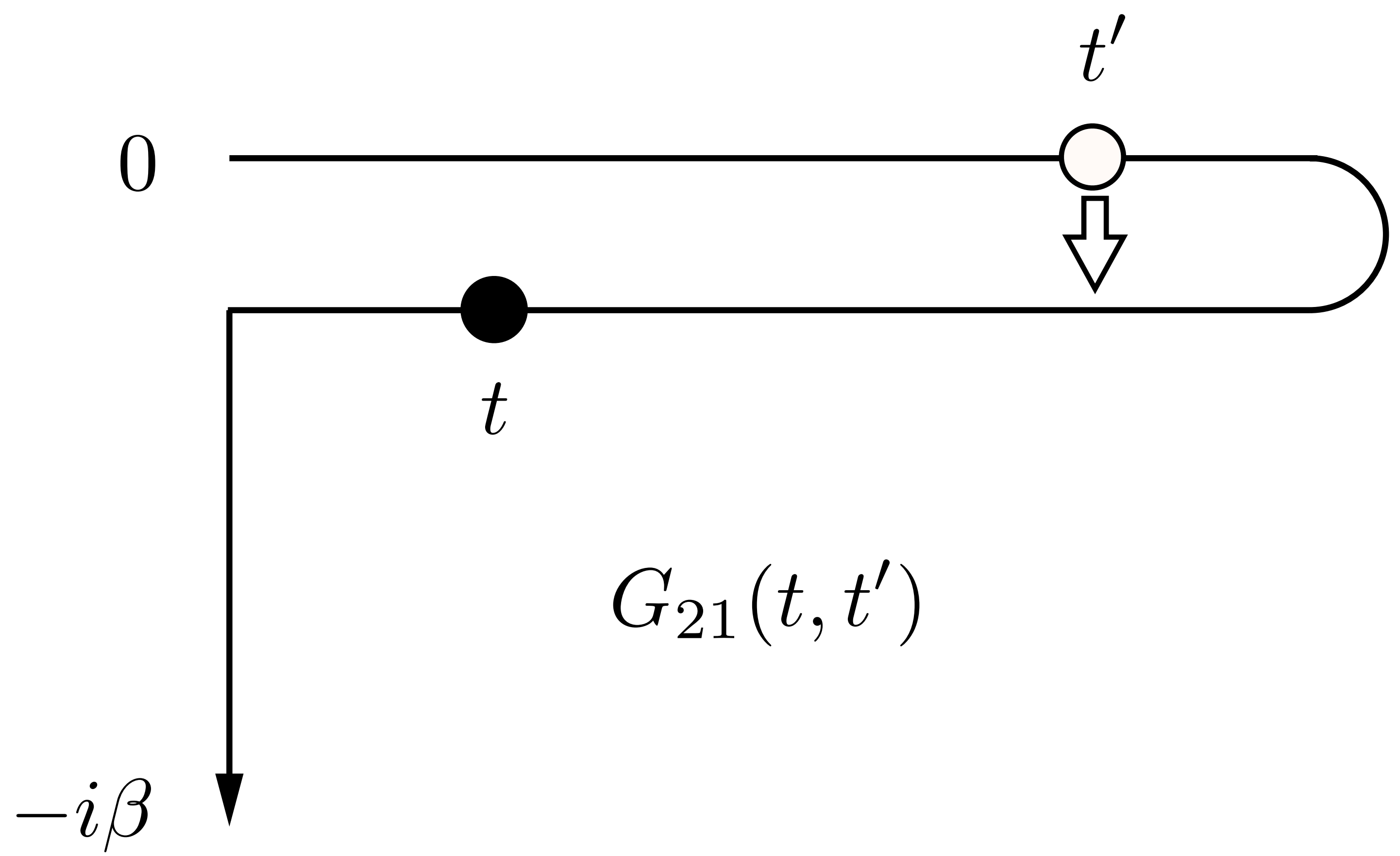

Spectroscopy

- “Physical” Green’s functions
- The 9 elements of the 3x3 Green’s function matrix

$$\hat{G} = \begin{pmatrix} G_{11} & G_{12} & G_{13} \\ G_{21} & G_{22} & G_{23} \\ G_{31} & G_{32} & G_{33} \end{pmatrix}$$

are not independent:

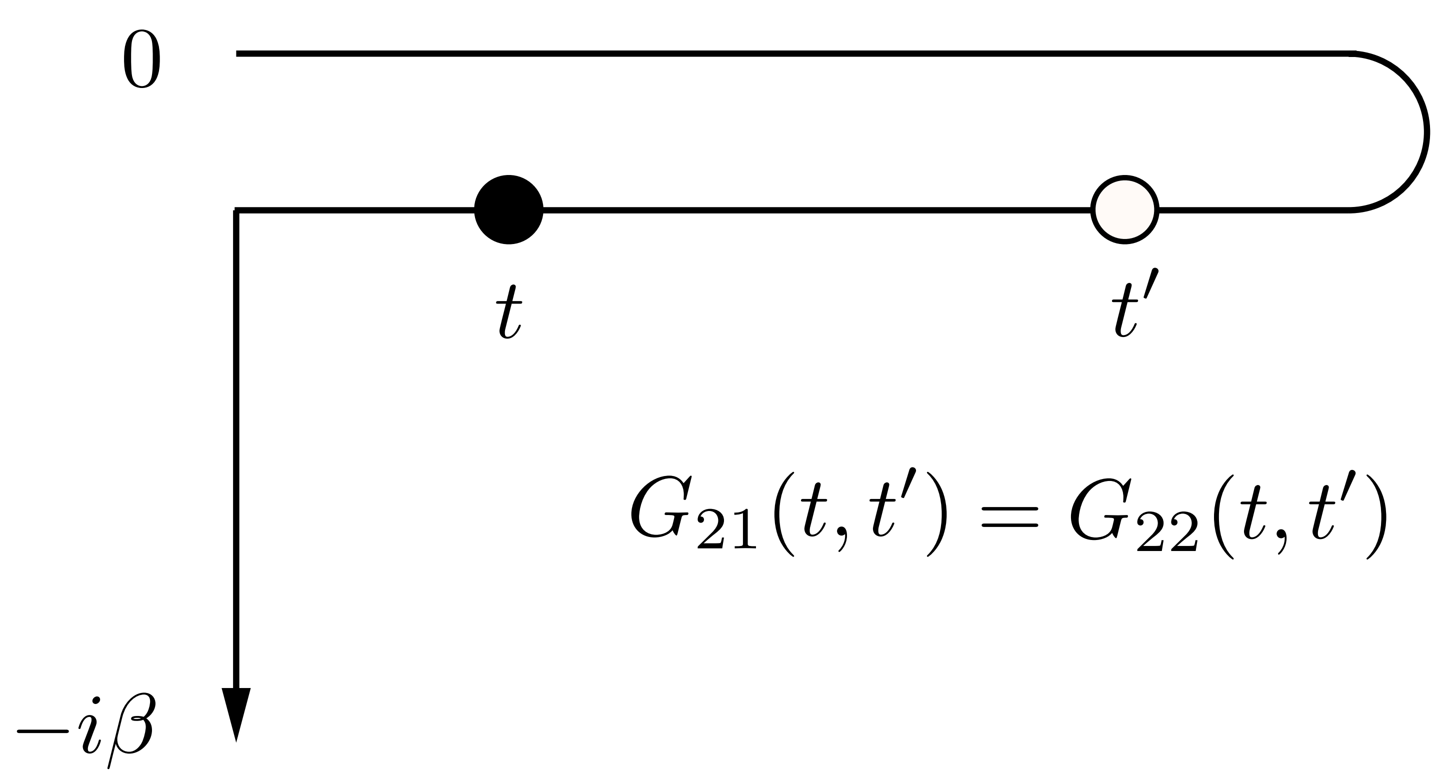

$$G_{21}(t, t') = G_{22}(t, t') \quad (\text{for } t < t')$$

Spectroscopy

- "Physical" Green's functions
- We have the following redundancies

$$
\begin{aligned}
G_{11}(t,t') &= G_{12}(t,t') \quad (\text{for } t \leq t') \\
G_{11}(t,t') &= G_{21}(t,t') \quad (\text{for } t > t') \\
G_{22}(t,t') &= G_{21}(t,t') \quad (\text{for } t < t') \\
G_{22}(t,t') &= G_{12}(t,t') \quad (\text{for } t \geq t') \\
G_{13}(t,\tau') &= G_{23}(t,\tau') \\
G_{31}(\tau,t') &= G_{32}(\tau,t')
\end{aligned}
$$

which allow to eliminate 3 of the 9 components

$\longrightarrow$ define 6 "physical" Green's functions

$$G^R, G^A, G^K, \ldots$$

Spectroscopy

- "Physical" Green's functions
- Relevant for the following discussion: Retarded Green's function

$$G^R(t,t') = \frac{1}{2}(G_{11} - G_{12} + G_{21} - G_{22}) = -i\theta(t-t')\langle\{d(t), d^\dagger(t')\}\rangle$$

and lesser Green's functions

$$G^<(t,t') = G_{12} = i\langle d^\dagger(t')d(t)\rangle$$

- In equilibrium:
  - Spectral function: $A(\omega) = -\frac{1}{\pi}\mathrm{Im}\, G^R(\omega)$
  - Occupation: $N(\omega) = \frac{1}{2\pi}\mathrm{Im}\, G^<(\omega)$
  - Distribution function: $N(\omega)/A(\omega) = f(\omega)$ *Fermi function*

Spectroscopy

- "Physical" Green's functions
- Relevant for the following discussion: Retarded Green's function

$$G^R(t,t') = \frac{1}{2}(G_{11} - G_{12} + G_{21} - G_{22}) = -i\theta(t-t')\langle\{d(t), d^\dagger(t')\}\rangle$$

and lesser Green's functions

$$G^<(t,t') = G_{12} = i\langle d^\dagger(t')d(t)\rangle$$

- Out of equilibrium: $t_{\mathrm{av}} = (t+t')/2, t_{\mathrm{rel}} = t - t'$
  - Spectral function: $A(\omega, t_{\mathrm{av}}) = -\frac{1}{\pi}\mathrm{Im}\int dt_{\mathrm{rel}} e^{i\omega t_{\mathrm{rel}}} G^R(t,t')$
  - Occupation: $N(\omega, t_{\mathrm{av}}) = \frac{1}{2\pi}\mathrm{Im}\int dt_{\mathrm{rel}} e^{i\omega t_{\mathrm{rel}}} G^<(t,t')$
  - "Distribution function": $N(\omega, t_{\mathrm{av}})/A(\omega, t_{\mathrm{av}})$

Spectroscopy

- Time-resolved photoemission spectrum *Freericks et al. (2009)*

$$\cos[\Omega(t - t_p + \phi)]S(t - t_p)$$

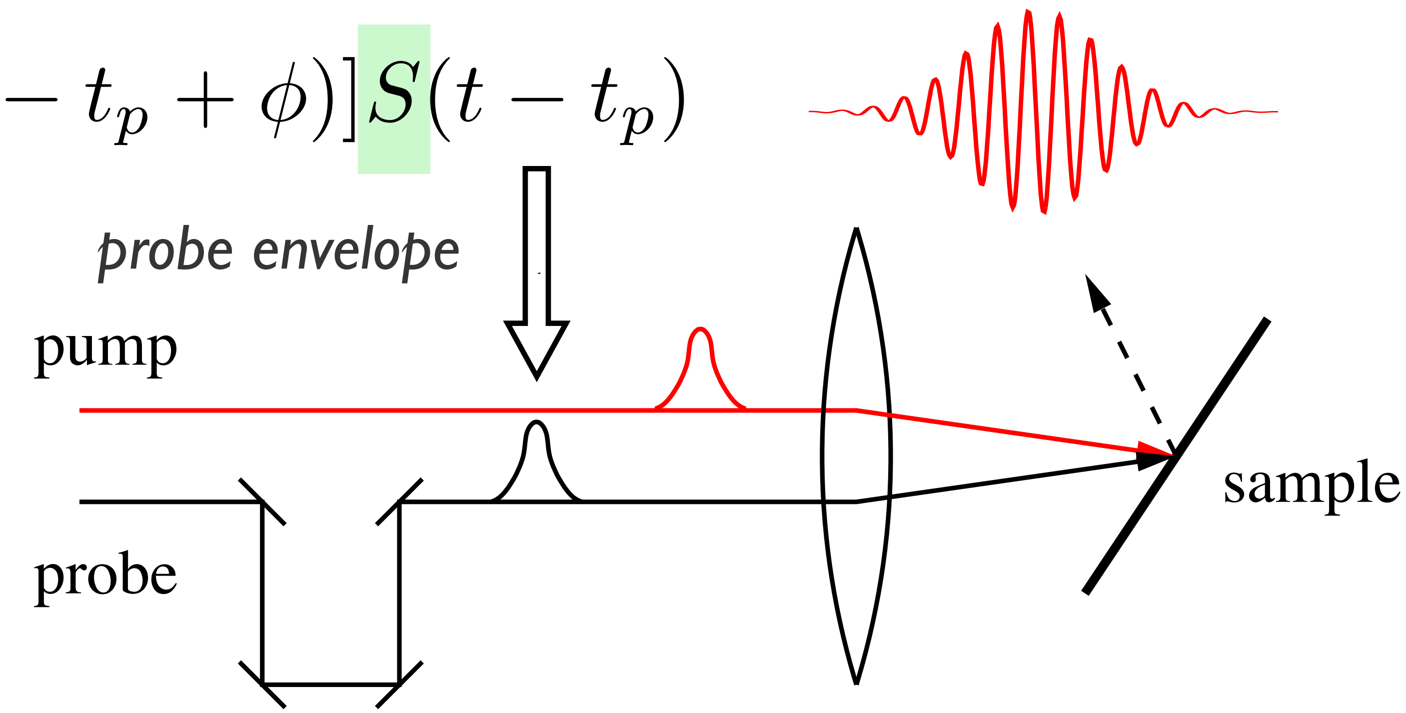

$$I_k(\omega; t_p) = -i \int dt dt' \, S(t) S(t') e^{i\omega(t'-t)} G_k^<(t + t_p, t' + t_p)$$

probe time

Spectroscopy

- Time-resolved photoemission spectrum *Freericks et al. (2009)*

$$\cos[\Omega(t - t_p + \phi)]S(t - t_p)$$

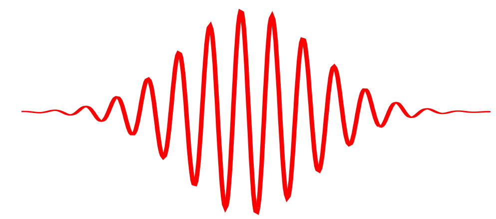

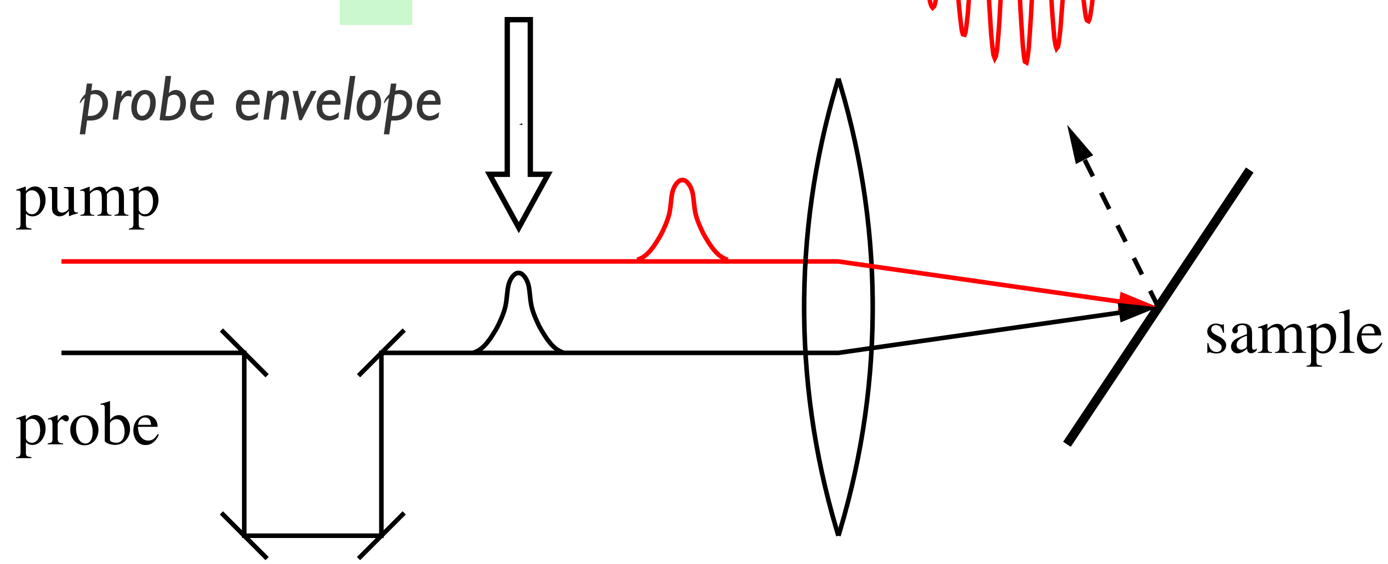

$$I_k(\omega; t_p) = -i \int dt dt' \, S(t) S(t') e^{i\omega(t'-t)} G_k^<(t + t_p, t' + t_p)$$

- Formula contains time-energy uncertainty

$$S(t) \sim \delta(t - t_p) : \text{ measure occupation } n_k(t_p)$$

$$S(t) \sim \text{const} : \text{ measure spectral function } A_k(\omega, t_p)$$

Accuracy of nonequilibrium DMFT

- Benchmark against DMRG for 1D Hubbard model
  - Quench from *U=0* to *U=1*

    Tsuji, Barmettler, Aoki & Werner (2014)

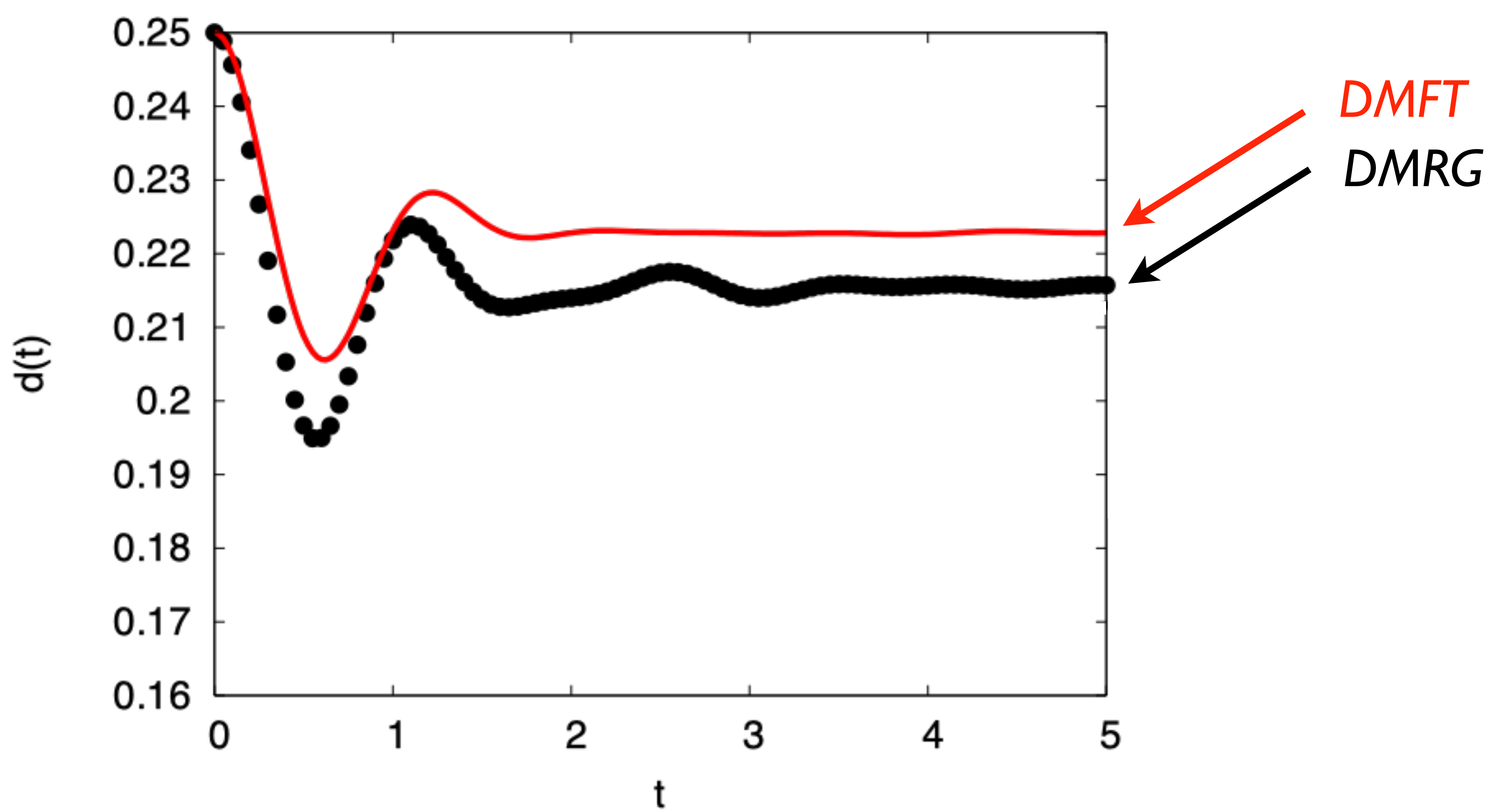

Accuracy of nonequilibrium DMFT

- Benchmark against DMRG for 1D Hubbard model
  - Quench from *U=0* to *U=1*

    Tsuji, Barmettler, Aoki & Werner (2014)

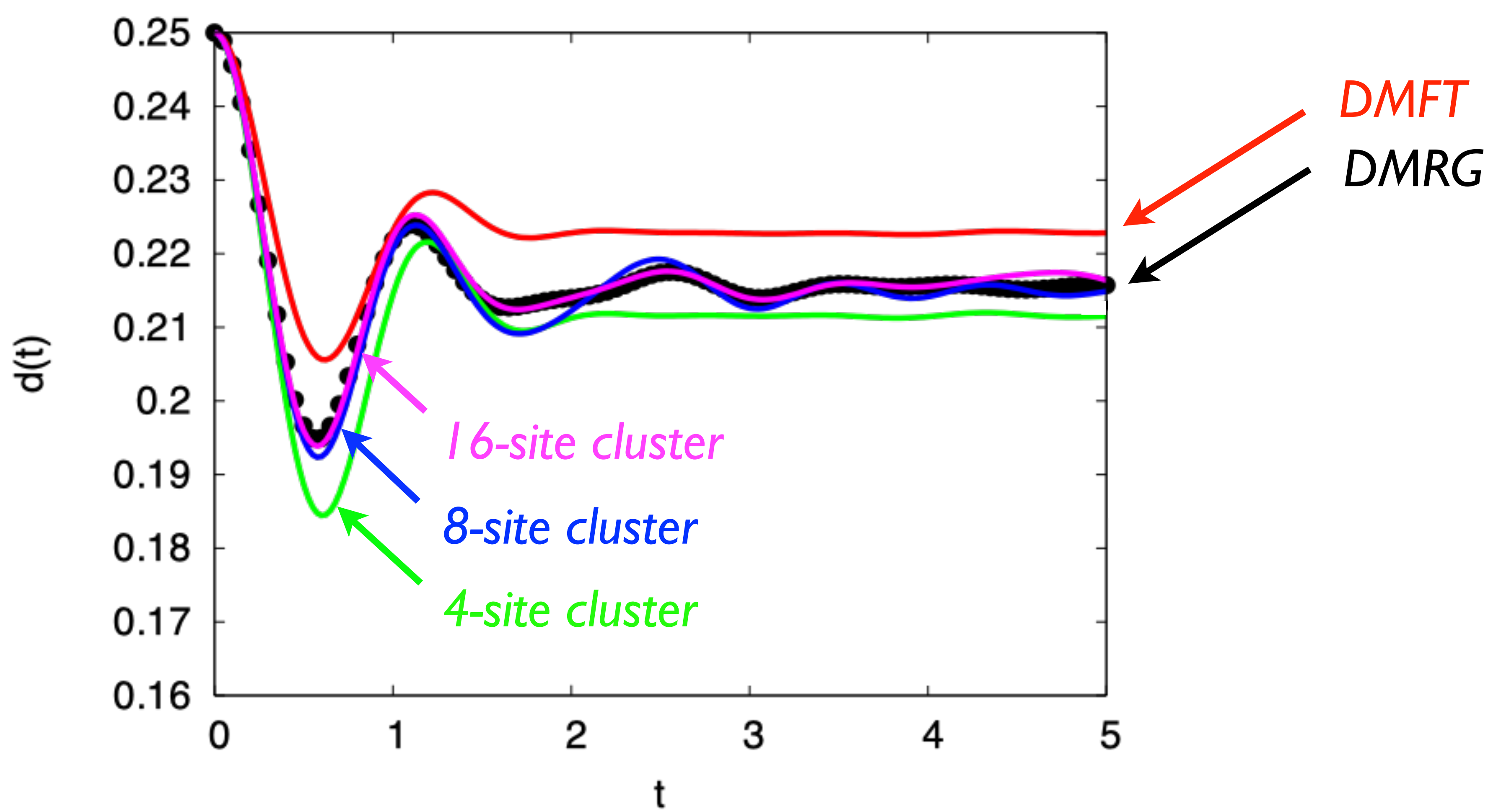

- Cluster extensions of DMFT capture short-range correlations

  Tsuji et al. (2014); Eckstein & Werner (2016); Bittner et al. (2019)

Accuracy of nonequilibrium DMFT

- Benchmark against cold atom simulator *Sandholzer et al. (2019)*
  - Resonant excitation ($\Omega = U$) of Mott insulating Hubbard model
  - linear ramp of pulse amplitude K_0

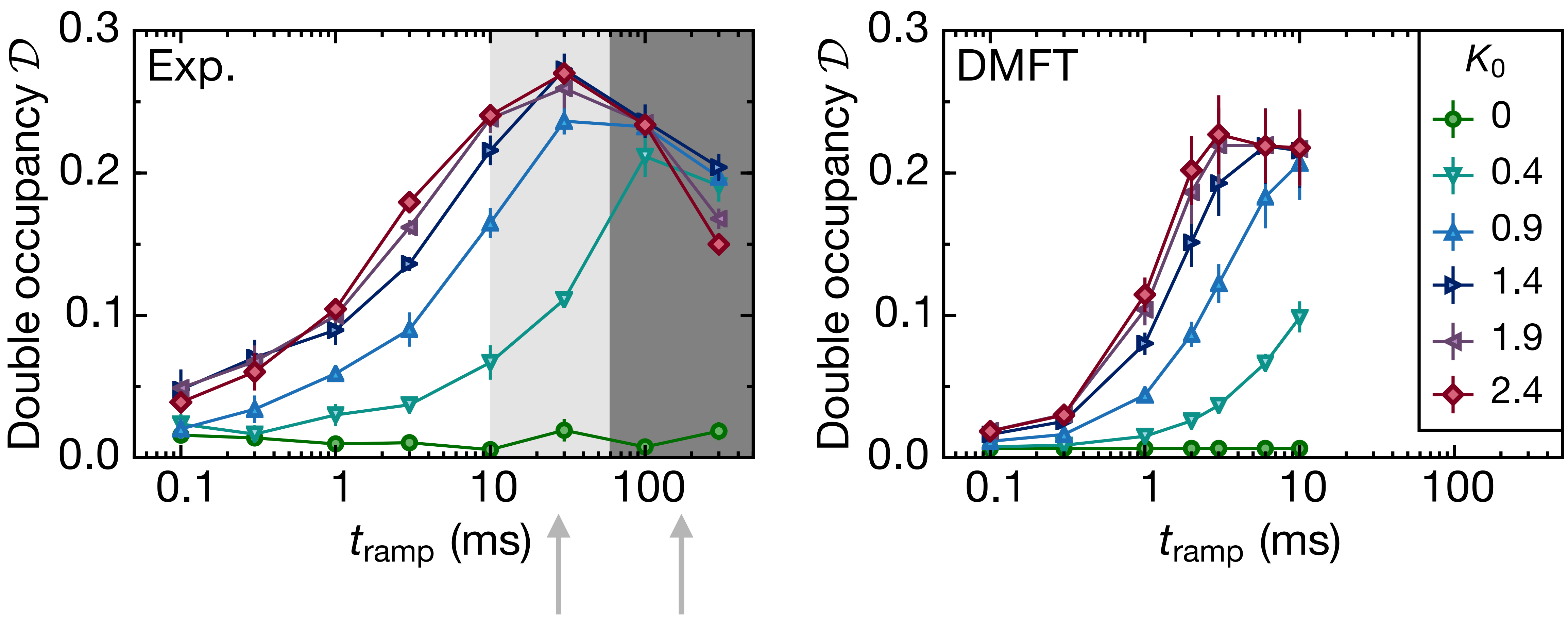

redistribution in the trap

atom loss

1. Periodic electric fields

- AC-field quench in the Hubbard model (metal phase)

  Tsuji, Oka, Werner and Aoki (2011)

Electric field (amplitude E, frequency Ω) applied at t=0

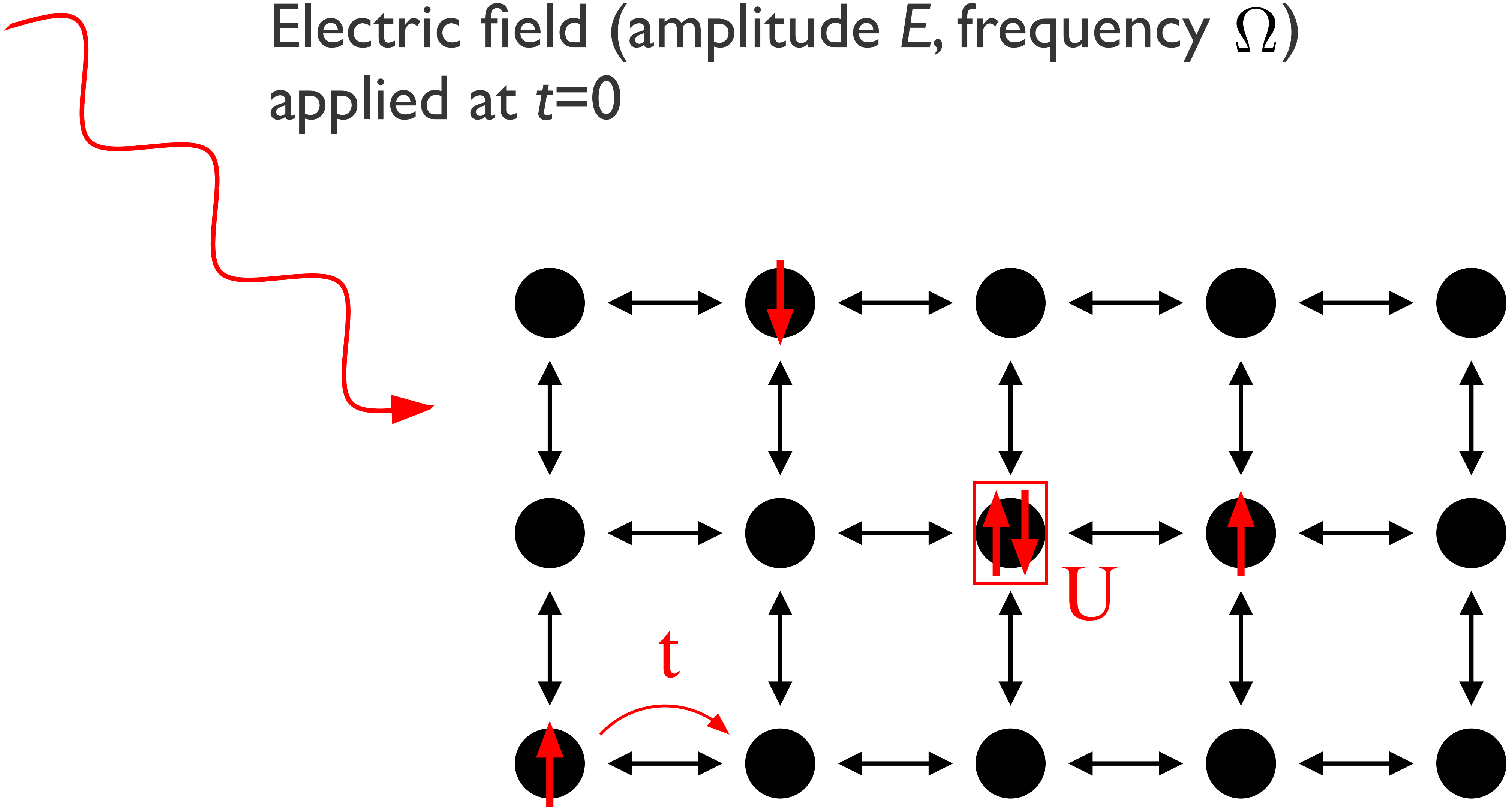

1. Periodic electric fields

- AC-field quench in the Hubbard model (metal phase)

Tsuji, Oka, Werner and Aoki (2011)

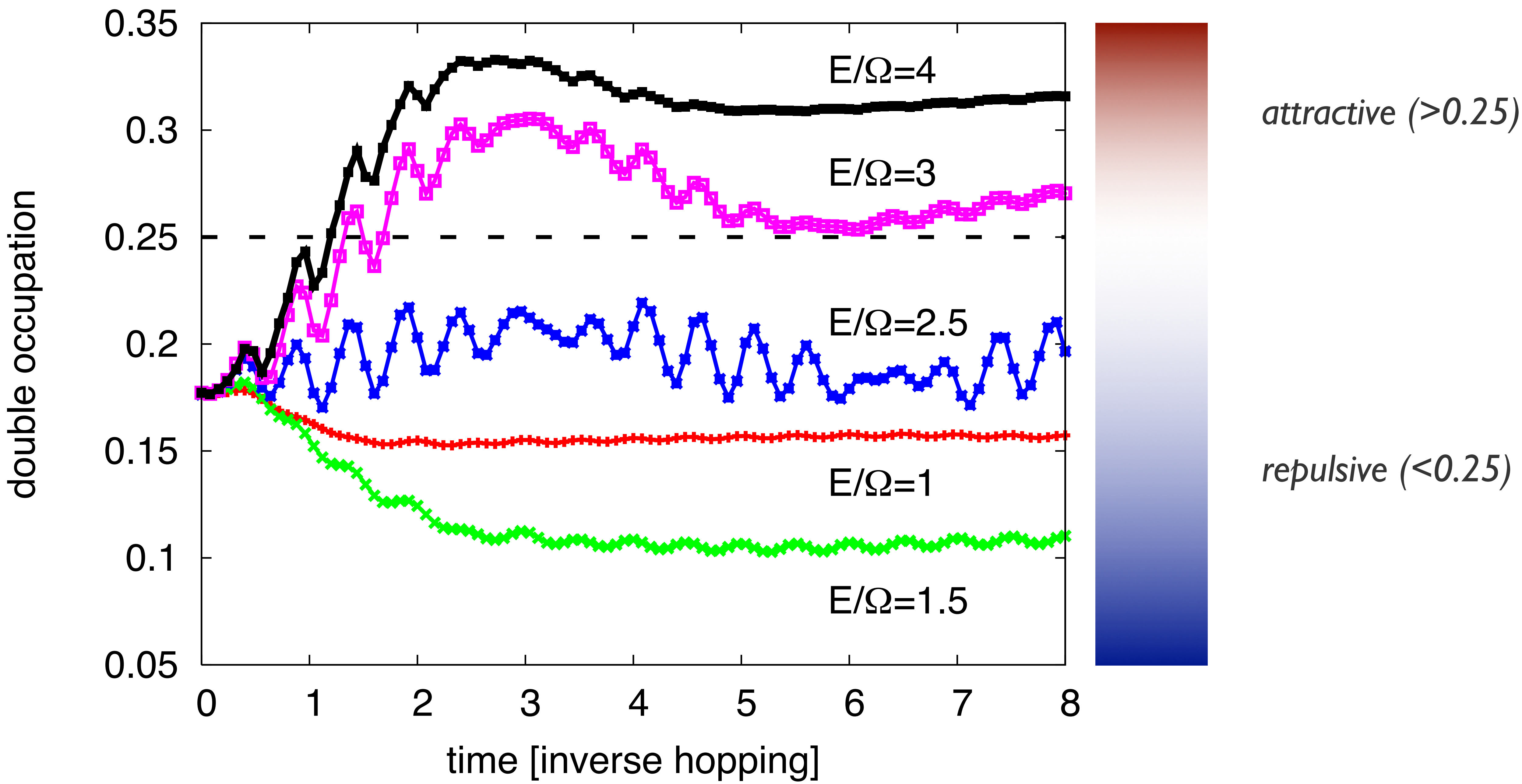

1. Periodic electric fields

- AC-field quench in the Hubbard model (metal phase)
  - Sign inversion of the interaction: repulsive ↔ attractive
  - *Dynamically generated* high-Tc superconductivity?

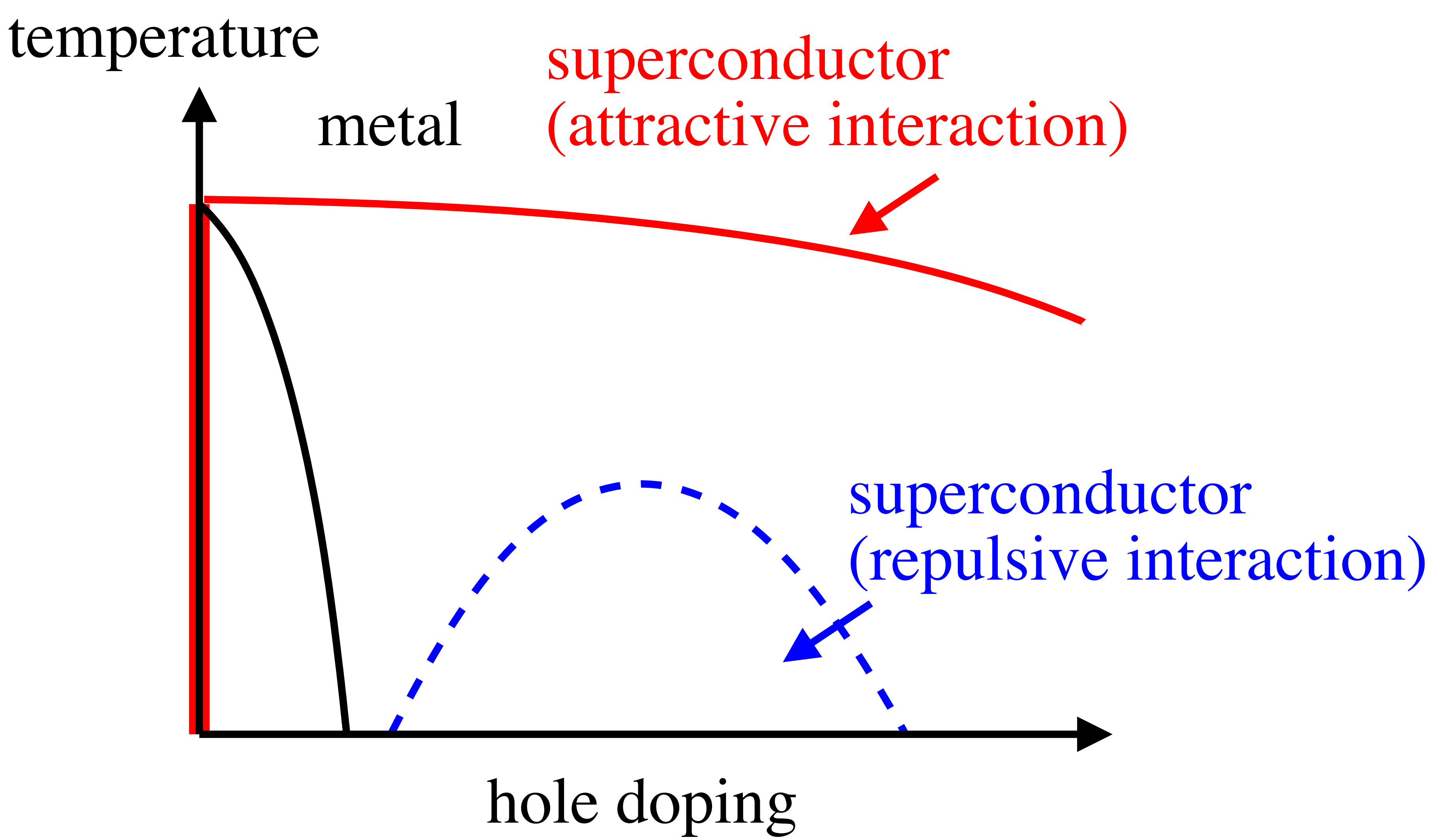

I. Origin of the attractive interaction

- Periodic E-field leads to a population inversion

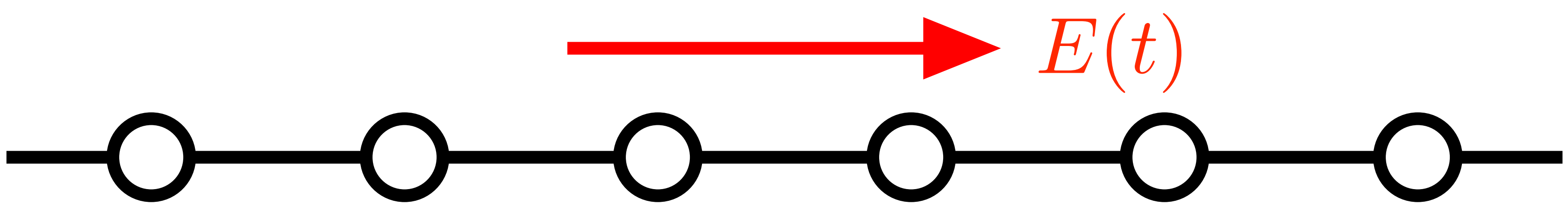

- Gauge with pure vector potential

$$E(t) = E\cos(\Omega t) = -\partial_t A(t)$$
$$\Rightarrow A(t) = -(E/\Omega)\sin(\Omega t)$$

- Peierls substitution $\epsilon_k \longrightarrow \epsilon_{k-A(t)}$

- Renormalized dispersion

$$\overline{\epsilon_k} = \frac{\Omega}{2\pi}\int_0^{2\pi/\Omega} dt\epsilon_{k-A(t)} = \mathcal{J}_0(E/\Omega)\epsilon_k$$

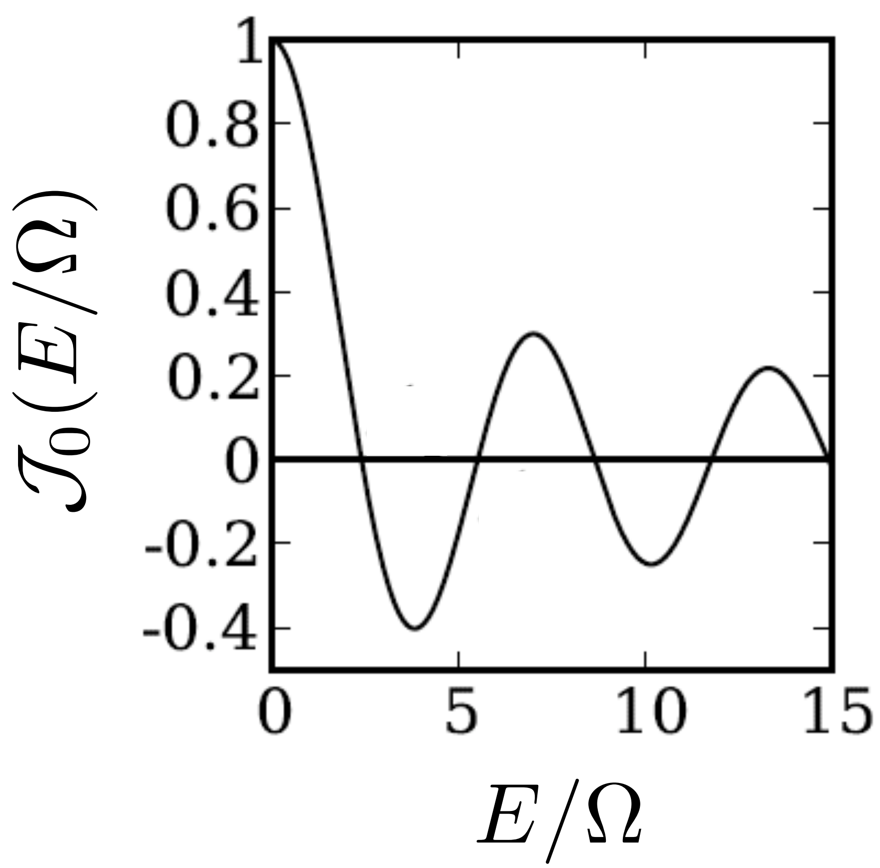

I. Origin of the attractive interaction

- Periodic E-field leads to a population inversion

$\mathcal{J}_0(E/\Omega) = 1$

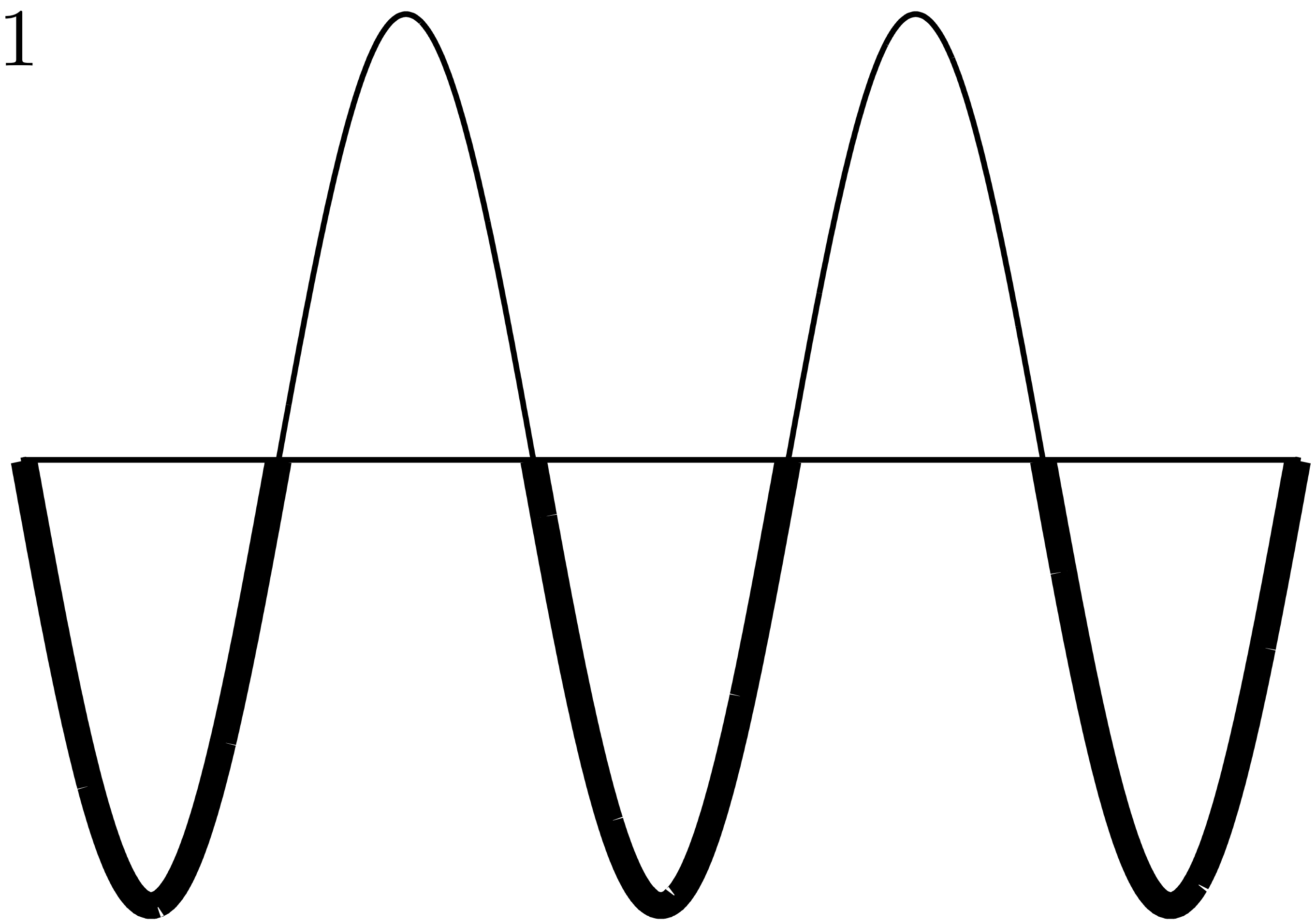

- Renormalized dispersion

$$\overline{\epsilon_k} = \frac{\Omega}{2\pi} \int_0^{2\pi/\Omega} dt \epsilon_{k-A(t)} = \mathcal{J}_0(E/\Omega) \epsilon_k$$

I. Origin of the attractive interaction

- Periodic E-field leads to a population inversion

$\mathcal{J}_0(E/\Omega) = 0.8$

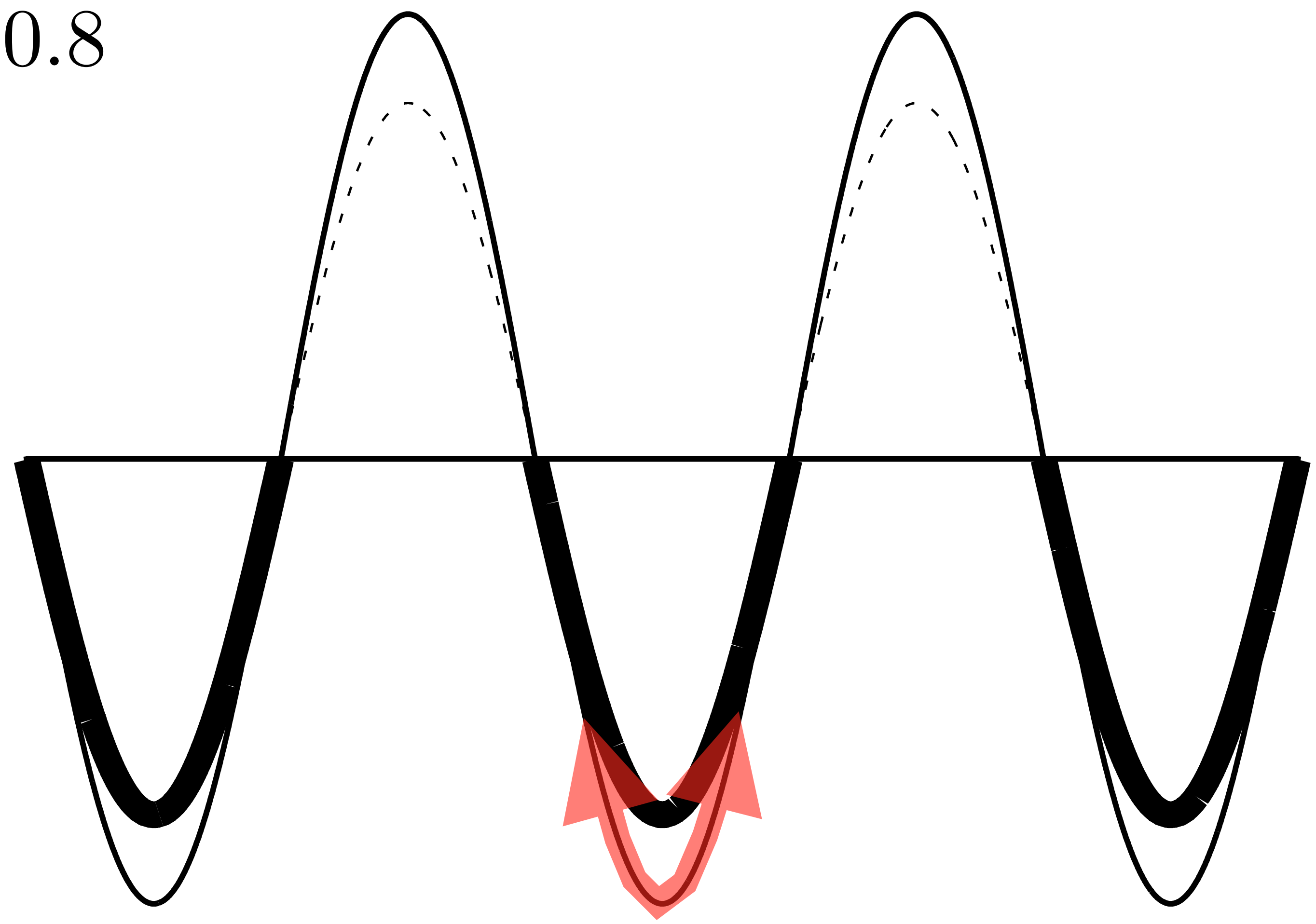

- Renormalized dispersion

$$\overline{\epsilon_k} = \frac{\Omega}{2\pi}\int_0^{2\pi/\Omega} dt \epsilon_{k-A(t)} = \mathcal{J}_0(E/\Omega)\epsilon_k$$

1. Origin of the attractive interaction

- Periodic E-field leads to a population inversion

$\mathcal{J}_0(E/\Omega) = 0.3$

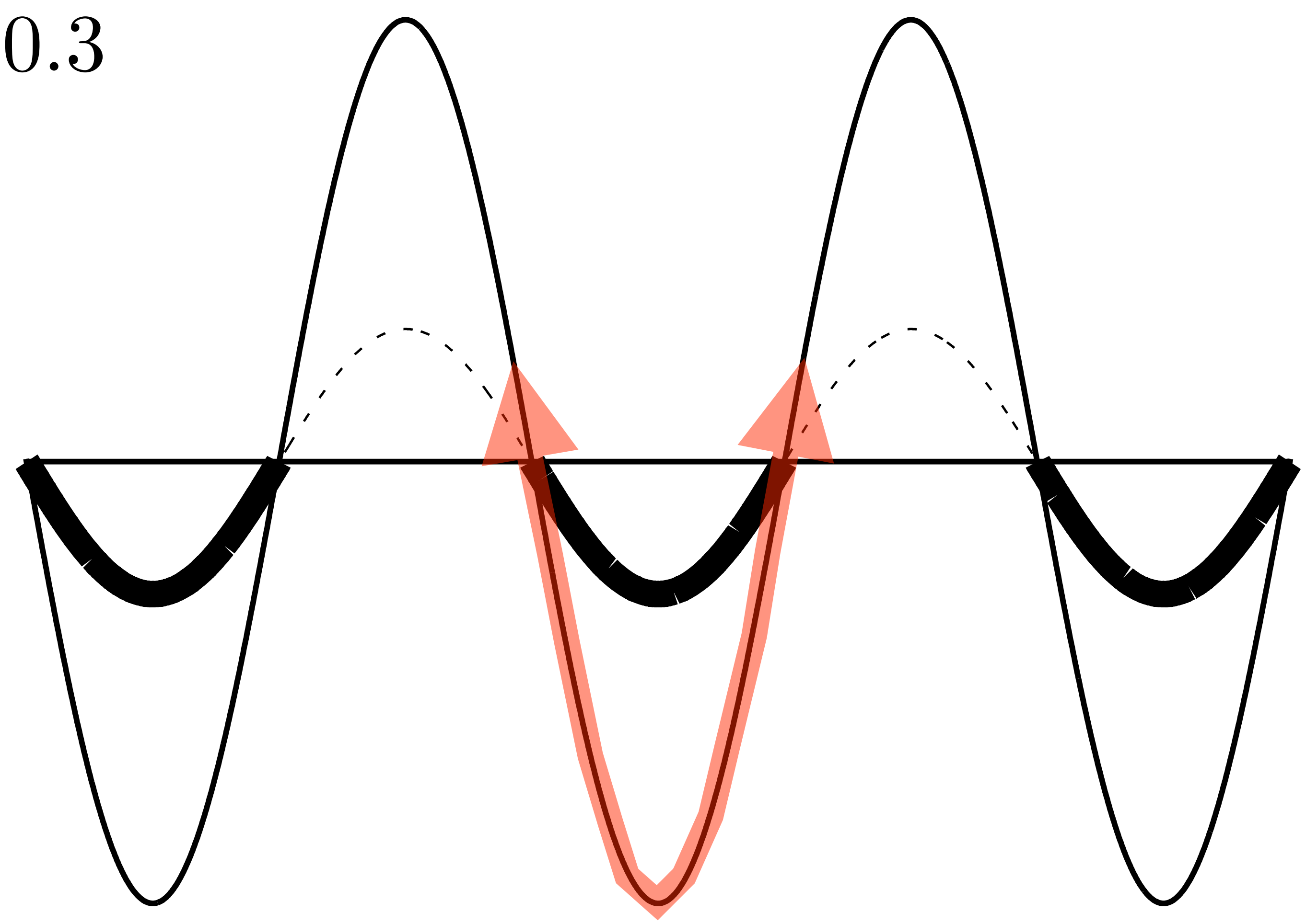

- Renormalized dispersion

$$\overline{\epsilon_k} = \frac{\Omega}{2\pi} \int_0^{2\pi/\Omega} dt \epsilon_{k-A(t)} = \mathcal{J}_0(E/\Omega)\epsilon_k$$

1. Origin of the attractive interaction

- Periodic E-field leads to a population inversion

$$\mathcal{J}_0(E/\Omega) = -0.2$$

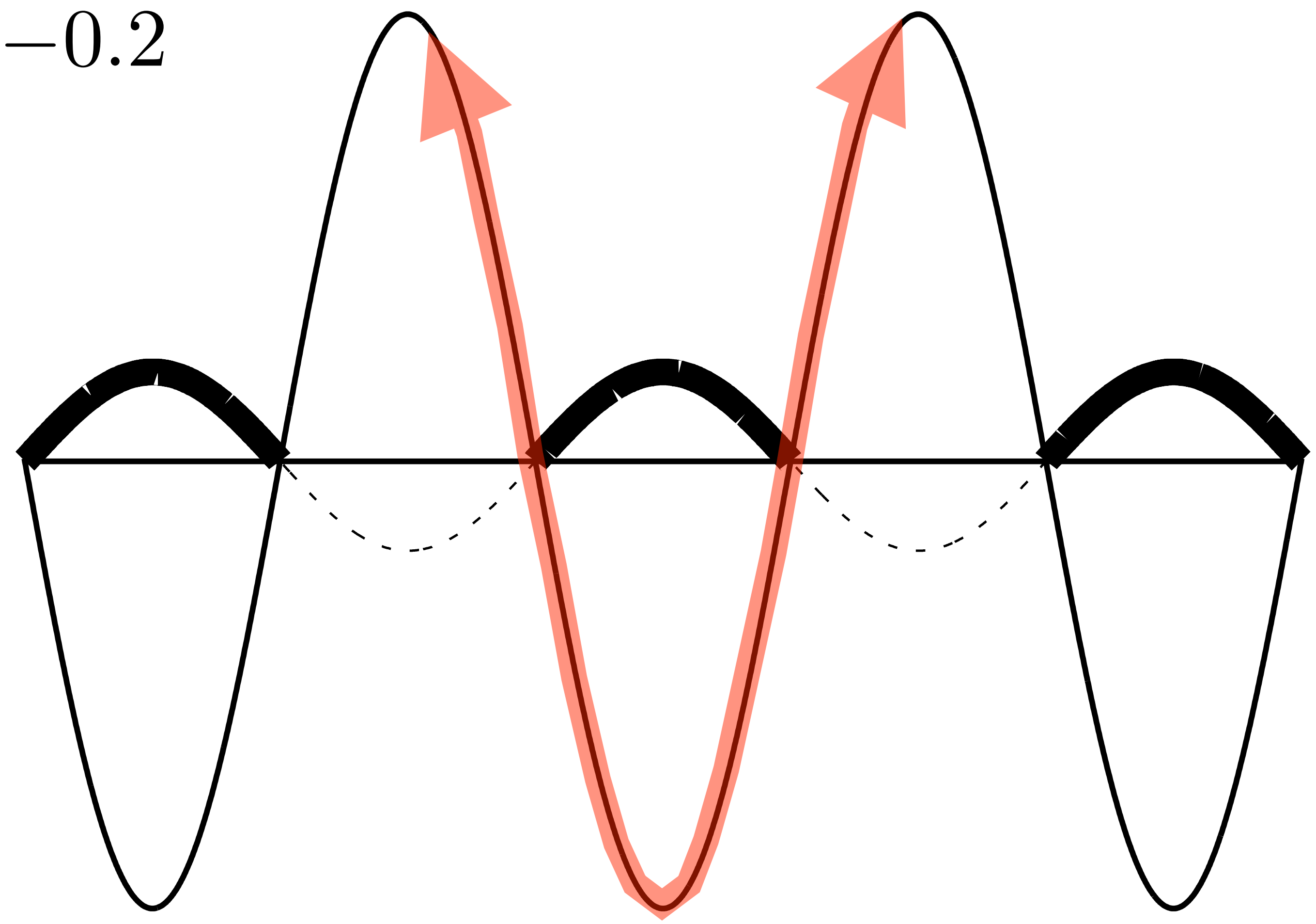

- Renormalized dispersion

$$\overline{\epsilon_k} = \frac{\Omega}{2\pi}\int_0^{2\pi/\Omega} dt\,\epsilon_{k-A(t)} = \mathcal{J}_0(E/\Omega)\epsilon_k$$

1. Origin of the attractive interaction

- Inverted population = negative temperature

- State with $U > 0, T < 0$ is equivalent to state with $U < 0, T > 0$

$$\tilde{T} < 0, \mathcal{J}_0 < 0 \qquad \rho \propto \exp\left(-\frac{1}{\tilde{T}}\left[\sum_{k\sigma} \mathcal{J}_0 \epsilon_k n_{k\sigma} + U \sum_i n_{i\uparrow} n_{i\downarrow}\right]\right)$$

$$T_{\text{eff}} = \frac{\tilde{T}}{\mathcal{J}_0} > 0 \qquad = \exp\left(-\frac{1}{T_{\text{eff}}}\left[\sum_{k\sigma} \epsilon_k n_{k\sigma} + \frac{U}{\mathcal{J}_0} \sum_i n_{i\uparrow} n_{i\downarrow}\right]\right)$$

- Effective interaction of the $T_{\text{eff}} > 0$ state

$$U_{\text{eff}} = \frac{U}{\mathcal{J}_0(E/\Omega)}$$

1. Effect on superconductivity

- AC-field quench from $U = 1$ to $U_{\mathrm{eff}} = -2.5$ (NCA solver)

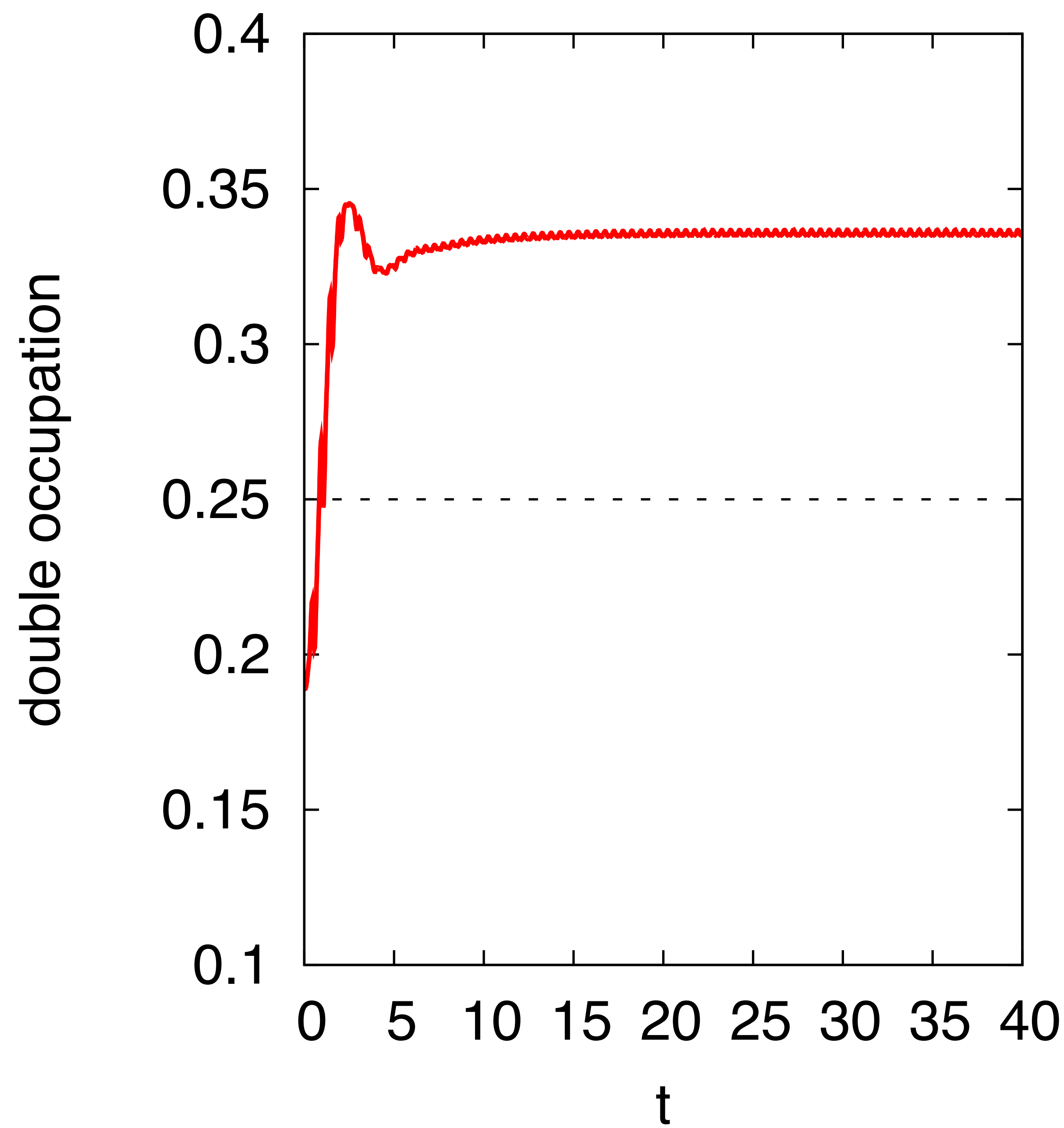

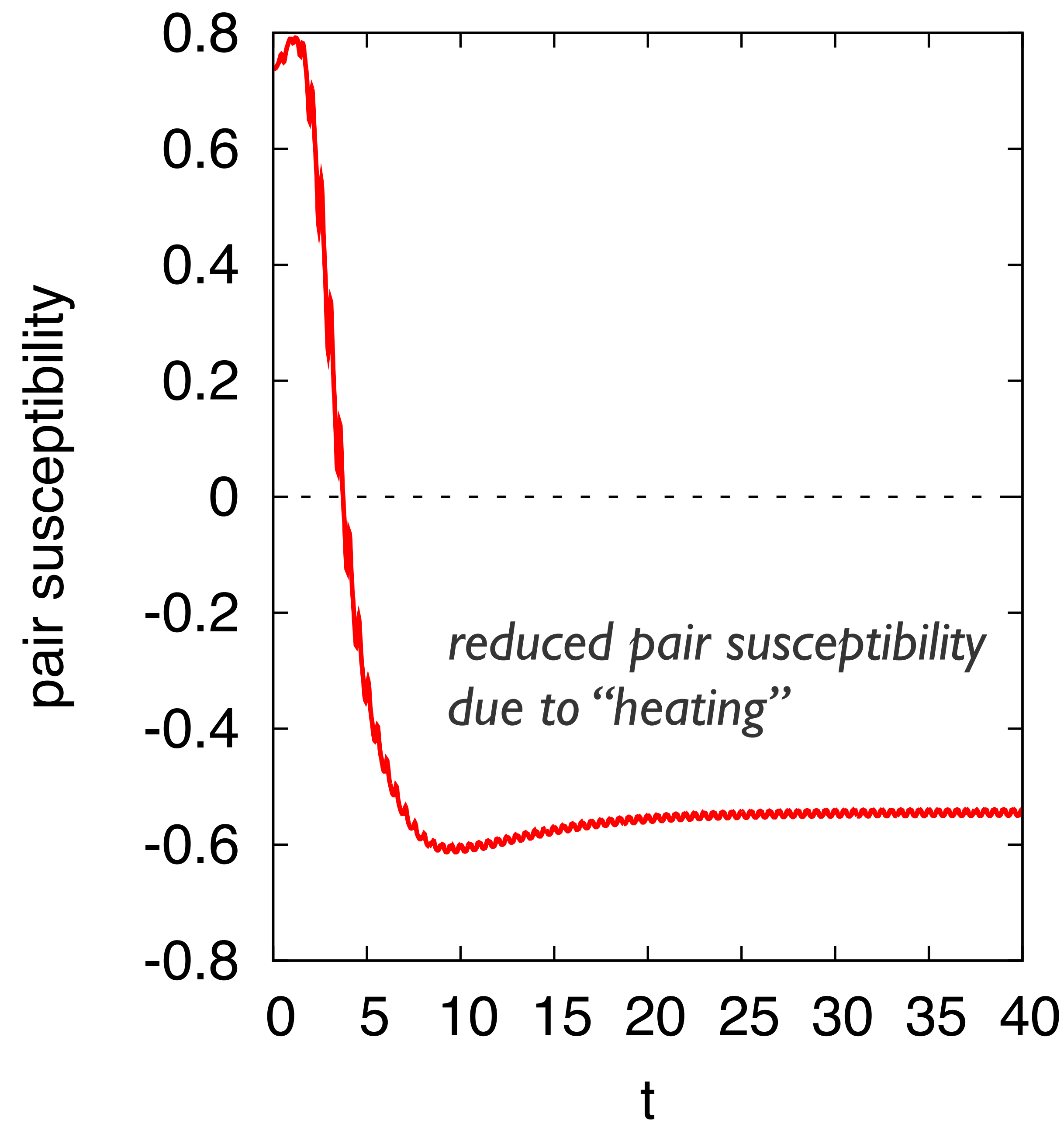

II. Nonthermal symmetry-broken states

- Equilibrium DMFT phase diagram (half-filling)
- Half-filling: transformation $c_{i\uparrow} \to c_{i\uparrow}^{\dagger} \quad (i \in A), \quad c_{i\uparrow} \to -c_{i\uparrow}^{\dagger} \quad (i \in B)$

  maps repulsive model onto attractive model

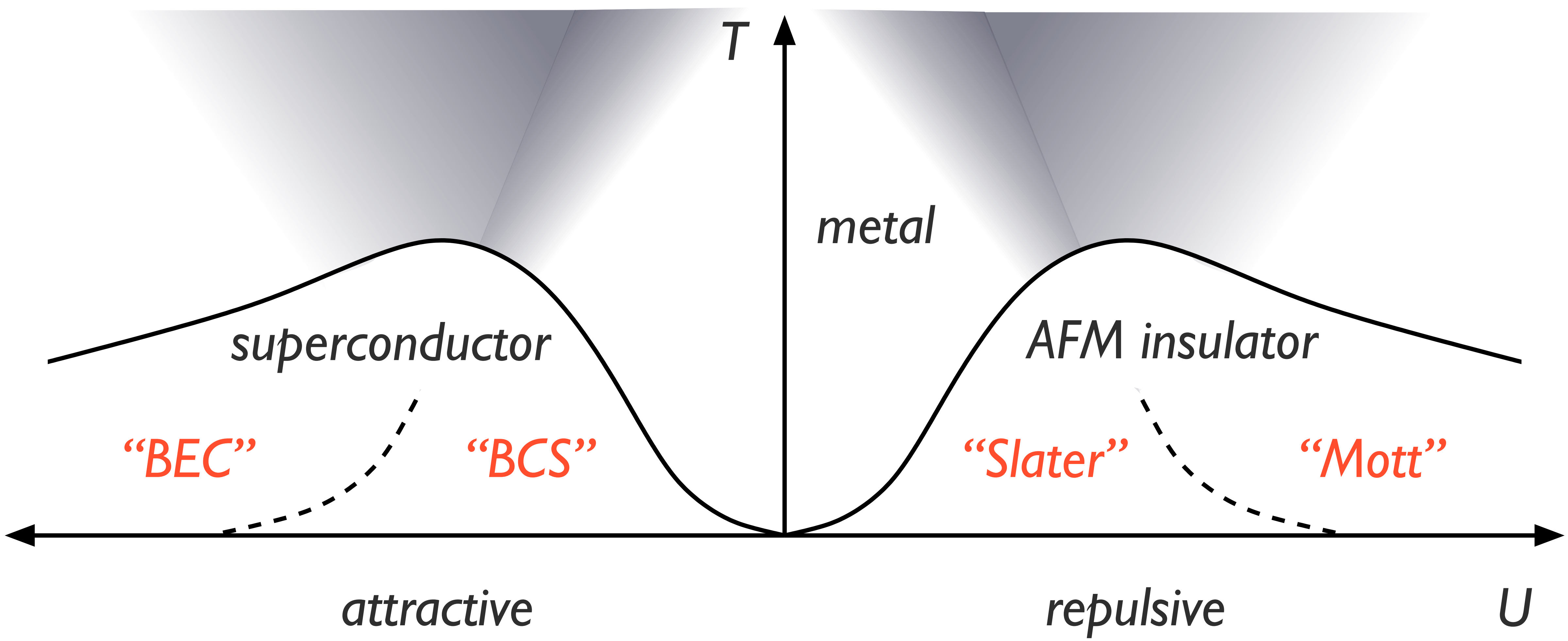

II. Nonthermal symmetry-broken states

- Weak-coupling regime

  Tsuji, Eckstein & Werner (2012)

- Slow ramp from (Slater-)Antiferromagnet to Paramagnet

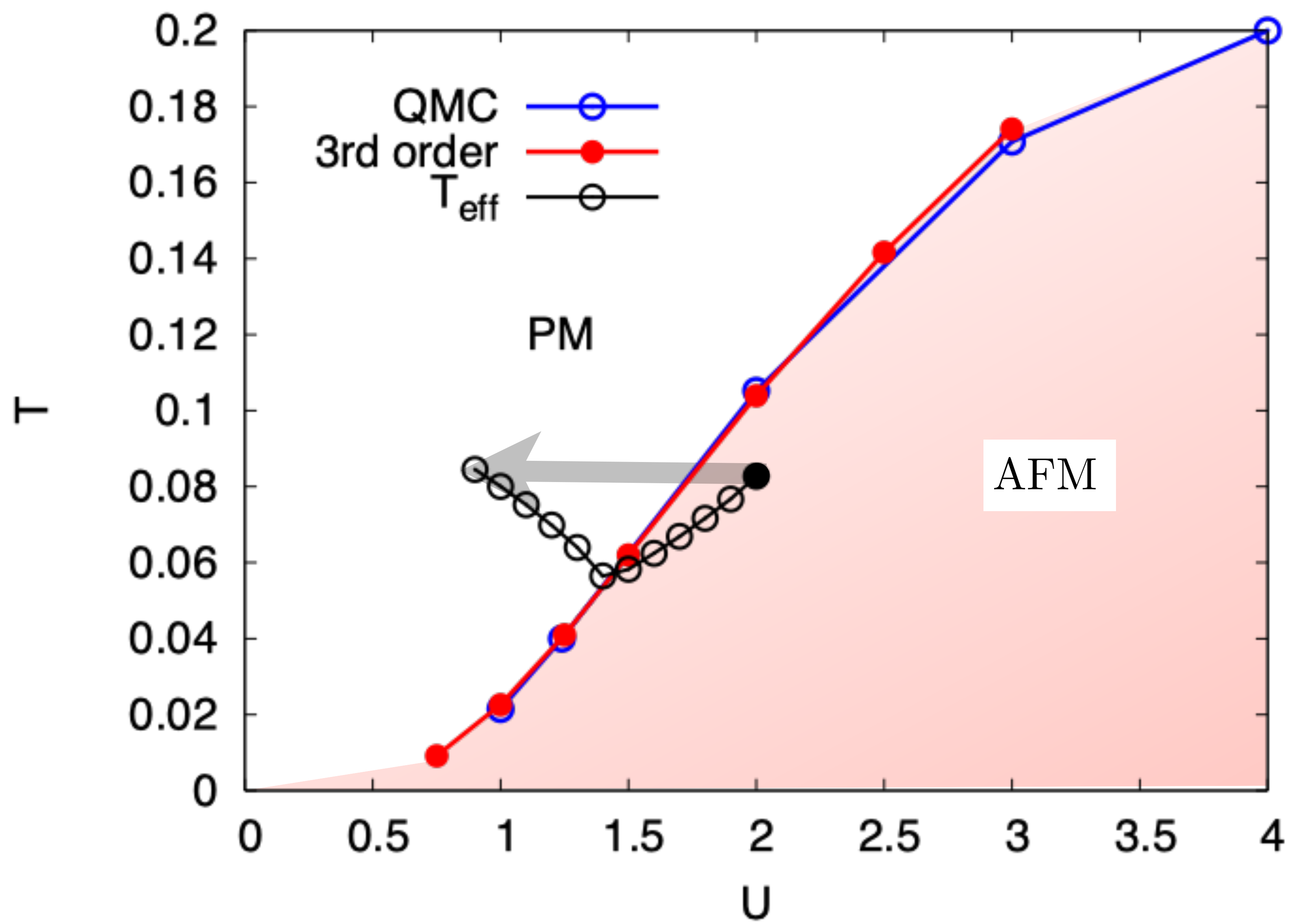

II. Nonthermal symmetry-broken states

- Weak-coupling regime

  Tsuji, Eckstein & Werner (2012)

- Time-evolution of the magnetization for different final *U*

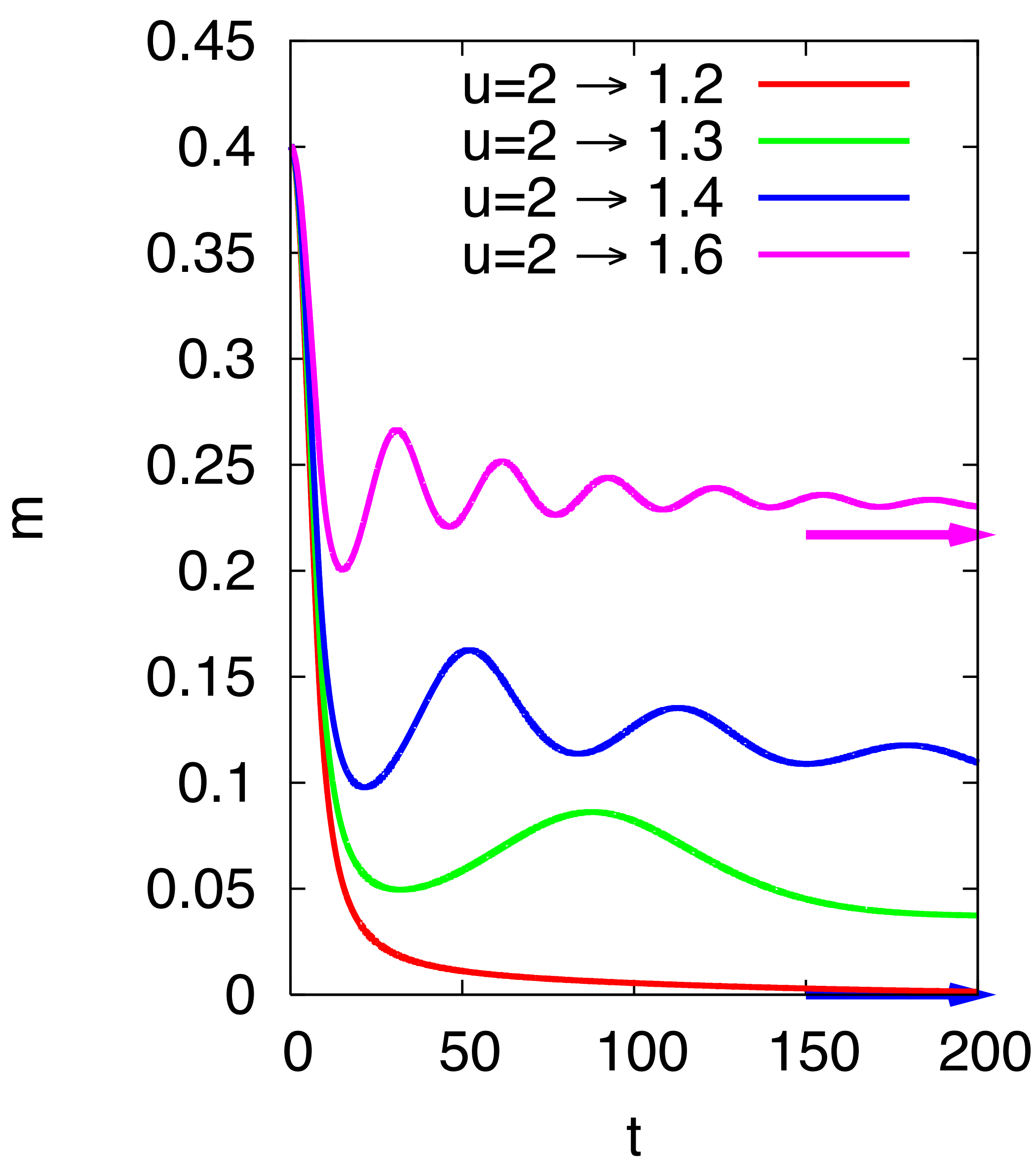

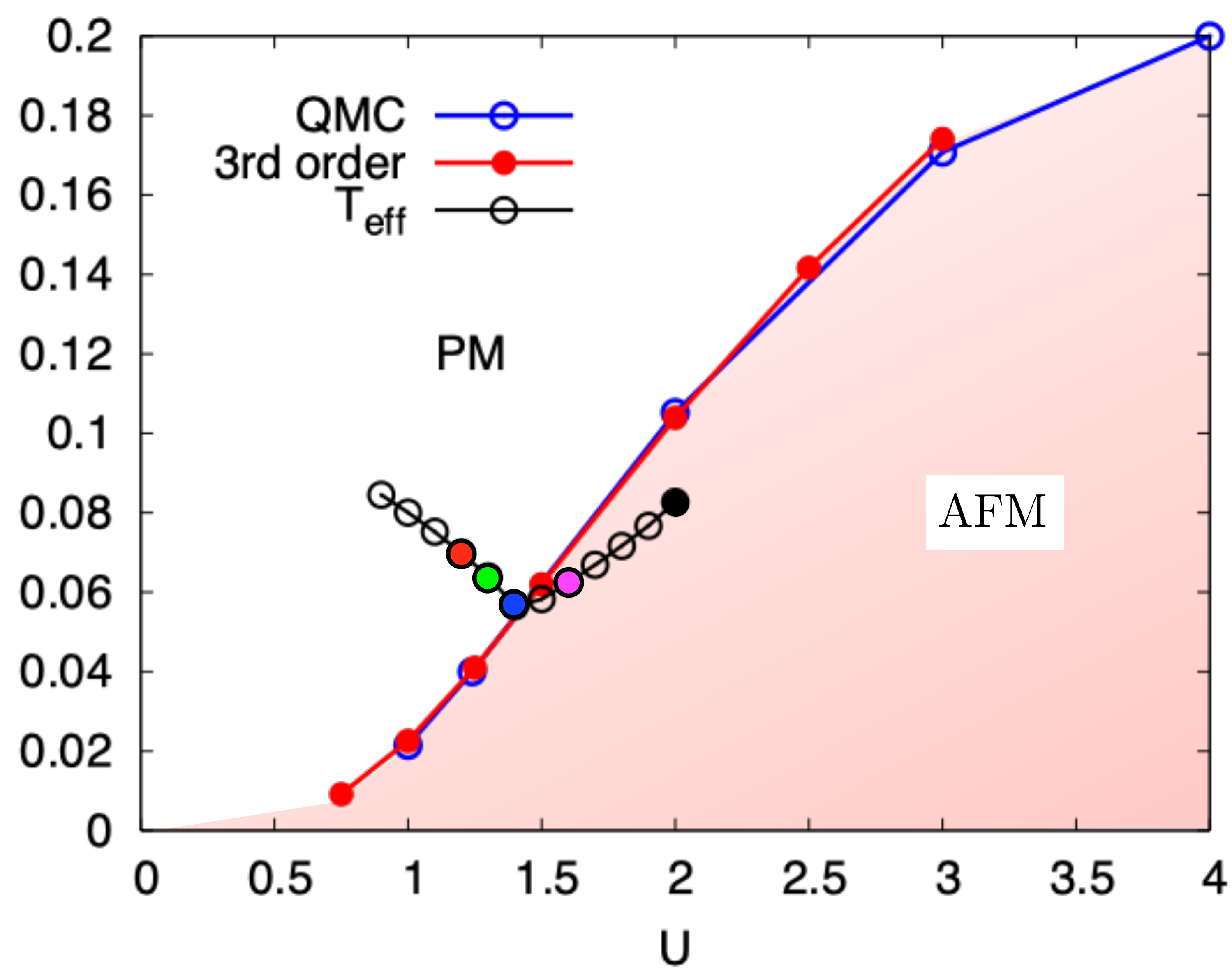

II. Nonthermal symmetry-broken states

- Weak-coupling regime

  Tsuji, Eckstein & Werner (2012)

- Time-evolution of the magnetization for different final *U* (Hartree)

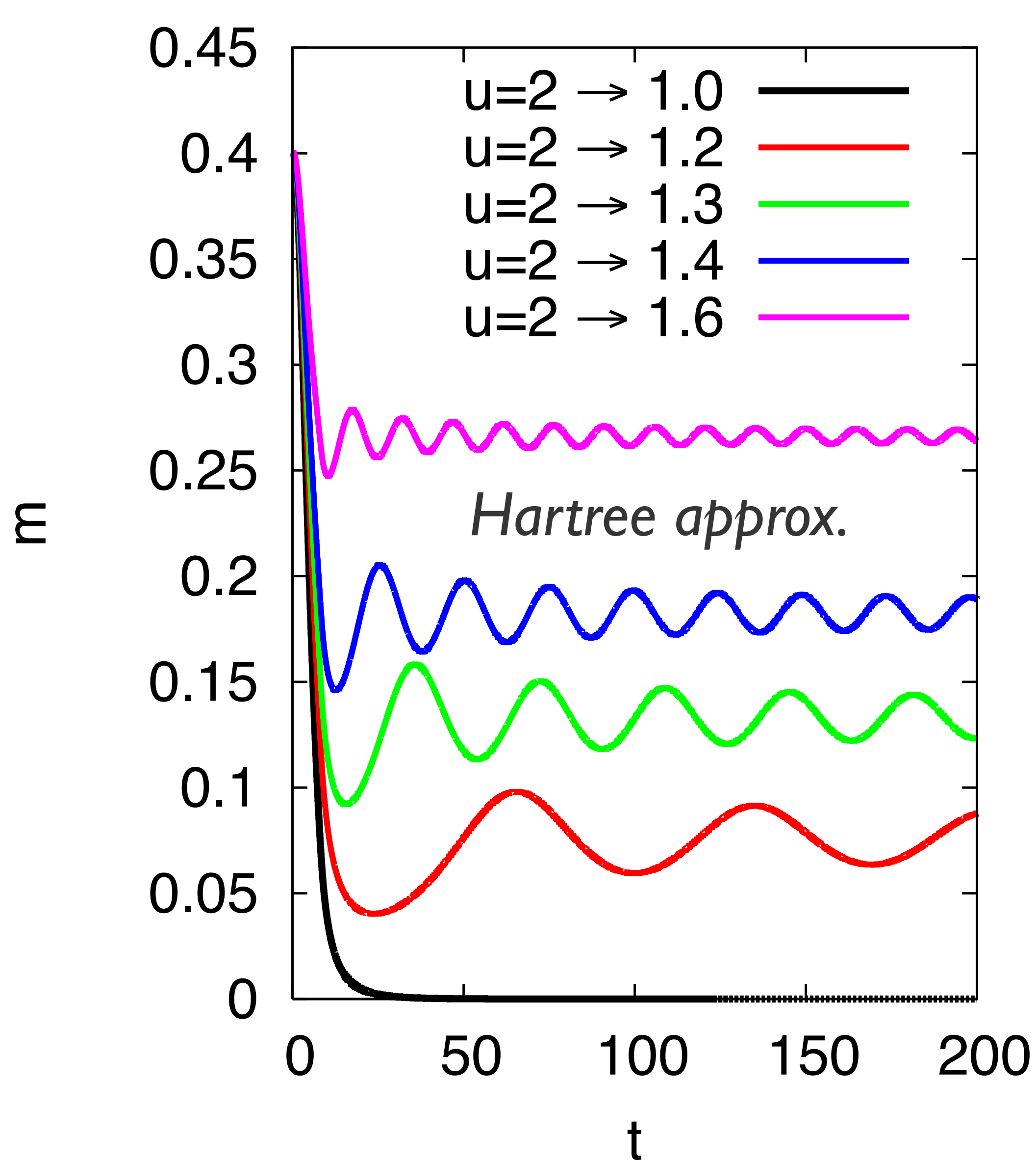

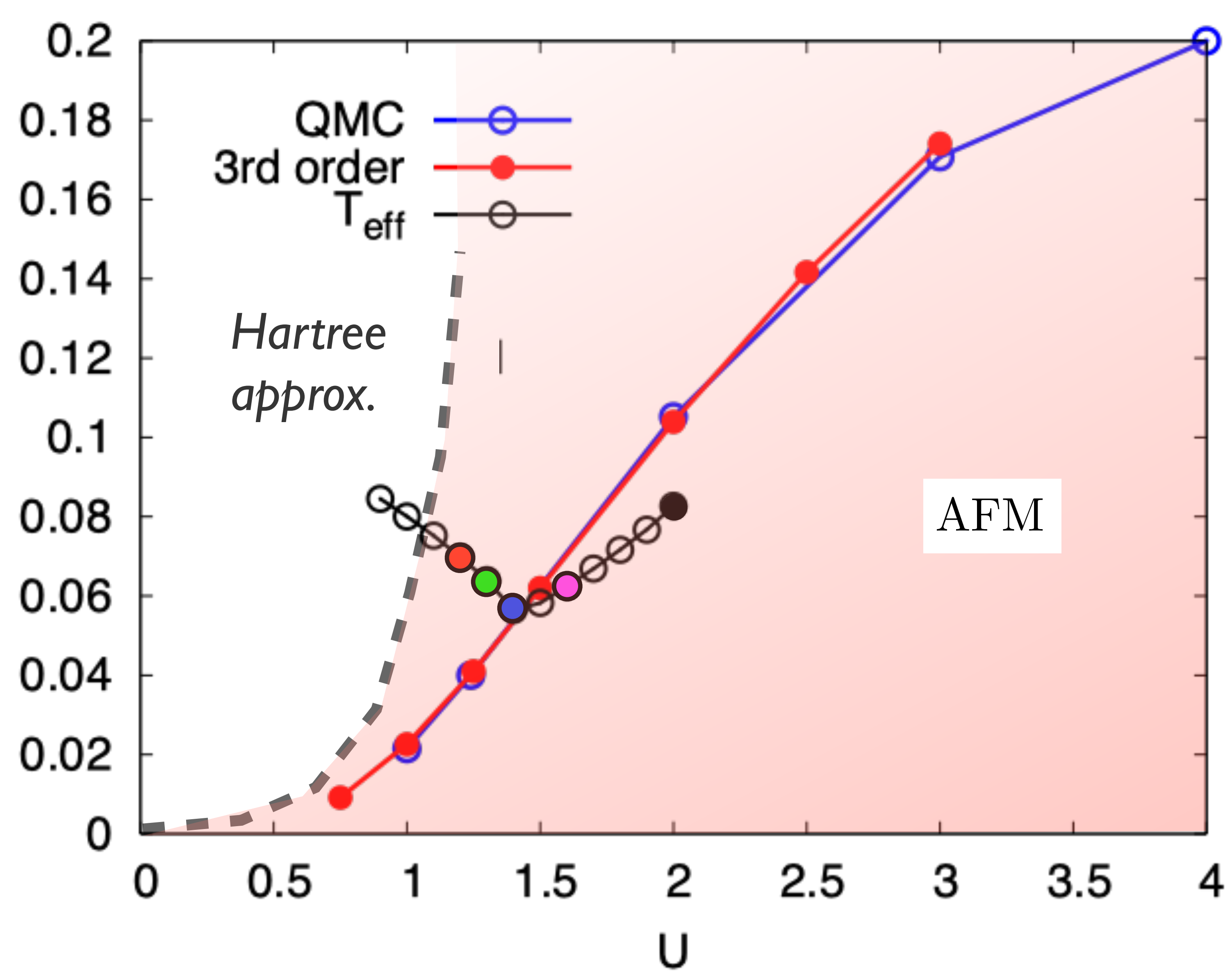

II. Nonthermal symmetry-broken states

- Weak-coupling regime

  Tsuji, Eckstein & Werner (2012)

- Time-evolution of the magnetization for different final *U*

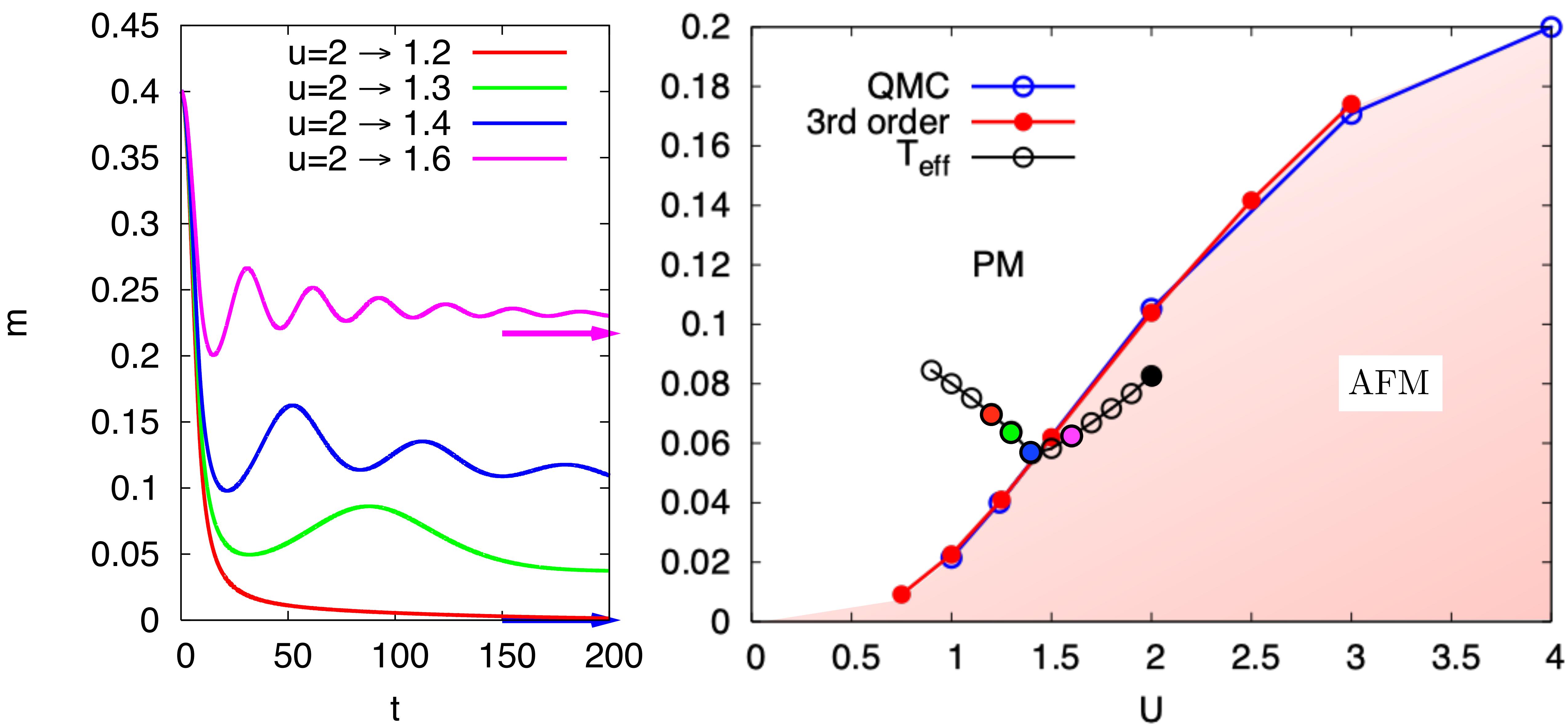

II. Nonthermal symmetry-broken states

- Weak-coupling regime

  Tsuji, Eckstein & Werner (2012)

- Evidence for a nonthermal critical point

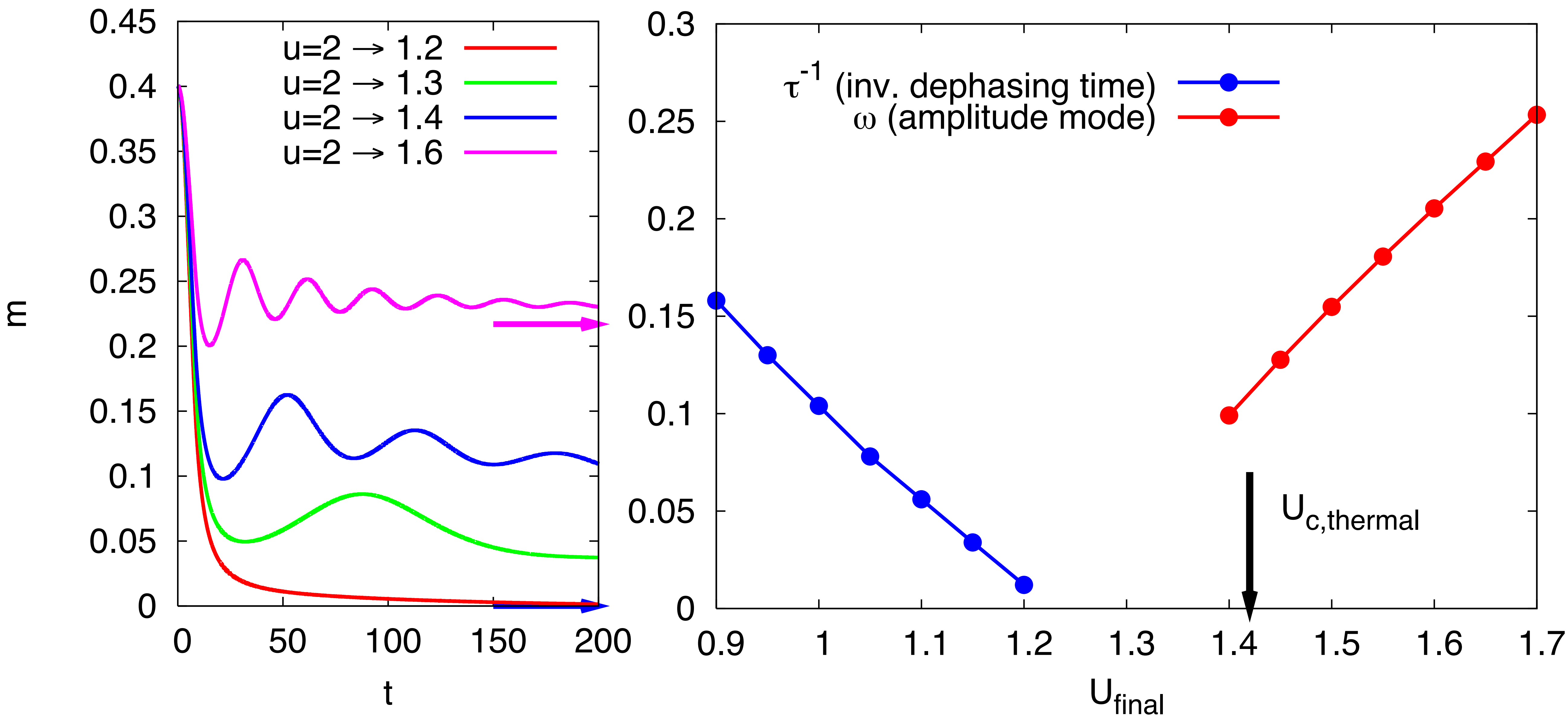

II. Nonthermal symmetry-broken states

- Weak-coupling regime

  Tsuji, Eckstein & Werner (2012)

- Evidence for a nonthermal critical point

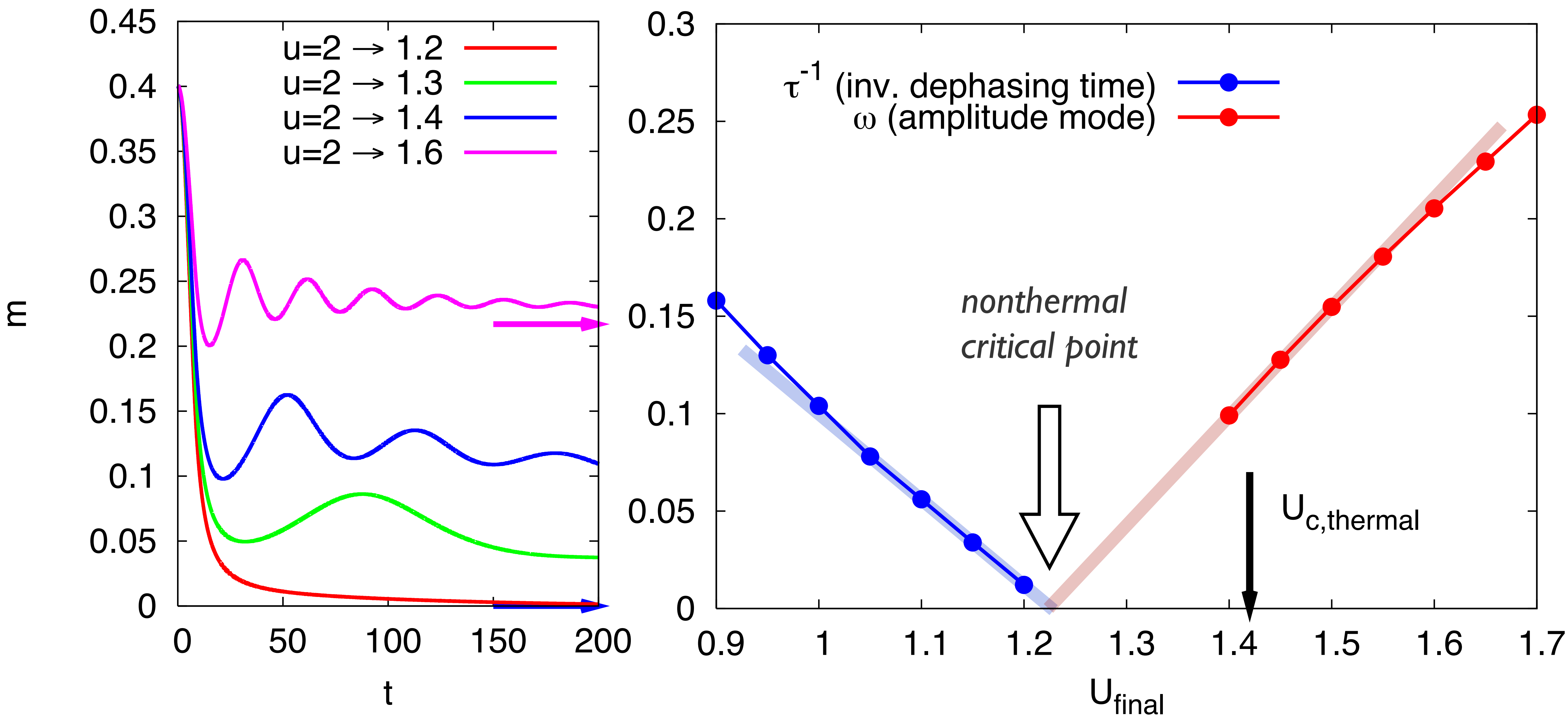

II. Nonthermal symmetry-broken states

- Weak-coupling regime

  Tsuji, Eckstein & Werner (2012)

- Evidence for a nonthermal critical point

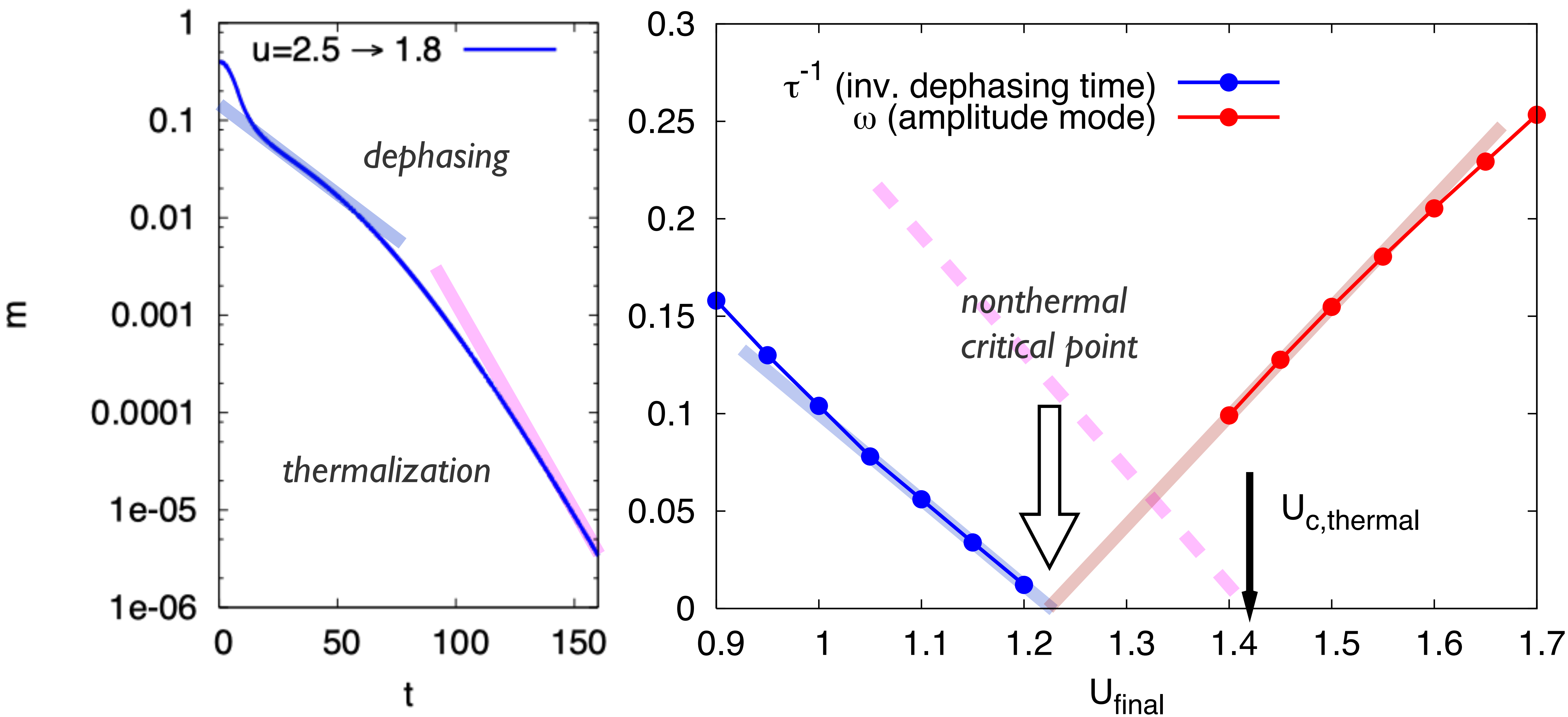

II. Nonthermal symmetry-broken states

- Weak-coupling regime

  Tsuji, Eckstein & Werner (2012)

- Evidence for a nonthermal critical point

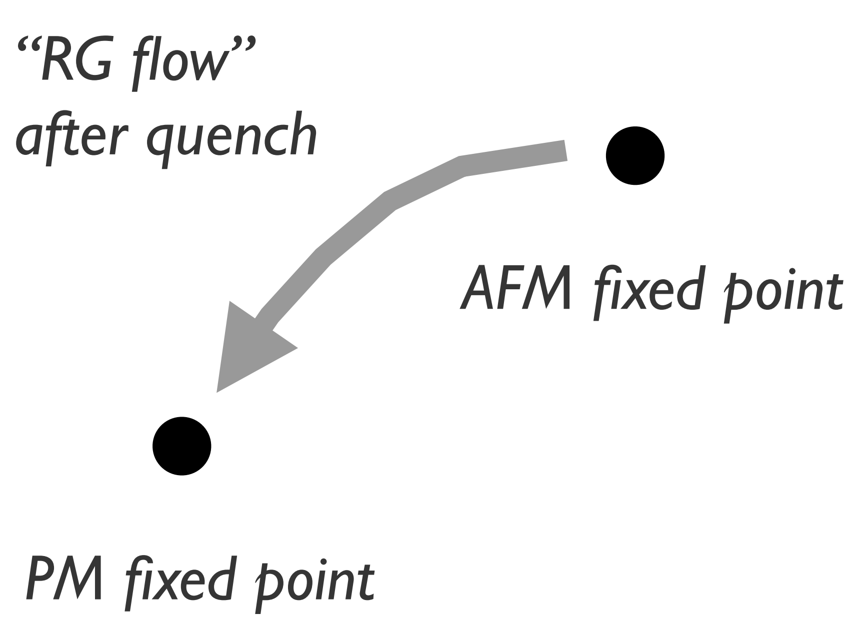

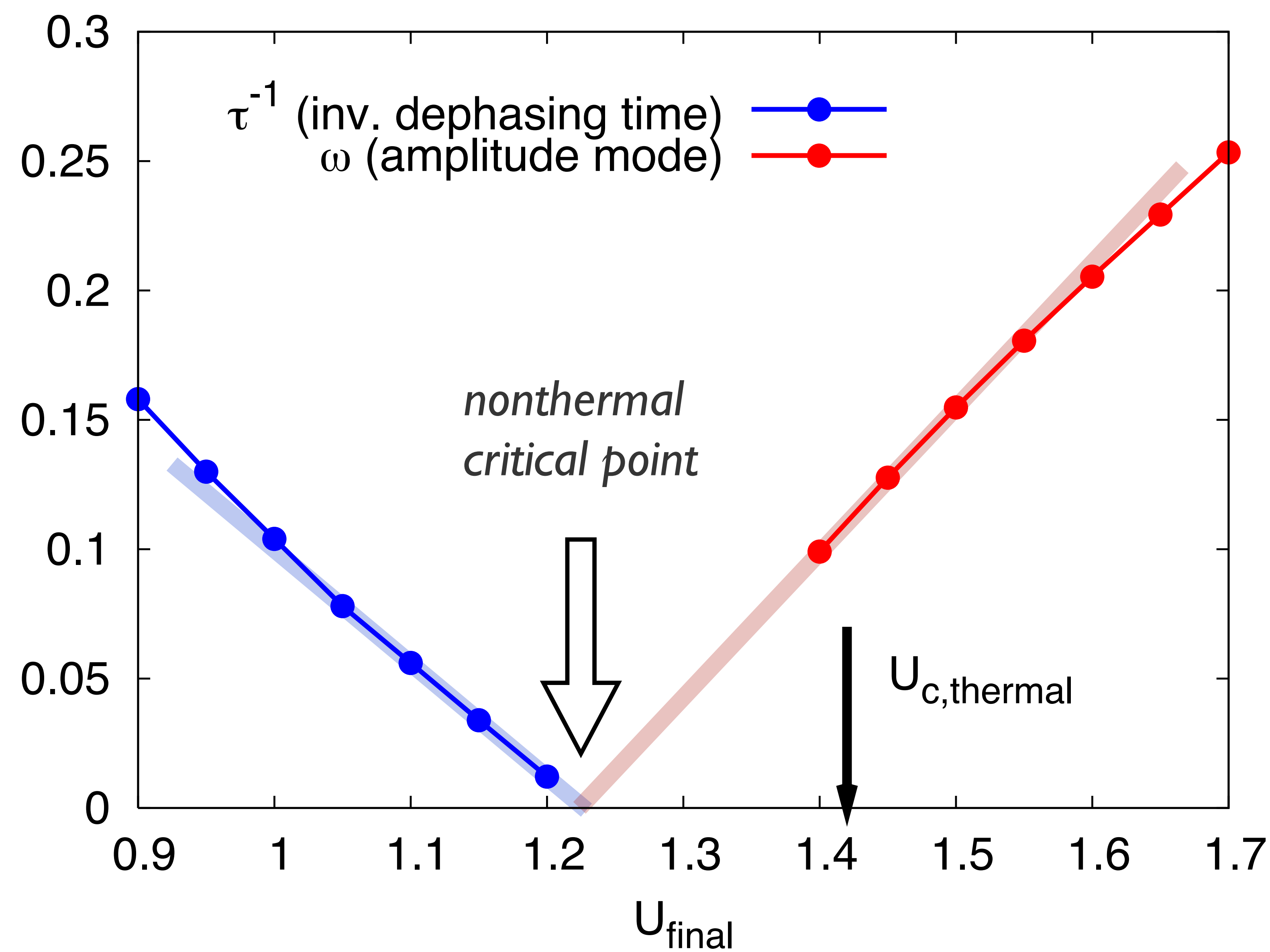

II. Nonthermal symmetry-broken states

- Weak-coupling regime

  Tsuji, Eckstein & Werner (2012)

- Evidence for a nonthermal critical point

Berges et al. (2004)

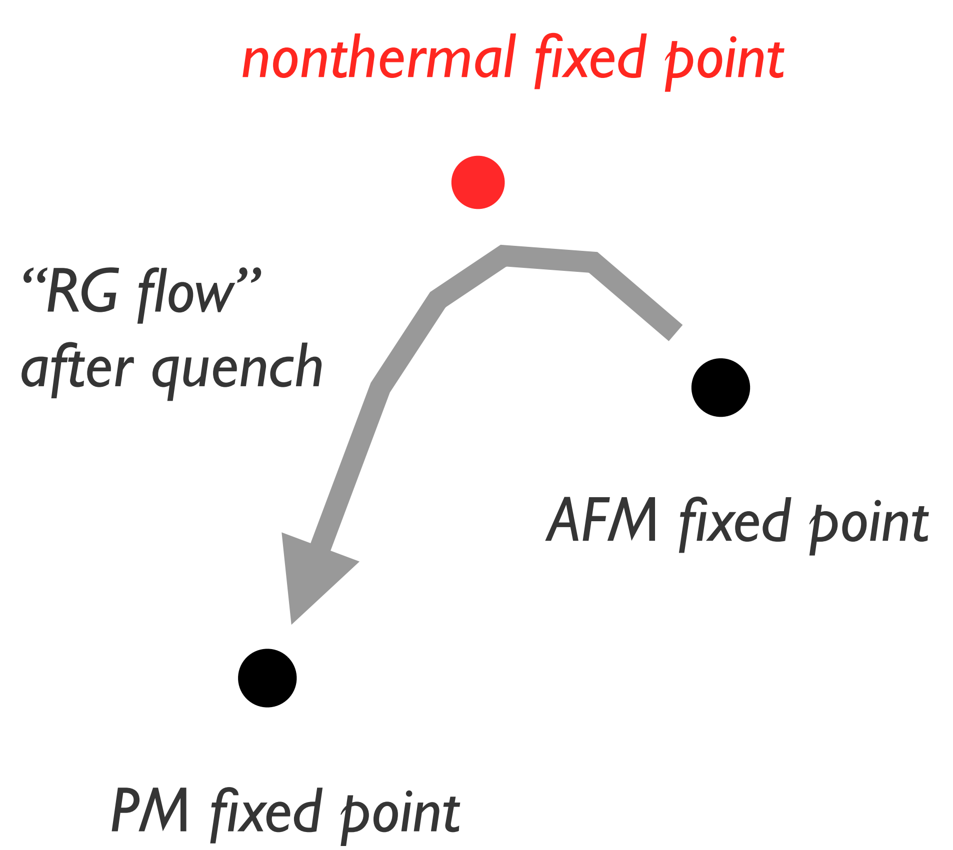

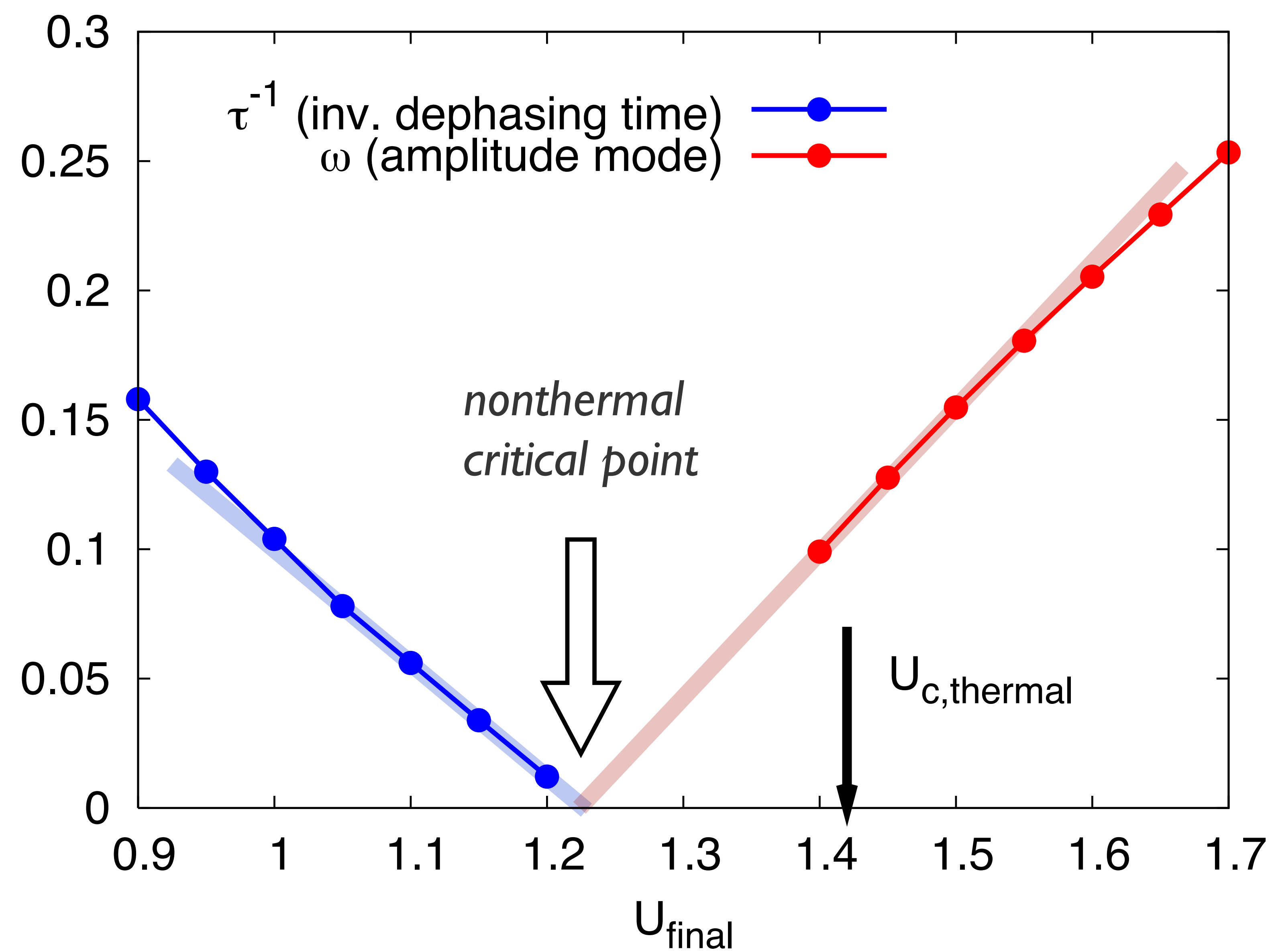

III. Cooling by photo-doping

- Photo-doping from core levels *Werner, Eckstein, Mueller & Refael (2019)*
  - Dipolar excitations with appropriate frequency Ω transfer electrons from core to system and cool down the system

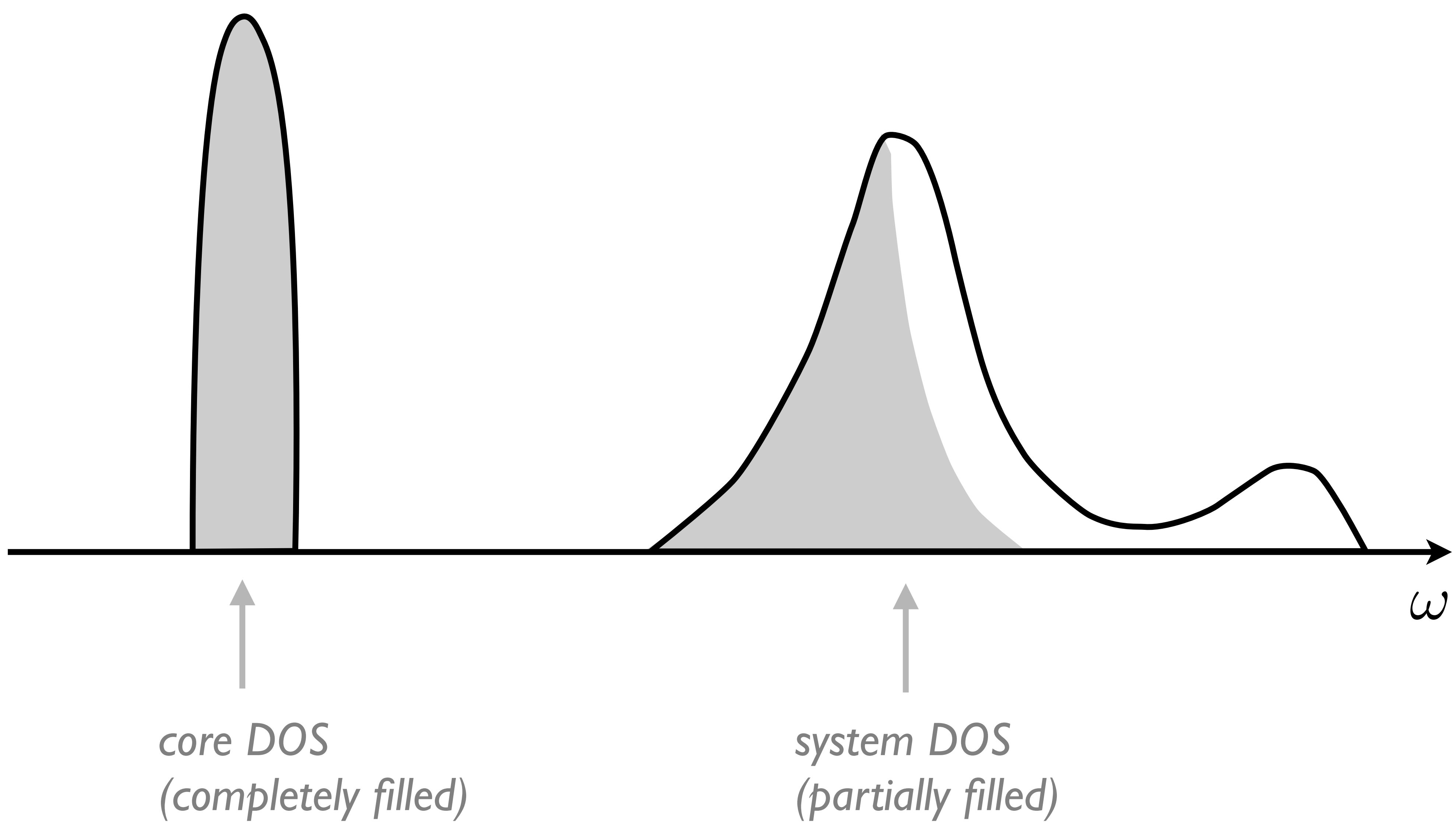

III. Cooling by photo-doping

- Photo-doping from core levels *Werner, Eckstein, Mueller & Refael (2019)*
  - Dipolar excitations with appropriate frequency Ω transfer electrons from core to system and cool down the system

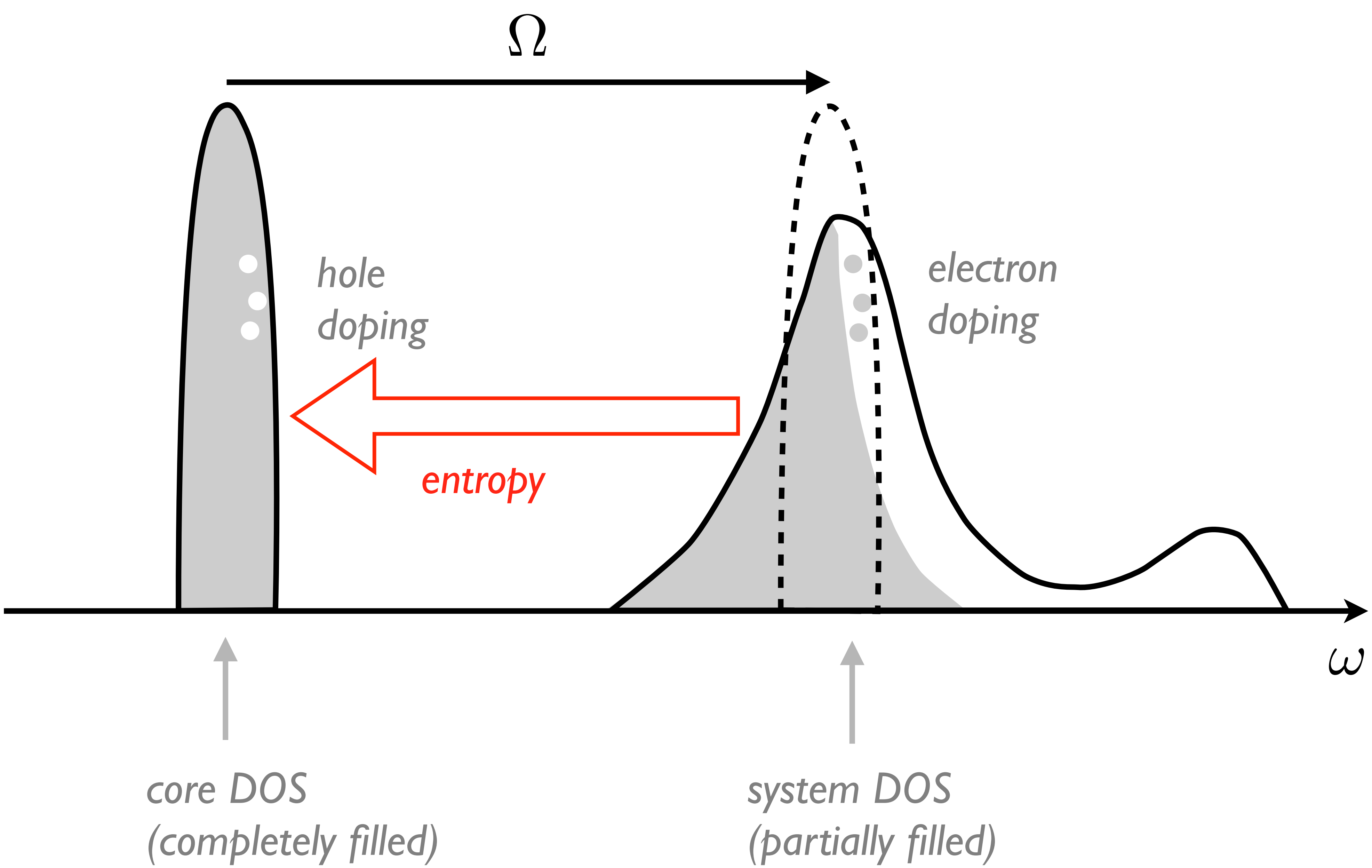

III. Cooling by photo-doping

- Photo-doping from core levels *Werner, Eckstein, Mueller & Refael (2019)*
  - Entropy of the core band in the narrow band (atomic) limit:

$$S_{\rm core} = -2n_\sigma \ln(n_\sigma) - 2(1-n_\sigma)\ln(1-n_\sigma)$$

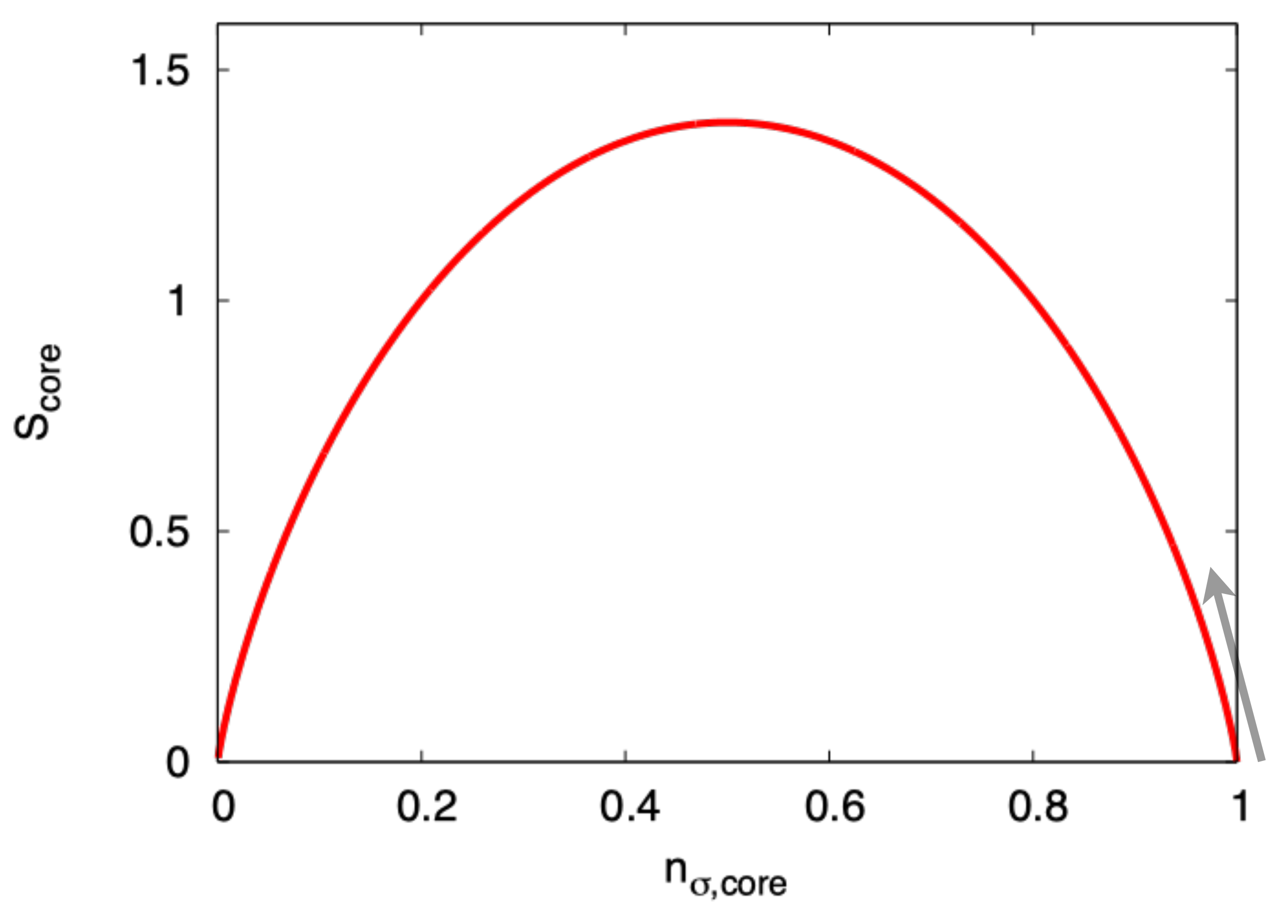

rapid increase of entropy of the core upon hole doping

  - In case of isentropic doping process:

$$\Delta S_{\rm core} \nearrow \;\Rightarrow\; \Delta S_{\rm system} \searrow$$

cooling of system due to entropy reshuffling

III. Cooling by photo-doping

- Photo-doping from core levels *Werner, Eckstein, Mueller & Refael (2019)*
  - Constant entropy contours in the filling-temperature plane

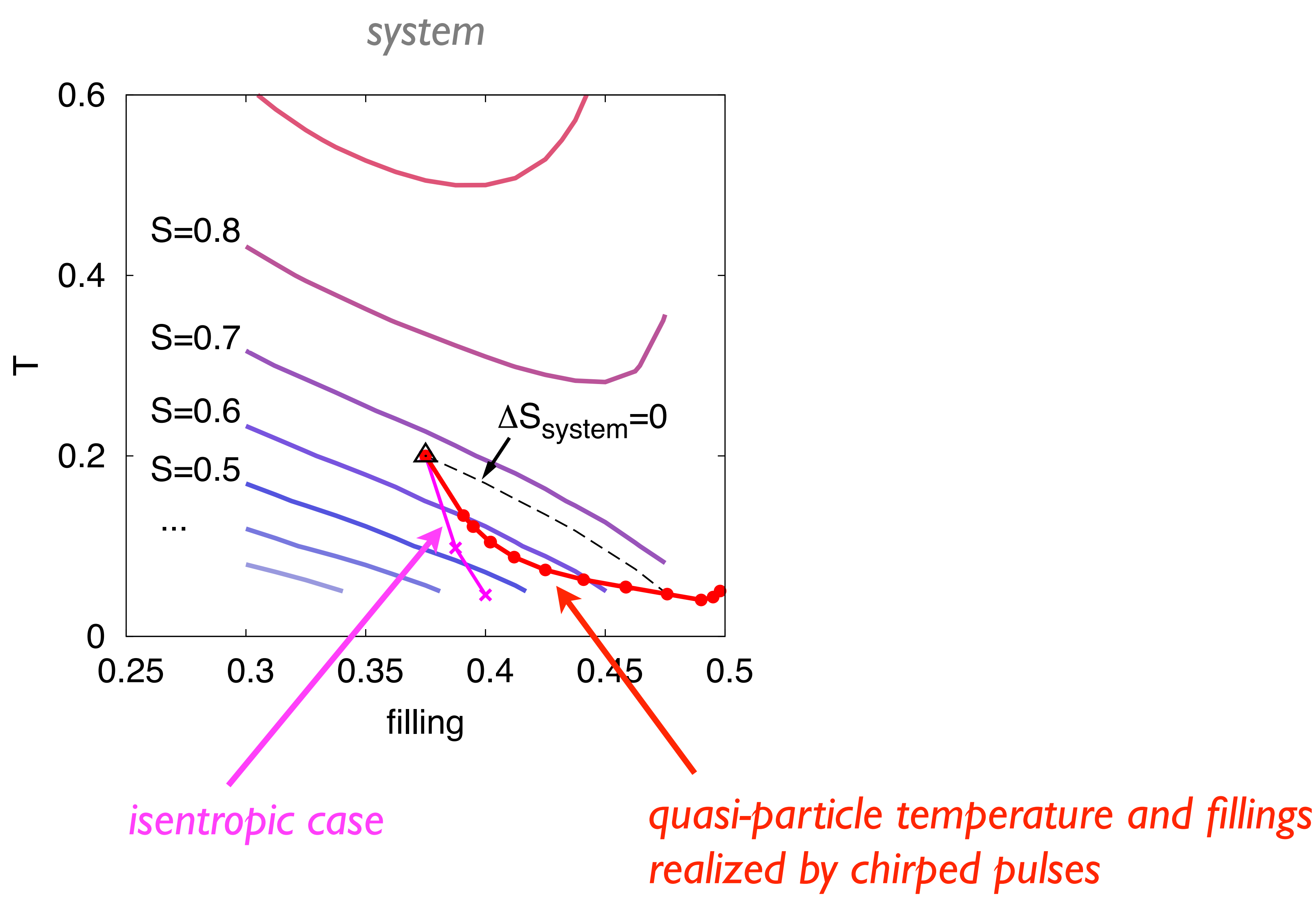

III. Cooling by photo-doping

- Photo-doping from core levels *Werner, Eckstein, Mueller & Refael (2019)*
  - Constant entropy contours in the filling-temperature plane

system

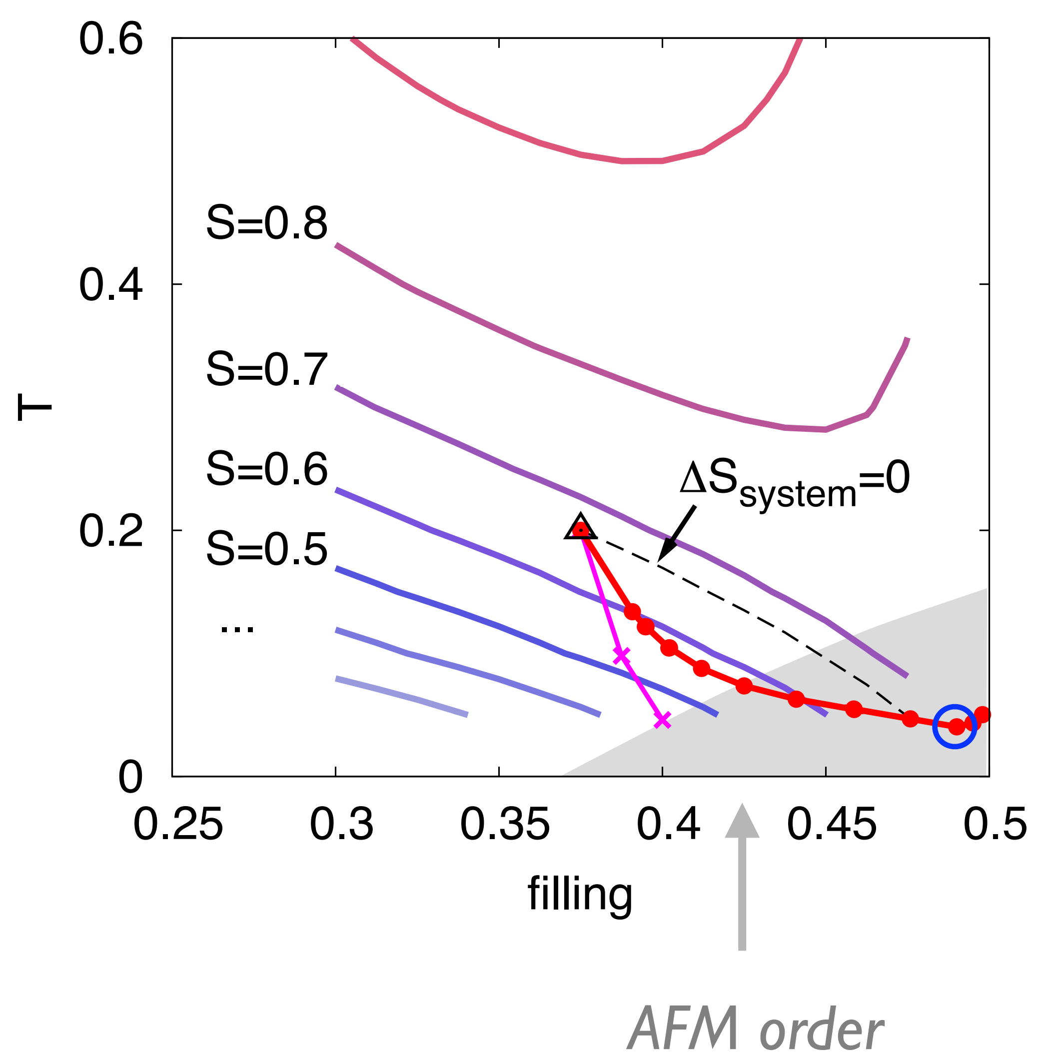

light-induced AFM order

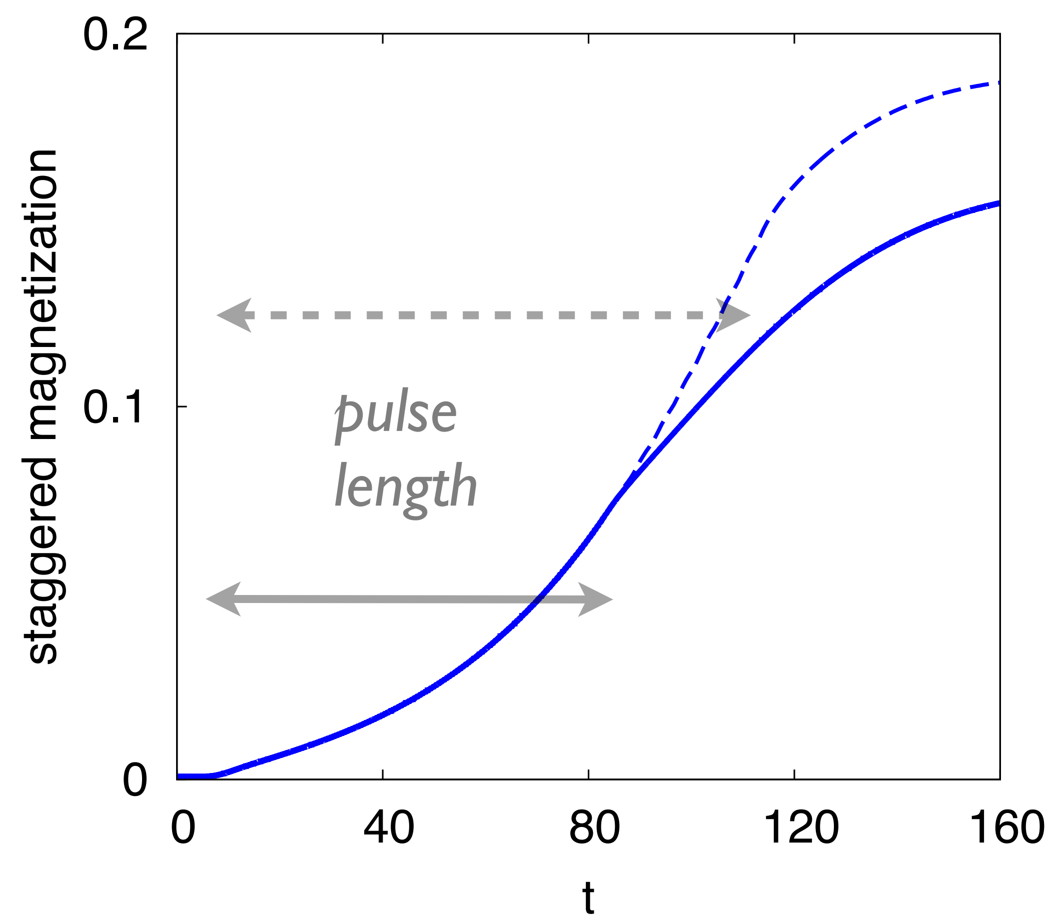

III. Cooling by photo-doping

- Related example of a nonthermal superconducting state
  - η-pairing in a repulsive Hubbard model with inverted population

    Rosch, Rasch, Binz & Vojta (2008); Kaneko et al. (2019); Werner, Li, Golez & Eckstein (2019)

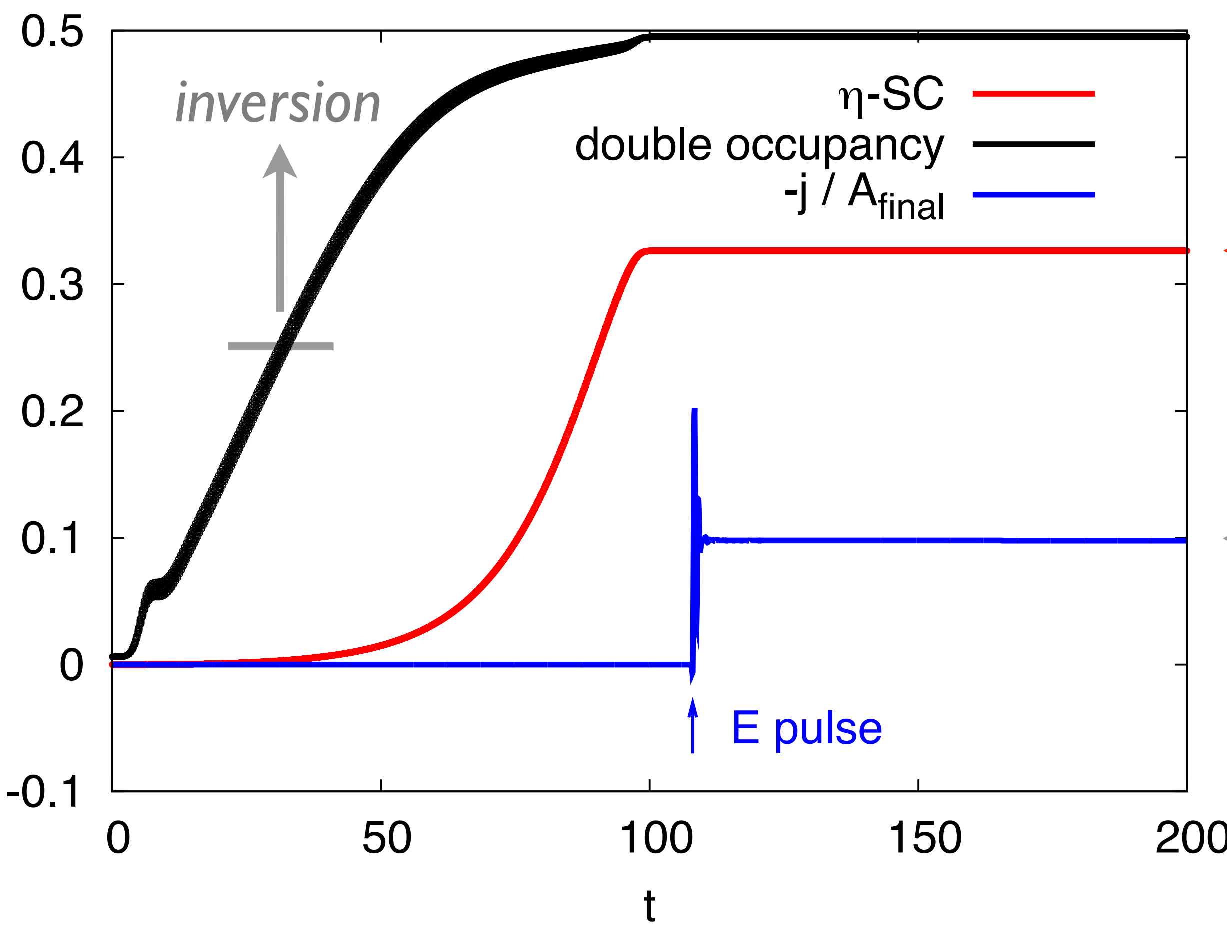

light-induced η-pairing

non-decaying current consistent with superconductivity

uniform pairing

staggered η-pairing

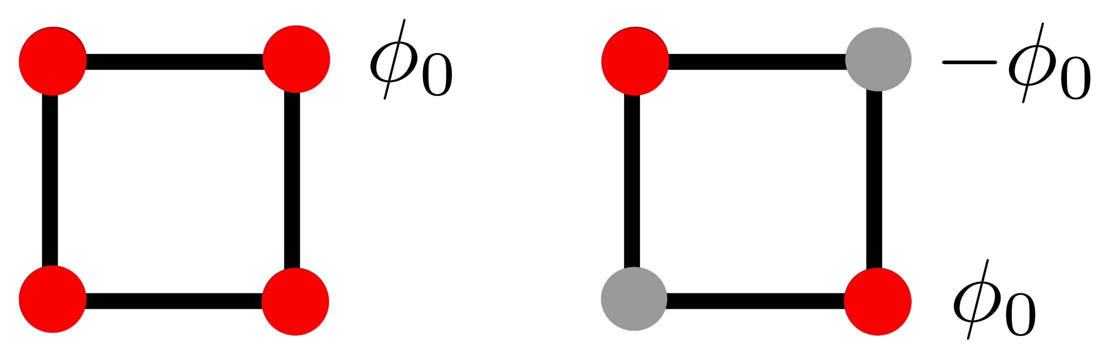

III. Cooling by photo-doping

- Related example of a nonthermal superconducting state
  - Nonequilibrium phase diagram from steady-state DMFT
  - Use coupling to baths to control doublon concentration and T_{eff}

Li, Golez, Werner & Eckstein, PRB (2020)

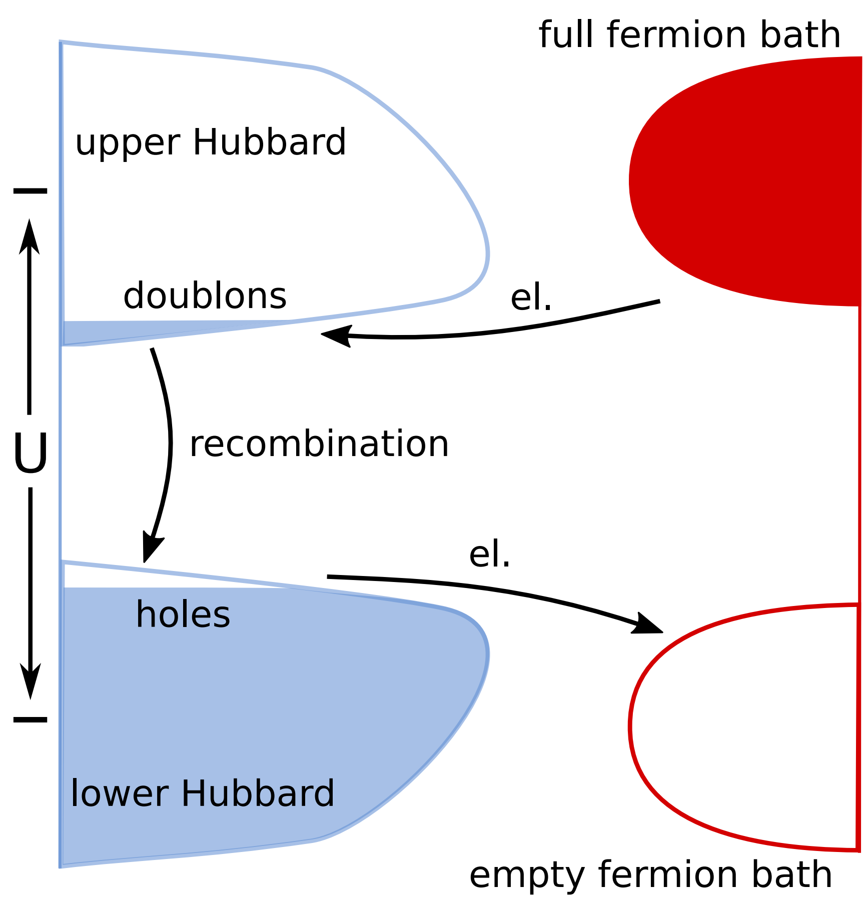

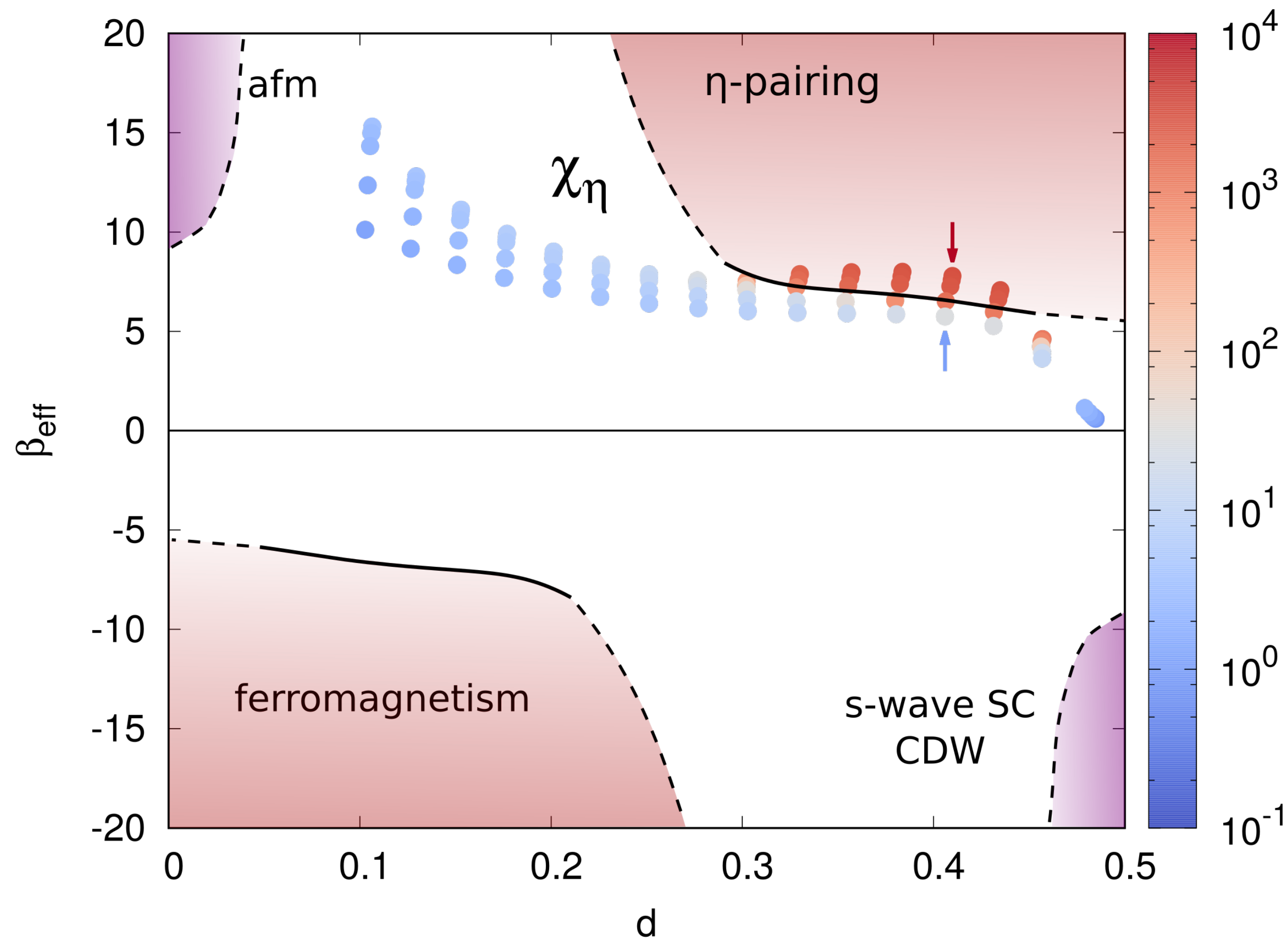

References

- Dynamical mean field theory of strongly correlated fermion systems and the limit of infinite dimensions

  A. Georges *et al.*, Rev. Mod. Phys. 68, 13 (1996)

- Nonequilibrium dynamical mean field theory and its applications

  H. Aoki *et al.*, Rev. Mod Phys. 86, 779 (2014)

- Photo-induced nonequilibrium states in Mott insulators

  Y. Murakami *et al.*, arXiv:2310.05201 (2023)

- Acknowledments:

  Martin Eckstein (Hamburg), Marcus Kollar (Augsburg), Naoto Tsuji (Tokyo University), Takashi Oka (Tokyo University), Hideo Aoki (Tsukuba), Hugo Strand (Oerebro), Denis Golez (Ljubljana), Yuta Murakami (RIKEN), Michael Schueler (PSI), Nikolaj Bittner (Zeiss)